Trade, Infrastructure and Supply Chain

by

Weizhao Sun

B.A., Michigan State University, 2017

M.A., Duke University, 2019

M.A., University of Colorado Boulder, 2021

A thesis submitted to the

Faculty of the Graduate School of the

University of Colorado in partial fulfillment

of the requirements for the degree of

Doctor of Philosophy

Department of Economics

2025

Committee Members:

Sergey Nigai, Chair

Jeronimo Carballo

Wolfgang Keller

Taylor Jaworski

Guofeng Cao

Sun, Weizhao (Ph.D., Economics)

Trade, Infrastructure and Supply Chain

Thesis directed by Prof. Sergey Nigai

Chapter one quantifies the trade effects of effective bilateral elevation (EBE), representing the transportation cost incurred when trucks go uphill and downhill between countries. Introducing an instrumental variable for EBE, the paper reveals that a one-percent rise in EBE leads to a 0.046 percent reduction in trade. This impact varies across regions and industries, with landlocked countries experiencing effects more than nine-fold. The impact is more pronounced in industries with higher weight-to-value ratios. Employing a multi-sector Armington model, the paper estimates that removing bilateral elevations could lead to an average 1 percent increase in real wages.

Chapter two develops a quantitative spatial equilibrium model to study endogenous infrastructure under a two-tier government structure where a benevolent national government, followed by self-interested provincial governments, optimally solves the planners' problems by allocating highways and tunnels to maximize aggregated welfare within their jurisdictions. I estimate the trade-cost mitigating effect of highways and tunnels by introducing two novel instrumental variables and incorporating bilateral elevation. The model is calibrated to 309 prefectures across 23 Chinese provinces. Results show that, compared to complete centralization, a two-tier approach promotes equality, lowering inequality measures at the expense of lowering expected utility. In contrast, complete decentralization leads to a substantial decrease in expected utility and a significant increase in inequality.

Chapter three examines the impact of the 2018 US-China trade war on mergers and acquisitions (M&A) activity in China. Using industry-level data, it explores whether rising protectionism and tariff exposure influenced domestic M&A patterns, particularly in trade-sensitive sectors. The analysis reveals a significant drop in overall M&A deals post-2018, with a sharper decline among Chinese acquirers compared to foreign ones. It also finds that industries facing higher tariff ex-

posure saw an increase in M&A activity. These industries engaged in strategic consolidation to mitigate risks and improve supply chain resilience. The study highlights the trade war's role in shaping M&A behavior, with firms adapting to the new trade environment through restructuring.

Acknowledgements

I am grateful to Sergey Nigai for his invaluable guidance and support throughout this research. I also appreciate the insightful feedback from Jeronimo Carballo, Wolfgang Keller, Taylor Jaworski, Richard Mansfield, Scott Savage, Yongmin Chen, and Daniel Kaffine, which helped refine this work. Special thanks to the Department of Economics at the University of Colorado Boulder for providing the necessary resources and funding. I would also like to acknowledge the helpful discussions with Peter Egger, James Markusen, Esteban Rossi-Hansberg, Treb Allen, Tibor Besedes, Marta Santamaria, John Jairo Posada Henao, Huixuan Li, Kyle Butts, Ge Song, and Chunyang Huang that enriched my understanding of the topic. Finally, I extend my deepest gratitude to my family and friends for their unwavering encouragement and support.

Contents

Chapter

List of Tables

Table

List of Figures

Figure

Chapter 1

The Earth Is Not Flat: Bilateral Elevation as a Component of Trade Costs

1.1 Introduction

Prior to 2016, residents of the 800 meter-high cliff homes in China's Sichuan province had a unique challenge when it came to traveling outside their village. Their only option was to descend these cliffs using precarious rattan ladders (Gan (2020)). In the mountainous regions of the Himalayas, other villages faced similar isolation until modern roads were constructed. These villages had minimal contact with the outside world, importing goods only once a year and engaging in limited exports (NHK (2010)). Despite their proximity to potential trading partners when measured by geographical great circle distance, the rugged terrain and rapid elevation changes kept these locations in a state of economic self-sufficiency or autarky.

This paper tries to understand the significance of bilateral elevation in the context of trade. The research assesses the costs associated with elevation changes and explores the implications of electric vehicles that may enhance the efficiency of transporting goods on uneven terrain. Two novel terms are introduced: "physical bilateral elevation (PBE)" and "effective bilateral elevation (EBE)." PBE quantifies the cumulative elevation changes along the shortest route from the origin to the destination. Building upon PBE, EBE evaluates the costs incurred when a vehicle transports goods along this route, considering both uphill and downhill travel. The study then employs a gravity framework to quantify the influence of EBE on trade outcomes.

To compute bilateral elevations along the actual shortest trade routes, I constructed a global transportation network database using ArcGIS. This network database incorporates the world roads

(GRIP global roads database, Meijer et al. (2018)), railway networks (Source: Esri and DeLorme), frequently used shipping routes (Halpern et al. (2015)), and cities (Source: Esri and ArcWorld). Each country's capital city is selected as the origin and destination for trade routes. The *Network Analysis* tool in ArcGIS is then utilized to find the shortest trade routes between the capital cities. The path-finding process prioritizes railroads, higher-quality roads, and maritime routes while attempting to avoid smaller roads. After establishing the trade routes, elevation data is merged with them. Specifically, the U.S. Geological Survey's Global Multi-resolution Terrain Elevation Data 2010 (GMTED2010) at the 15-arc-second level is employed. The calculation of Physical Bilateral Elevation (PBE) involves summing the absolute values of elevation changes along the routes. Effective Bilateral Elevation (EBE), which builds upon PBE, is a weighted average of elevation changes, assigning greater weight to changes with steeper average slopes. These weights are sourced from the transportation literature MOPU (1990) and represent trucks' fuel-cost ratios of traveling on a sloped road compared to flat roads. EBE, the preferred measure of bilateral elevation in this study, can be interpreted as an index representing the cost associated with ascending and descending terrain.

To empirically assess the significance of Effective Bilateral Elevation (EBE), I introduce it as a new key explanatory variable in a gravity model with distance and standard gravity controls. The gravity model is estimated using a log-linear ordinary least-squares approach and a Poisson pseudo-maximum likelihood (PPML) model. This paper also introduces an instrumental variable (IV) for bilateral elevations designed to capture elevation changes near each route but not directly on the routes themselves. This IV strategy is employed to address the endogeneity that arises from terrain modifications on roads. The OLS, PPML, and IV analyses formally demonstrate that EBE constitutes a quantitatively substantial component of international trade costs. On average, a one-percent increase in EBE leads to a 0.046 percent reduction in bilateral trade value. Notably, the impact of EBE varies across regions and industries. If countries are landlocked, the effect of EBE can be nine times more pronounced, highlighting the substantial impact on landlocked nations. Additionally, industries dealing with cheaper but heavier products are more significantly affected

by EBE.

Finally, this paper uses a multi-sector Armington model and conducts counterfactual analyses to answer the following questions: (1) What happens when bilateral elevations are treated as nonexistent (or if they are overlooked)? (2) How will the regenerative braking system of electric vehicles affect bilateral elevations and welfare? Overlooking the impact of bilateral elevations could imply increased wages for most countries by an average of 1 percent. Furthermore, the regenerative braking systems on electric vehicles help recharge the battery when going downhill. The dominance of electric vehicles (in the future) would further decrease EBE and increase wages by, on average, 0.2 percent.

This paper is closely related to Nunn and Puga (2012) and Hirte et al. (2020), who create measures to quantify the impact of geographical barriers to trade. Nunn and Puga (2012) devise a measure of ruggedness to account for regional small-scale terrain irregularities. Hirte et al. (2020) calculate a measure of geographic heterogeneity at the country level based on the number of mountains higher than 1500 meters between different regions within a country. I build on this literature and create two encompassing measures of bilateral elevation by combining data on shortest trade routes with route-segment-specific elevation data. This allows me to measure the actual changes in elevation that vehicles must traverse from the origin to the destination.

Relative to the existing literature, the approach proposed in this paper has several advantages. First, the proposed measure of EBE captures asymmetry that arises because transporting uphill is generally more expensive than going downhill. Second, the measures can capture relative changes in elevation due to both high-elevation mountains and low-elevation hills. Third, the proposed framework can account for changes in transportation technology, e.g., electric vehicles, and the associated effects on EBE. Lastly, PBE and EBE can be directly incorporated into standard gravity equations for trade and will constitute important empirical measures of bilateral trade barriers.

This paper is related to two broad strands of the literature on geographical barriers and trade. First, it contributes to the strand of research that studies how transportation infrastructure mediates geographical barriers and facilitates trade within and between countries (see Combes

and Lafourcade (2005); Hummels (2007); Faber (2014); Coşar and Demir (2016); Martincus et al. (2017); and Coşar et al. (2021)). For example, Allen and Arkolakis (2022) evaluate the welfare impact of transportation infrastructure improvements in a general equilibrium model featuring endogenous transportation costs and traffic congestion. Jaworski and Kitchens (2019) quantify the impact of highways on regional development in the Appalachian Mountains in the United States.[1] This paper contributes to this strand by highlighting a novel mechanism: New infrastructures and advancing automobile technology can change the magnitude and significance of bilateral elevations, leading to trade cost reductions, higher trade, and improvements in welfare.

Second, this paper contributes to the literature that focuses on the role of geographical barriers on trade and development. For example, it is well established that geographical great circle distance impedes international trade (see Hummels (1999); Borchert and Yotov (2017); Feyrer (2021)) as well as domestic trade (see Hillberry and Hummels (2008); Agnosteva et al. (2019)). International and intranational border effects also play a significant role in impeding trade flows (see Nitsch (2000); Coughlin and Novy (2016); Wrona (2018)). This paper contributes to this strand by devising and quantifying two innovative measures of geographic barriers to trade and development- PBE and EBE.

1.2 Calculating Bilateral Elevation

1.2.1 Bilateral Elevation

I construct two measures of bilateral elevations along the shortest trade route for each country pair. To do so, first, I build a world transportation network database, including world roads, railways, maritime trade routes, and representative cities in each country. Secondly, I calculate the shortest trade routes between representative cities using the network database and the *Network*

[1] Also see Donaldson (2018) who studied the historical impact of railroads in India and De Soyres et al. (2019), Bird et al. (2020), Baniya et al. (2020), and Chen and Lin (2020) who focus on infrastructures built under the belt and road initiative. See Combes and Lafourcade (2005), who calculate a transport cost measure based on the real transport network and characteristics of the infrastructure, vehicle, and energy used. The IV strategy in this paper is related to Ducruet et al. (2020), who use natural ocean depth in buffer rings around the ports to proxy modified port depth and measure port-city development.

Analysis tool of ArcGIS. Thirdly, I create the elevated trade routes by merging the shortest trade routes with the world elevation database, allowing detailed changes in elevation along the routes to be observed. Finally, I propose a method to measure physical and effective bilateral elevations using elevated trade routes.

1.2.1.1 World Network Database

I build a world network database, which is a collection of world roads, railways, maritime trade routes, and representative cities. The world roads network comes from the Global Roads Inventory Project (GRIP), Meijer et al. (2018). The GRIP database used in this paper contains the updated road network from 2014. Information on the railroad network comes from the Esri "World Railroads" database. The Esri "World Cities" database collects data on the world's cities. Information on the world shipping routes comes from Halpern et al. (2015). The origin and destination of the trade routes are the capitals of each country. Using capitals as endpoints of routes has been the standard approach in the past, and it is consistent with the methods used by Centre d'Études Prospectives et d'Informations Internationales (CEPII). [2]

1.2.1.2 Shortest Trade Routes

The *Network Analysis* toolbox of ArcGIS is used to calculate the shortest trade routes along the existing networks between the representative cities. Each route prioritizes railroads, high-quality roads, and maritime routes and tries to avoid local roads. This also yields the bilateral distance along the network, a variable in the gravity regression in Section 1.3. [3]

The routes are expanded into three dimensions by integrating them with elevation data, enabling a detailed assessment of elevation changes along each route. This elevation data is at

[2] One alternative strategy is to use the economic hubs of countries as the starting and ending points for routes. However, it's important to consider that elevation tends to be spatially correlated: Areas adjacent to elevated terrain are also likely to be elevated. Consequently, routes originating from or terminating at economic centers are highly likely to pass through regions with elevation profiles similar to those connecting the capital cities. Therefore, using economic centers as the origin and destination points is not expected to produce substantially divergent outcomes.

[3] An alternative method is to utilize the least-cost routes for trucks instead of the shortest ones. However, due to the spatial correlation of elevation, using the least-cost routes is unlikely to produce significantly different results.

a 15-arc-second resolution level and is sourced from the U.S. Geological Survey's Global Multi-resolution Terrain Elevation Data 2010 (GMTED2010) database.

1.2.1.3 Two Measures of Bilateral Elevation

In this section, I establish two metrics for bilateral elevations. The first metric is referred to as "Physical Bilateral Elevation" (PBE), as defined in equation (1.1). For a given shortest route between ij, PBE is calculated by summing the absolute values of elevation changes along the route and dividing this sum by the route's distance. PBE provides insight into elevation changes along the route, serving as a descriptor of the physical characteristics of the terrain along roads. Its unit of measurement is in meters per kilometer.

$$PBE_{ij} = \frac{\sum_{n=2}^{N_{ij}} |Elev_n - Elev_{n-1}|}{Dist_{ij}} \tag{1.1}$$

The subscript, $n = (1, ..., N_{ij})$, represents sampled points along each shortest trade route whose elevation will be recorded. $Elev_n$ is the average elevation of the pixel in which point n is located. (The elevation data employed in this paper is at the 15-arc-second level, so a pixel is an area of approximately 450 meters by 450 meters.) N_{ij} is the maximum sampled point, depending on the country pair ij. It's important to note that as one travels further, more hills are encountered, leading to larger absolute differences in elevation. This could pose a problem if the sum of elevation differences strictly increases with distance. Equation (1.1) divides the sum of absolute elevation differences, $\sum_{n=2}^{N_{ij}} |Elev_n - Elev_{n-1}|$, by the distance, $Dist_{ij}$. This adjustment ensures that PBE does not exhibit a strictly increasing relationship with distance. The absolute value is applied to $Elev_n - Elev_{n-1}$ to create positive measures suitable for use with logarithms, which are commonly employed in gravity-estimating trade equations. Two critical limitations of PBE are worth mentioning: firstly, by using the absolute value, PBE treats uphill and downhill segments equally, making it symmetric. Secondly, PBE doesn't differentiate between rapid and mild elevation changes. Consequently, this paper does not explore the trade implications of PBE. Instead, a modified version of PBE will be introduced.

The second metric for bilateral elevation is referred to as "effective bilateral elevation" (EBE), defined in equation (1.2). EBE is a weighted average serving as an index representing the costs associated with going uphill and downhill. Denoted as $Elev_{ij}$, EBE is the preferred measure for bilateral elevation. In contrast to PBE, EBE introduces a weighting factor, denoted as w_{grade}, for the absolute value of the elevation difference between two consecutive points.

$$EBE_{ij} \equiv Elev_{ij} = \frac{\sum_{n=2}^{N_{ij}} |Elev_n - Elev_{n-1}| * w_{grade}}{Dist_{ij}} \tag{1.2}$$

The weighting metric, w_{grade}, is calculated as follows: Let $interval$ be the distance between two sample points, which is 20 miles in the baseline regressions.[4] Let $grade = \frac{Elev_n - Elev_{n-1}}{interval}$ denote the average grade (road slope) going from point $n-1$ to point n.[5] The fuel consumption, c, on roads with different grades, p, is calculated in equation (1.3). The weighting metric, $w_{grade} = \frac{c_{grade}}{c_{grade=0}}$, represents the fuel-consumption ratio of driving on a sloped road with respect to driving on flat roads. Examples of fuel-consumption ratios can be found in Table A.13 in the Appendix.[6]

Equation (1.3) quantifies the impact of vehicle speeds and road slopes on trucks' fuel consumption, taken from the transportation literature MOPU (1990).

For uphill and flat roads($p \geq 0$):

$$c = 388.18 - 7.32 * Vcp + 0.0700 * Vcp^2 + 101.28 * p + 0.019 * Vcp * p + 7.85 * 10^{-3} * Vcp^2 * p$$

For downhill roads($p < 0$):

$$c = 213.31 - 6.15 * Vcp + 0.0742 * Vcp^2 + 6.08 * p + 0.0382 * Vcp * p + 7.27 * 10^{-4} * Vcp^2 * p \tag{1.3}$$

where p denotes the slope of roads in percentage. A positive value of p denotes uphill roads, whereas a negative value of p signifies downhill roads. c represents fuel consumption per kilometer measured

[4] To test whether 20 miles is an appropriate interval length, I conduct a robustness check in which the interval is shrunk to 10 miles. This almost doubles N_{ij}. In brief, the choice of interval length does not impact the measure's significance or effect. More details can be found in the Appendix.

[5] The average grade in data is zero. The maximum grade is 0.086, and the minimum grade is -0.087.

[6] For instance, $w_{grade} = 3$ implies that driving uphill on the road consumes three times more fuel than driving on a flat road. A value of 0.2 indicates that driving downhill on the road saves 80 percent of the fuel compared to driving on a flat road. w_{grade} can be negative, if w_{grade} = -0.2 for a specific grade, it suggests that driving on the road with this specific grade helps the vehicle regain 20 percent of the energy consumed on a flat road.

in cubic centimeters(milliliters), and Vcp indicates speed in kilometers per hour. In the baseline analysis of this paper, the speed is assumed to remain constant at 50 km/h.

Equation (1.3) was derived from investigating the fuel consumption patterns of four representative types of trucks in Spain. These truck models included the Pegaso 1216, 1217, and 1234 and Renault D-210. These selections were drawn from transportation authorizations in 1983 (*las autorizcciones de transporte de 1983*). They had an average maximum weight capacity (*carga maxima autorizada*) of 12.4 tons and an average manufacturer price (*precio franco fabrica*) of 6,800,000.00 Spanish Pesetas in December 1987. Price was taken from *GANVAM*. Half-loaded trucks were used in the study. The paper argued that if the percentage of fully loaded, half-loaded, and empty vehicles was available, the specific fuel consumption could be calculated in each case. However, the paper asserted that equation (1.3), based on half-loaded trucks, was a sufficient approximation.

MOPU (1990) did not specify an average speed in their experimental setup. Instead, speed was another variable in their study, varying from 30km/h to 110km/h. A more recent paper, Posada-Henao et al. (2022), conducts experiments with carefully chosen representative trucks[7] in Colombia. The evaluation of trucks' fuel consumption focused solely on uphill roads, with downhill roads being overlooked. In Posada-Henao et al. (2022), speed varied from 25 km/h to 70 km/h. For analytical purposes, a constant speed assumption of 50 km/h is adopted in this paper, roughly corresponding to the median of the speed range observed in Posada-Henao et al. (2022). A robustness check presented in the Appendix explores the impact of increased speed, set at 90 km/h. Results of the robustness check align with baseline findings, suggesting that the selection of speed insignificantly influences the trade effect of bilateral elevation.

Based on the available literature, it appears that MOPU (1990) remains the sole paper allowing for the calculation of trucks' fuel consumption on both uphill and downhill roads at the time of composing this paper. Notably, Posada-Henao et al. (2022) exclusively focuses on uphill roads, omitting analysis of downhill roads. Other studies, such as Hooker (1988), Boriboonsomsin

[7] The trucks used in Posada-Henao et al. (2022) are rigid-type trucks with three axles, and articulated trucks with six axles (C3 and C3S3 as the official classification in Colombia, respectively), with engine powers of 350 HP (10,800 cc) and 400 HP (15,000 cc).

and Barth (2009), and Faria et al. (2019), endeavor to measure fuel consumption on both uphill and downhill roads, albeit for passenger cars. In the Appendix, it is demonstrated that if w_{grade} is computed utilizing the statistics from uphill roads in Posada-Henao et al. (2022) or from studies involving passenger cars like Faria et al. (2019), the obtained results remain consistent with those derived from the baseline regression. A comparison of fuel-consumption ratios from different literature can be found in Table A.13 of the Appendix.

The calculation and application of the weighting metric to bilateral elevation yield several notable effects. An increase in elevation is scaled by a weight greater than one, signifying the added difficulty of ascending. Conversely, a decrease in elevation is scaled by a weight smaller than one, indicating that descending is less challenging. EBE allows rapid changes in elevation to have a more pronounced impact than gradual changes. Moreover, the weighting metric makes EBE an asymmetric measure, and the asymmetry indicates the relative altitude between the origin and destination. For instance, if location i has a higher altitude than location j, then traveling from j to i (ascending uphill) results in a larger EBE than the reverse direction, meaning $EBE_{ij} < EBE_{ji}$. Note that EBE is the preferred measure of bilateral elevation in this paper.[8] Examples of EBE are provided below. The density and cumulative distribution of EBE can be found in Figure A.1 in the Appendix.

Although this paper focuses on international bilateral elevation, it is simple to create regional (intra-national) bilateral elevation using its methodologies. Regional PBE and EBE can be computed by replacing origins and destinations with regional population or economic centers, such as state capitals or county seats.

1.2.2 Examples

Let's consider two country pairs: Iran-Turkey and Iran-Uzbekistan. The routes for these pairs originate in Tehran, Iran's capital, and terminate in the capital cities of Ankara, Turkey, and

[8] PBE is introduced and defined separately for several reasons. Firstly, PBE provides a characterization of the terrain along routes independently of vehicle attributes, meaning it only changes when routes change. In areas where new road construction is infrequent, PBE can remain constant for extended periods. Secondly, defining PBE separately offers flexibility for future researchers to depart from PBE and create alternative EBE versions.

Tashkent, Uzbekistan. In Figure 1.1, the stars on the map indicate the locations of these capital cities. The dashed lines on the map represent the shortest and most realistic driving routes, as calculated by ArcGIS's *Network Analyst* tool, using a road network database. Along the dashed lines, each point signifies a sampled location, spaced 20 miles apart, except for the final two points at the destinations. The distances for both routes are approximately 2150 kilometers. However, there is a difference in the terrain characteristics along these routes; the Iran-Turkey route traverses regions with varying elevations, while the Iran-Uzbekistan route primarily crosses flat areas with minimal elevation changes. Rows 1-2 of Table 1.1 provide a summary of statistics for the routes in Figure 1.1. "G-C Distance" stands for the great-circle distance, which represents the shortest distance between two points and is obtained from CEPII. "Points Along Route" indicates the number of sampled points taken along the route, spaced 20 miles apart in the baseline model, except for the last two points at the destination. The EBE for the trade route between Iran and Uzbekistan

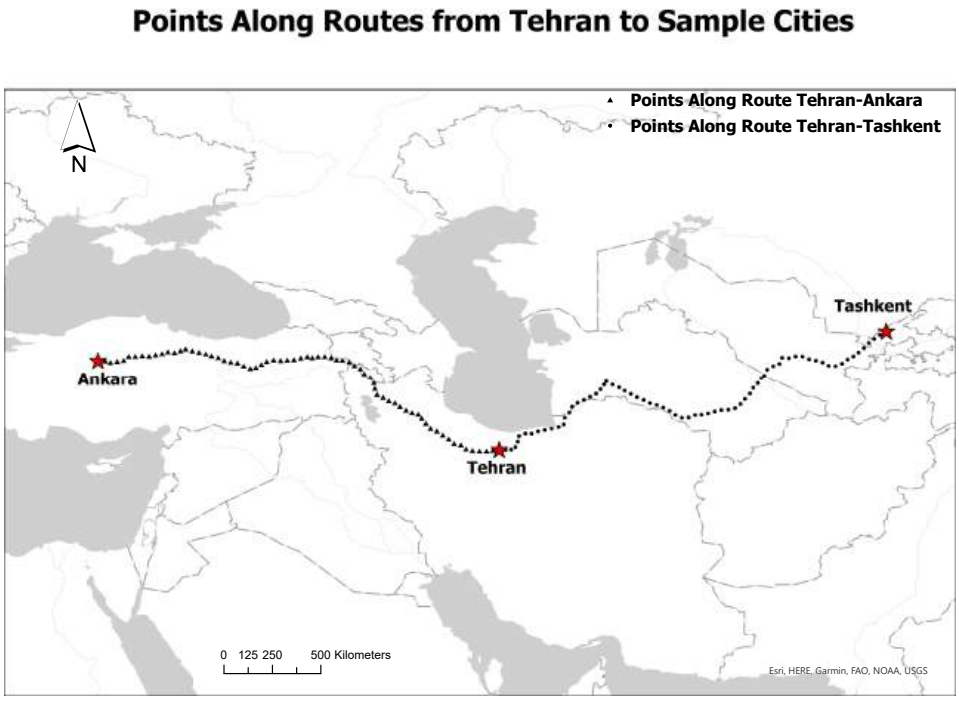

Figure 1.1: Illustration of Two Country Pairs and Sample Points Along Routes

measures 2.43, whereas it is notably higher at 4.90 for the Iran-Turkey route. This translates to a

101.6 percent increase in EBE for the Iran-Turkey route compared to the Iran-Uzbekistan route. As indicated by the findings presented in the results section, when other factors are held constant, this 101.6 percent elevation difference contributes to a 3.2 percent decrease in the value of bilateral trade between Iran and Turkey.[9]

Row	Country Pair	G-C Distance	Route Distance	Points Along Route	EBE
1	**Iran-Turkey**	1697km	2100km	69	4.90
2	**Iran-Uzbekistan**	1671km	2200km	71	2.43
3	**Uzbekistan-Iran**	1671km	2200km	71	3.86
4	**France-Spain**	1055km	1204km	40	1.94
5	**France-Czech Republic**	885km	1120km	42	2.25
6	**France-Italy**	1110km	1428km	49	3.50
7	**France-Andorra**	712km	832km	27	6.89

Table 1.1: Statistics of Country Pairs in Figures 1.1 and 1.2

Note: EBE stands for effective bilateral elevation. "G-C Distance" stands for the great-circle distance, the shortest distance between two points on the sphere of the earth. "Route Distance" is the shortest distance on the road network. "Points Along Route" is the number of sampled points taken along the route. Points are 20 miles apart in the baseline model (except for the last two points before and at the destination).

Rows 2 and 3 in Table 1.1 illustrate asymmetric bilateral elevation. For the trade route from Uzbekistan to Iran, EBE is 58.8 percent higher compared to the reverse route. With other factors held constant, this elevation disparity results in a 2.1 percent reduction in trade value.[10] It's worth noting that this asymmetry also signifies that Tehran, the capital of Iran, is situated at a higher elevation level than Tashkent, the capital of Uzbekistan.

Figure 1.2 presents four example routes in Europe: France-Spain, France-Czech Republic, France-Italy, and France-Andorra. Their statistics can be found in rows 4 to 7 of Table 1.1. Using France-Spain route (Paris-Madrid) as the reference, France-Czech Republic (or Paris-Prague) has elevations that are 16 percent higher, France-Italy (or Paris-Rome) features elevations that are 80 percent higher, and France-Andorra (or Paris-Andorra La Vella) experiences a remarkable 254 percent elevation increase in relation to the reference route. My calculations show that the

[9] $((1+1.016)^{-0.046}-1)*100\% = -3.2\%$
[10] $((1+0.588)^{-0.046}-1)*100\% = -2.1\%$

differences in bilateral elevations are responsible for a decrease in trade by 0.68[11] percent for France-Czech Republic, 2.67[12] percent for France-Italy and 5.65[13] percent for France-Andorra.

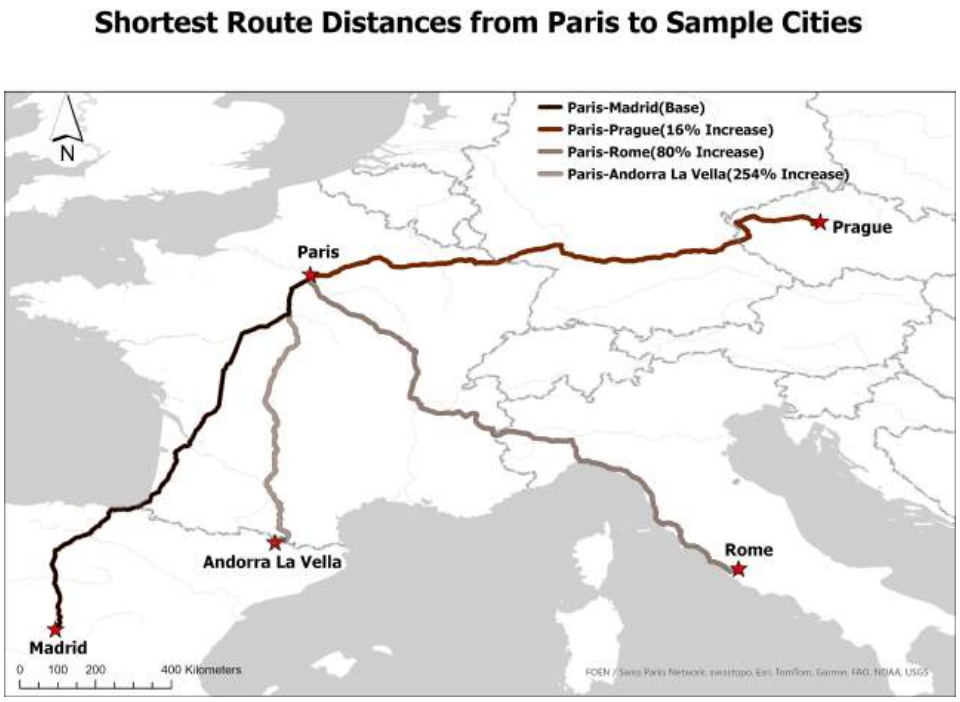

Figure 1.2: Example of Changes in Effective Bilateral Elevations

Notes: In the legend, the percentage changes in effective bilateral elevation compared to the base route are in parentheses. For example, the effective bilateral elevation along the Paris-Prague is 16 percent larger than the effective bilateral elevation along Paris-Madrid, which is the base route.

Table 1.2 summarizes some of the smallest and largest EBEs. Notably, country pairs with small EBEs often feature capital cities situated on the coast, affording them easy access to maritime transportation. While it's important to acknowledge that the ocean's elevation level is not precisely zero, this paper makes a simplification assumption that routes over oceans entail zero elevation changes.[14]

[11] $((1+0.16)^{-0.046}-1)*100\% = -0.68\%$
[12] $((1+0.80)^{-0.046}-1)*100\% = -2.67\%$
[13] $((1+2.54)^{-0.046}-1)*100\% = -5.65\%$
[14] The variations in ocean elevation are characterized by Mean Dynamic Topography (MDT), which represents the average over 12 years of the difference between the time-averaged sea surface and the geoid. The geoid is the

Some of the Lowest	EBE	Some of the Largest	EBE
Singapore-Vietnam	0.01	**Lebanon-Syria**	43.58
UAE-Kuwait	0.02	**Israel-Jordan**	32.11
Denmark-Finland	0.02	**Tajikistan-Uzbekistan**	31.52
Greece-Lebanon	0.04	**Nepal-Bhutan**	20.88
UK-Norway	0.05	**Georgia-Armenia**	18.94

Table 1.2: Country Pairs with Extreme Bilateral Elevations

Note: EBE stands for effective bilateral elevation. This table shows some examples of extreme EBE. Some country pairs like Singapore-Vietnam and Syria-Lebanon are omitted to avoid information redundancy.

1.3 Bilateral Elevation and Gravity

1.3.1 OLS and PPML

The impact of effective bilateral elevation (EBE) on trade is estimated. I employ a standard gravity specification as follows and estimate it using Ordinary least square (OLS) and Poisson Pseudo Maximum Likelihood (PPML):

$$X_{ijt}^k = e^{\beta_0 + log(D_{ij}) + \beta log(C_{ijt}^k) + \phi_{it}^k + \phi_{jt}^k} \epsilon_{ijt}^k \tag{1.4}$$

$$D_{ij} = Dist_{ij}^{\alpha_1} \; Elev_{ij}^{\alpha_2} \tag{1.5}$$

X_{ijt}^k is the trade value from country i to country j in year t for industry k. Trade data come from the UN Statistical Division Commodity Trade (*UN Comtrade*) database made available by the World Integrated Trade Solution (WITS). D_{ij} is a collection of bilateral resistance terms between country i and j that consists of two factors: distance, $Dist_{ij}$, and effective bilateral elevation, $Elev_{ij}$. ϕ_{it}^k and ϕ_{jt}^k are industry-origin-year and industry-destination-year fixed effects. ϵ_{ijt}^k is the

equipotential surface of the Earth's gravity field that best fits the average sea surface. Mulet et al. (2021) show that the range of Mean Dynamic Topography (MDT) extends from -1.6 meters to 1.6 meters. In simpler terms, this suggests that, on average, the highest point on the ocean's surface is approximately 3.2 meters higher than the lowest point. Although MDT changes throughout time, compared with the elevation difference on land, the elevation changes at different locations on the ocean are almost negligible.

error term. C_{ijt}^{k} is a vector of controls including the dummy indicating that railway connections are available, the log of maritime distance from the CERDI-SeaDistance database (see Bertoli et al. (2016)), and other bilateral terms from CEPII, including being in the European Union, common language, contiguity, common ethnicity, common religion, sibling relation, and colonial relation. The variable $tariff_{ijt}^{k}$ is also included in the controls, representing the tariff rate that importing country j imposes on exporting country i in year t for industry k. Tariff data are sourced from the World Integrated Trade Solution (WITS). These data have been aggregated using the International Standard Industrial Classification (ISIC) of All Economic Activities codes to the two-digit industry level, and then grouped similarly to the categorization in the World Input-Output Database. In total, there are sixteen groups of industries.[15]

VARIABLES	**mean**	**sd**	**min**	**max**
Year			2014	2019
Effective Bilateral Elevation	2.51	2.07	0.01	43.58
Bilateral Elevation IV	4.00	3.32	0.00	52.14
Trade Value ($million)	184.17	1,275.68	0.00	121,683.04
Straight Distance (kilometer)	3,530.90	2,716.64	59.62	11,896.52
Route Distance (kilometer)	4,425.69	3,364.40	74.37	13,896.30
Origin is Landlocked	0.23	0.42	0.00	1.00
Observation				945,920

Table 1.3: Summary Statistics

Note: This table summarizes the sample in the baseline model. The effective bilateral elevation in the baseline model uses fuel-consumption formulas in MOPU (1990) for trucks, takes points along routes, and uses the 20-mile interval between sampled points, assuming the speed is 50km/h. "Route Distance" is the distance of the shortest route between the origin and destination. "Straight Distance" is the great circle distance from CEPII. The sample includes 75 countries on (or connected to) the Eurasian landmass. Island countries not connected to the continents are omitted. Island countries in Europe and Asia are included in the sample for robustness checks.

Table 1.3 summarizes the statistics.[16] The baseline EBE employs fuel-consumption formulas

[15] The industry groups include chemical, higher-tech equipment, leather and shoe, machinery, metal and steel, textile and apparel, fishing and agriculture, transportation, glass ceramic and concrete (non-metallic), rubber, paper and publishing, food and tobacco, fuel, wooden products, mining quarrying, oil, and other.

[16] In discussions with colleagues, I've realized a discrepancy in the treatment of bilateral elevation compared to distance. While colleagues might wish to treat EBE similarly to distance, a challenge arises because the minimum value of EBE is close to 0, resulting in $log(EBE)$ being less than 0 for many country pairs in the sample. In contrast, $log(distance)$ is always larger than 0.

Although unnecessary for the purposes of this paper, if one insists, it's possible to scale up the unit of EBE by a factor of, for example, one thousand. This adjustment would result in EBEs being expressed in (weighted) meters per 1000 kilometers, ensuring that all EBE values are larger than 1, and consequently, $log(EBE)$ would be greater

sourced from MOPU (1990) for trucks. It selects points along routes, adopts a 20-mile interval between sampled points, and assumes a 50km/h speed. For this paper, aimed at creating a bilateral measure that effectively captures the costs associated with traversing uphill and downhill terrain, the baseline EBE performs adequately well.

As robustness checks, I constructed additional versions of EBE measures, allowing shorter intervals, different speeds, and alternative fuel consumption formulas from other literature sources. I thoroughly examine their impacts in the Appendix. The coefficients on alternative EBE measures closely align with those obtained in the baseline regression.

The sample in the baseline regression includes 75 countries on (or connected to) the Eurasian landmass. A list of countries for empirical analysis can be found in Table A.8 in the Appendix.[17] Island countries in Europe and Asia are omitted in the baseline regressions but added back to the sample in one robustness check. The route distance is the distance of the shortest route between the origin and destination capitals. The shortest routes come from the path-finding process in ArcGIS. The straight distance comes from CEPII and is also known as the great circle distance or the air distance. Tariffs are ad valorem, expressed in fractions, and come from the UN Conference on Trade and Development (UNCTAD) Trade Analysis Information System (TRAINS). I added one to all tariffs and took the log.

1.3.2 Instrumental Variable

A concern regarding endogeneity has been raised, stemming from the mutual influence between trade activity and modifications to the surrounding terrain, particularly along roadways. As trade volumes increase, enhancements to transportation infrastructure often follow, resulting in improved terrain conditions that, in turn, facilitate further trade expansion. To address this issue, I propose an instrumental variable for effective bilateral elevation. The aim is to establish a

than 0. Importantly, scaling up the unit of EBE should not affect the ability to capture bilateral elevation or the regression results. This approach may align EBE more closely with the treatment of distance if necessary in future research.

[17] The United Kingdom and Singapore are technically island countries. Still, they are included in the baseline regression since they are connected to the Eurasian landmass by bridges and tunnels.

measure relevant to bilateral elevation without directly relying on elevation values on trade routes.

Suppose a driver departs from the origin i and drives a truck along the route to the destination j. For each country pair ij, two lines parallel to and 700 meters away from the actual route are created, which depart from points near i and keep track of the actual routes all the way to points near j. One of these lines, denoted as $line_{ij}^{left}$, lies to the left-hand side of the driver, while the other line, $line_{ij}^{right}$, is positioned to the right-hand side. To generate $line_{ij}^{left}$ in ArcGIS, I take an intermediate step and generate a left buffer around route ij. This left buffer forms a polygon with one side coinciding with the route ij. It has another side parallel to the route, situated exactly 700 meters away, and it is the desired "left line." The rest of the buffer is deleted. Similarly, $line_{ij}^{right}$ is generated starting with a right buffer polygon and keeping its proper side. Using buffer zones to proxy artificially modified terrain has been practiced in Ducruet et al. (2020), who measure port suitability using underwater elevation in a buffer ring 3-5 km around the port.

Second, for each country pair ij, I calculate an EBE, $Elev_{ij}^{left}$, along $line_{ij}^{left}$; and another EBE, $Elev_{ij}^{right}$, along $line_{ij}^{right}$, using the same methodology in Section 1.2. They represent weighted changes in elevation near the routes ij but not directly on the routes.

Lastly, the instrumental variable is the average between the two EBEs in the preceding step.

$$IV_{ij} = \frac{Elev_{ij}^{left} + Elev_{ij}^{right}}{2}$$

The 700-meter distance between the route and its parallel lines is carefully selected to balance two important considerations. First, the parallel lines must be sufficiently far from the route to avoid potentially modified terrain on the roads. Second, they need to be close enough to the routes to remain relevant.

This distance is chosen based on the granularity of the elevation data used in this paper, which is at the 15-arc-second level. This level divides the Earth's surface into roughly 450-by-450-meter grids, with the average elevation recorded for each grid. By positioning the parallel lines 700 meters away from the actual route, the elevation grids the lines pass through must differ from

those traversed by the actual routes. Consequently, the instrumental variable (IV) should capture natural elevation changes near the roads rather than any modified elevation due to road flattening. If elevation data at a different level were employed, the distance between the route and its parallel lines may need adjustment accordingly.

The exclusion restriction assumption requires that the IV affects trade flow only because it predicts EBE. The author believes the exclusion restriction is satisfied. A potential challenger to the exclusion restriction might question whether elevation near roads could influence productivity and then trade flow. It's important to note that bilateral elevation, distinct from elevation levels, captures the change in elevation between countries. The elevation level at a specific point where production occurs would have minimal impact on bilateral elevation because individual elevation levels are not directly included in the calculation of bilateral elevation. Instead, what matters is the change in elevation from one point to the next along the route. Additionally, any variation in elevation at specific points is averaged out by other sampled points along the routes. The averaging mechanism ensures that the elevation level at any specific point minimally influences bilateral elevation.

Lastly, the relevance restriction requires the IV to correlate with EBEs. The evidence from the first-stage regressions in Table A.11 in the Appendix suggests that the relevance restriction is satisfied.

1.4 Results

Table 1.4 shows the baseline results from OLS, PPML and IV estimations of equation (1.4). All columns control for set C and the fixed effects. Column (1) shows the results from PPML regression that includes only the log of route distance as the key independent variable. Column (2) adds the log of effective bilateral elevation (20-mile version), whose coefficient is -0.046, suggesting that a one-percent increase in EBE decreases trade value by 0.046 percent. This number looks small. However, compared to a country pair that mainly conducts maritime trade, a country pair that mainly trades overland can easily have a bilateral elevation that is 200 percent higher.

Column(4) shows the IV regression result in which $log(BilateralElevation)$ is instrumented by $log(IV)$. The IV regression confirms the causal relationship between EBE and bilateral trade value. The Kleibergen-Paap(KP) F-statistic is substantial, indicating no evidence of a weak instrument. Column (3) shows the OLS counterpart of Column (4). First-stage regression results for the IV can be found in Table A.11.

Columns (5)-(8) control for the great-circle distance from CEPII rather than the shortest route distance. They show evidence that the EBE measure works well with CEPII's distance measure. In Column (6), the coefficient of the log of bilateral elevation is -0.064, suggesting that a one-percent increase in bilateral elevation decreases trade value by 0.064 percent. Column (8) results from the IV regression with a substantial F-statistic, showing no evidence of a weak instrument. Column (7) is the OLS counterpart of Column (8).

	(1)	**(2)**	**(3)**	**(4)**	**(5)**	**(6)**	**(7)**	**(8)**
VARIABLES	X_{ijt}^k	X_{ijt}^k	**log**(X_{ijt}^k)	**log**(X_{ijt}^k)	X_{ijt}^k	X_{ijt}^k	**log**(X_{ijt}^k)	**log**(X_{ijt}^k)
log(Route Distance)	-0.619***	-0.594***	-0.987***	-0.983***				
	(0.031)	(0.030)	(0.027)	(0.027)				
log(Bilateral Elevation)		-0.046*	-0.039***	-0.057***		-0.064**	-0.075***	-0.091***
		(0.025)	(0.010)	(0.011)		(0.025)	(0.010)	(0.011)
log(Straight Distance)					-0.614***	-0.586***	-1.000***	-0.999***
					(0.030)	(0.029)	(0.024)	(0.024)
Model	PPML	PPML	OLS	IV	PPML	PPML	OLS	IV
Kleibergen-Paap F-Statistic				45441				45771

Standard errors in parentheses
**** p<0.01, ** p<0.05, * p<0.1*

Table 1.4: Regression Results

Notes: This table shows the baseline regression result from equation (1.4). Columns (1) and (5) use PPML and include only distance (route distance in (1) and great-circle distance in (4)). Columns (2) and (6) have both distance and EBE. Columns (4) and (8) show the results from IV regressions. Columns (3) and (7) are OLS counterparts of (2) and (6), respectively. All columns include the set of controls, including tariffs and sea distance. The independent variable of interest is the bilateral elevation measure. "Route Distance" is the distance of the shortest route. "Straight Distance" is the straight line distance or great-circle distance from CEPII. The dependent variable is bilateral trade value which is aggregated to two-digit ISIC industry levels. Standard errors are clustered at the country-pair-industry level in all regressions in this paper. Destination-industry-year and origin-industry-year fixed effects are included. The sample includes 75 countries on the Eurasian landmass. The sample year spans the period from 2014 to 2019. The number of observations is 869,709.

1.5 Quantifying Trade Effects of Effective Bilateral Elevation

This section specifies a multi-sector Armington model to quantify the trade effects of effective bilateral elevation. A step-by-step derivation of the model can be found in the Appendix. In the model, there are S countries. There is a representative consumer in each country $i \in S$. There are K sectors and L_i amount of identical labor in each country. Workers are immobile across countries but mobile across sectors that inelastically supply labor. Each sector $k \in K$ in country i is represented by a single firm with exogenous productivity A_i^k. Without loss of generality, let sector superscript k also denote the representative firms. The quantity produced by each firm k while employing L_i^k labor is

$$q_i^k = A_i^k L_i^k \tag{1.6}$$

There are iceberg trade costs τ_{ij}^k such that for each unit of good in sector k to arrive at destination country $j \in S$, τ_{ij}^k unit must be shipped from firm k in origin country i. τ_{ij}^k depends on sector k, indicating that different sectors face different levels of trade cost. Thus, the price in destination j of consuming one unit of good from origin i, sector k is

$$p_{ij}^k = \tau_{ij}^k \frac{c_i^k}{A_i^k} \tag{1.7}$$

where c_i^k is the cost of production and A_i^k is the productivity.

Additionally, τ_{ij} comprises distance and bilateral elevation. It is assumed that distance is symmetric. However, bilateral elevation is not assumed to be symmetric, allowing for variations between the two directions.

$$\tau_{ij} = f(Dist_{ij}, Elev_{ij}) \quad where \;\; Dist_{ij} = Dist_{ji}; \;\; Elev_{ij} \neq Elev_{ji} \tag{1.8}$$

In each country, there is a representative consumer who maximizes the following CES preferences:

$$U_j = \left(\sum_{i \in S} \sum_{k \in K} a_{ij}^{k\,\frac{1}{\sigma^k}} q_{ij}^{k\,\frac{(\sigma^k - 1)}{\sigma^k}}\right)^{\frac{\sigma^k}{\sigma^k - 1}} \tag{1.9}$$

subject to the budget constraints.

The model will be solved using hat-algebra. For any variable a, a' is the counterfactual value of a moving from policy τ to τ'. Define $\hat{a} = \frac{a'}{a}$ as the relative change in a after the policy.

To solve the model, the change in the production cost can be expressed as the following:

$$\hat{c}_i^k = \hat{w}_i{}^{\gamma_i^k} \prod_l \hat{P}_i^{l\,\eta_i^{lk}} \tag{1.10}$$

where γ_i^k is the share of value-added and η_i^{lk} is the share of goods in industry l produced in country i used as intermediate goods in sector k. Let P_j^k be the Dixit-Stiglitz price index. The hat-algebra of P_j^k can be expressed as the following

$$\hat{P}_j^k = \big(\sum_{i \in S} \lambda_{ij}^k (\hat{\tau}_i^k \hat{c}_i^k)^{1-\sigma}\big)^{\frac{1}{1-\sigma}} \tag{1.11}$$

where λ_{ij}^k is the trade share of country j with respect to country i in sector k, which is the proportion of goods in sector k shipped to country j from country i relative to the total amount of k shipped to country j. The hat-algebra of λ_{ij}^k is the following:

$$\hat{\lambda}_{ij}^k = \big(\frac{\hat{\tau_{ij}^k} \hat{c}_i^k}{\hat{P}_j^k}\big)^{1-\sigma} \tag{1.12}$$

Define the trade value of the sector from country i to country j by $X_{ij}^k \equiv q_{ij}^k p_{ij}^k$. Then, the trade deficit, D_i, can be solved using the trade balance equation.

$$D_i = \sum_k \sum_j \lambda_{ij}^k{}' Y_i^{k\prime} - \sum_k \sum_j \lambda_{ji}^k{}' Y_j^{k\prime} \tag{1.13}$$

The total expenditure on goods from sector k in country i is:

$$Y_i^{k\prime} = \sum_l \eta_i^{kl} \sum_j \lambda_{ji}^l{}' Y_j^{l\prime} + \mu_i^k I_i' \tag{1.14}$$

Let I_i represent the final absorption in country i.

$$I' = (w_i L_i)\hat{w}_i + D_i \tag{1.15}$$

The equilibrium is solved using equations (1.10), (1.11), (1.12), (1.13), (1.14) and (1.15). After the model is solved, the equilibrium change in welfare for each country is represented by the relative change in the real wage, $\frac{\hat{w}_i}{\hat{P}_i}$, where $\hat{P}_i$ is the change in the price index in country i.

$$\hat{P}_i = \prod_k \hat{P_i^k}^{\mu_i^k} \tag{1.16}$$

Parameters are calibrated using data from the 2014 World Input-Output Table with 32 countries and 47 sectors. Lists of countries and sectors in the counterfactual analysis can be found in Table A.9 and Table A.10. Specifically, the following parameters are calibrated: value-added share, γ_i^k; input-output share, η_i^{kl}; benchmark trade share, λ_{ij}^k; consumption share, μ_i^k; and deficit, D_i. $\sigma^k = 1 + \theta^k$, where θ^k is the trade elasticity, taken from Caliendo and Parro (2015).[18]

Trade cost is calibrated as follows:

$$\tau_{ij} = exp\left(\frac{\alpha_1 * log(Dist_{ij}) + \alpha_2^k * log(Elev_{ij})}{1 - \sigma^k}\right) \tag{1.17}$$

$$\hat{\tau}_{ij} = \frac{\tau_{ij}^{'}}{\tau_{ij}} \tag{1.18}$$

where $Dist_{ij}$ is the distance of the shortest trade routes. $Elev_{ij}$ is the effective bilateral elevation. Both $Dist_{ij}$ and $Elev_{ij}$ are generated in Section 1.2. $\alpha_1 = -0.594$, as obtained from the baseline PPML result in Table 1.4, serves as the estimated coefficient for route distance. It is assumed to remain constant across industries. α_2^k, the coefficients on the log of EBE, are assumed to vary across sectors k, introducing sector-specific heterogeneity to better suit the multi-sector model. α_2^k is estimated similarly to the approach outlined in Section 1.7.2.[19]

1.6 Counterfactual Experiment

1.6.1 Design of Counterfactual Analysis

In this section, I first examine what happens to the trade cost and real wages if bilateral elevation is overlooked. In this case, the counterfactual trade cost is calculated as follows.

$$\tau_{ij}^{'} = exp\left(\frac{\alpha_1 * log(Dist_{ij})}{1 - \sigma^k}\right) \tag{1.19}$$

[18] Caliendo and Parro (2015) estimated θ^K for agriculture, mining and manufacturing sectors. θ^k is assumed to be 10.4 for service sectors, the average for agriculture, mining, and manufacturing.

[19] To estimate industry-specific coefficients for bilateral elevation, I introduce interaction terms between EBE and industry dummies in an IV regression analysis using data from the 2014 World Input-Output Table. If a coefficient is positive (as discussed in Section 1.7.2 under problematic coefficients), I attempt to replace it with the corresponding coefficient from the full-gravity IV regression. If it remains positive, I replace it with the baseline coefficient, -0.046, as shown in Table 1.4. It's important to note that bilateral elevation is considered non-effective for service sectors. Nevertheless, the service sectors are included to enhance the reliability of the results.

Next, I study the impact of the regenerative braking system of electric vehicles (EVs) on bilateral elevations and real wages. The regenerative braking system (RBS) on EVs transfers the kinetic energy of the vehicle in motion into electricity to recharge the battery and, in the meantime, slows down the vehicle. Anecdotal evidence suggests that EVs reduce energy consumption while descending downhill and may even recharge the battery when encountering sufficiently steep roads. However, there is a lack of research on EV trucks' energy consumption ratios at different slopes of roads. In this paper, I modify the fuel consumption and the fuel consumption ratio, w_{grade}, to simulate the potential impact of Regenerative Braking Systems (RBS) based on speculative assumptions.

Equation (1.20) outlines a conservative scenario regarding the fuel consumption of EV trucks. $c^{'}$ represents the counterfactual fuel (electricity) consumption, and c denotes the benchmark fuel consumption derived from equation (1.3), and $c_{grade=0}$ denotes the benchmark fuel consumption when roads are perfectly flat. Under this framework, I assume that the fuel consumption for EVs remains consistent with the model presented in MOPU (1990) while ascending uphill. However, when traversing downhill terrain, the fuel consumption is reduced. Specifically, on mild downhill roads with slopes ranging from less than 0 to greater than -5 percent, Regenerative Braking Systems (RBS) are presumed to aid in decreasing energy consumption by 10 percent (multiplied by 0.9). If the downhill roads become steeper, with slopes less than -5 percent to greater than -6 percent, EV trucks cease to consume additional energy, maintaining a constant battery percentage. Further steepening of the road slopes, between less than -6 percent and greater than -7 percent, prompts the RBS to help recover 10 percent of the energy consumed when driving on flat roads. Notably, a negative fuel consumption indicates an energy recovery, resulting in reduced trade costs. For roads steeper than -7 percent, the RBS is assumed to assist in recovering 20 percent of the energy consumed when driving on flat roads.

Subsequently, the counterfactual fuel consumption values are utilized to compute counterfactual fuel consumption ratios, denoted as w_{grade}, as discussed in Section 1.2. Ultimately, these counterfactual fuel consumption ratios are employed to calculate counterfactual EBE tailored specif-

ically for EV trucks.

$$c^{'} = \begin{cases} c & \text{road slopes} \in [0\%, \text{inf}) \\ 0.9 * c & \text{road slopes} \in (-5\%, 0\%) \\ 0 & \text{road slopes} \in (-6\%, -5\%] \\ -\frac{c_{grade=0}}{10} & \text{road slopes} \in (-7\%, -6\%] \\ -\frac{c_{grade=0}}{5} & \text{road slopes} \in (-\text{inf}, -7\%,] \end{cases} \tag{1.20}$$

Equation (1.21) presents a moderate scenario regarding the fuel consumption of EV trucks. Here, I assume that on mild downhill roads with slopes ranging from less than 0 to greater than -5 percent, Regenerative Braking Systems (RBS) facilitate a more substantial reduction in energy consumption, amounting to 50 percent (multiplied by 0.5). Similar to the conservative scenario, EV trucks cease to consume additional energy if the downhill roads become sufficiently steep, with slopes ranging from less than -5 percent to greater than -6 percent. Furthermore, if the road slopes are less than -6 percent and greater than -7 percent, the RBS is postulated to assist in recovering 20 percent of the energy consumed when driving on flat roads. In scenarios where the roads are steeper than -7 percent, the RBS is presumed to aid in regaining 40 percent of the energy consumed when driving on flat roads. Examples and comparisons of fuel-consumption ratios for EV trucks can be found in Table A.13.

$$c^{'} = \begin{cases} c & \text{road slopes} \in [0\%, \text{inf}) \\ 0.5 * c & \text{road slopes} \in (-5\%, 0\%) \\ 0 & \text{road slopes} \in (-6\%, -5\%] \\ -\frac{c_{grade=0}}{5} & \text{road slopes} \in (-7\%, -6\%] \\ -\frac{c_{grade=0}}{2.5} & \text{road slopes} \in (-\text{inf}, -7\%,] \end{cases} \tag{1.21}$$

The impact of bilateral elevation varies across country pairs. To facilitate a clearer presentation of the results, I aggregate bilateral elevations to the country level by averaging them across each origin. Panel (a) of Figure 1.3 illustrates that the prevalence of electric vehicles (EVs) equipped

with conservatively speculated regenerative braking systems (RBS) is expected to reduce bilateral elevation by 1.8 to 3.2 percent compared to trucks equipped solely with internal combustion engines. Moreover, as RBS technology advances in efficiency, the reductions in bilateral elevation could reach up to 15 percent, as depicted in panel (b) of Figure 1.3. Panels (c) and (d) further illustrate that countries with a higher proportion of steep roads (steeper than 5 percent) tend to experience a more significant reduction in bilateral elevation with EV trucks. This phenomenon is driven by the assumption that EV trucks cease consuming additional energy if the road slope is less than -5 percent and regain energy if the downhill roads are steeper. While the "-5 percent" threshold remains speculative due to limited research, the analyses highlight a crucial insight: RBS technology presents greater welfare gains to countries with more rugged trade routes. The subsequent section delves into the counterfactual results of welfare gains. Additional details on how changes in EBE translate to changes in trade costs can be found in Figure A.3 in the Appendix.

1.6.2 Counterfactual Results

Figure 1.4 poses the question: "What happens to real wages if bilateral elevations are overlooked or treated as nonexistent?" To address this inquiry, I excluded bilateral elevations from the model. It's important to note that different origins possess varying levels of average EBE to the rest of the world. Removing bilateral elevations for all countries would particularly benefit origins endowed with larger average EBE to the rest of the world. Consequently, eliminating bilateral elevations would lead to a decrease in trade costs by an average of 0.4 percent. In other words, overlooking bilateral elevations would result in an underestimation of trade costs by 0.4 percent. Additionally, the removal of bilateral elevation would correspond to an increase in real wages by an average of 1 percent.

Figure 1.5 presents a scenario envisioning the widespread adoption of EV trucks equipped with conservatively speculated Regenerative Braking Systems (RBS). In this scenario, as vehicles descend on roads with a 6-8 percent slope, the RBS can recharge 10-20 percent of the electricity consumed when driving on flat roads. Although this recharging capacity is assumed to be relatively

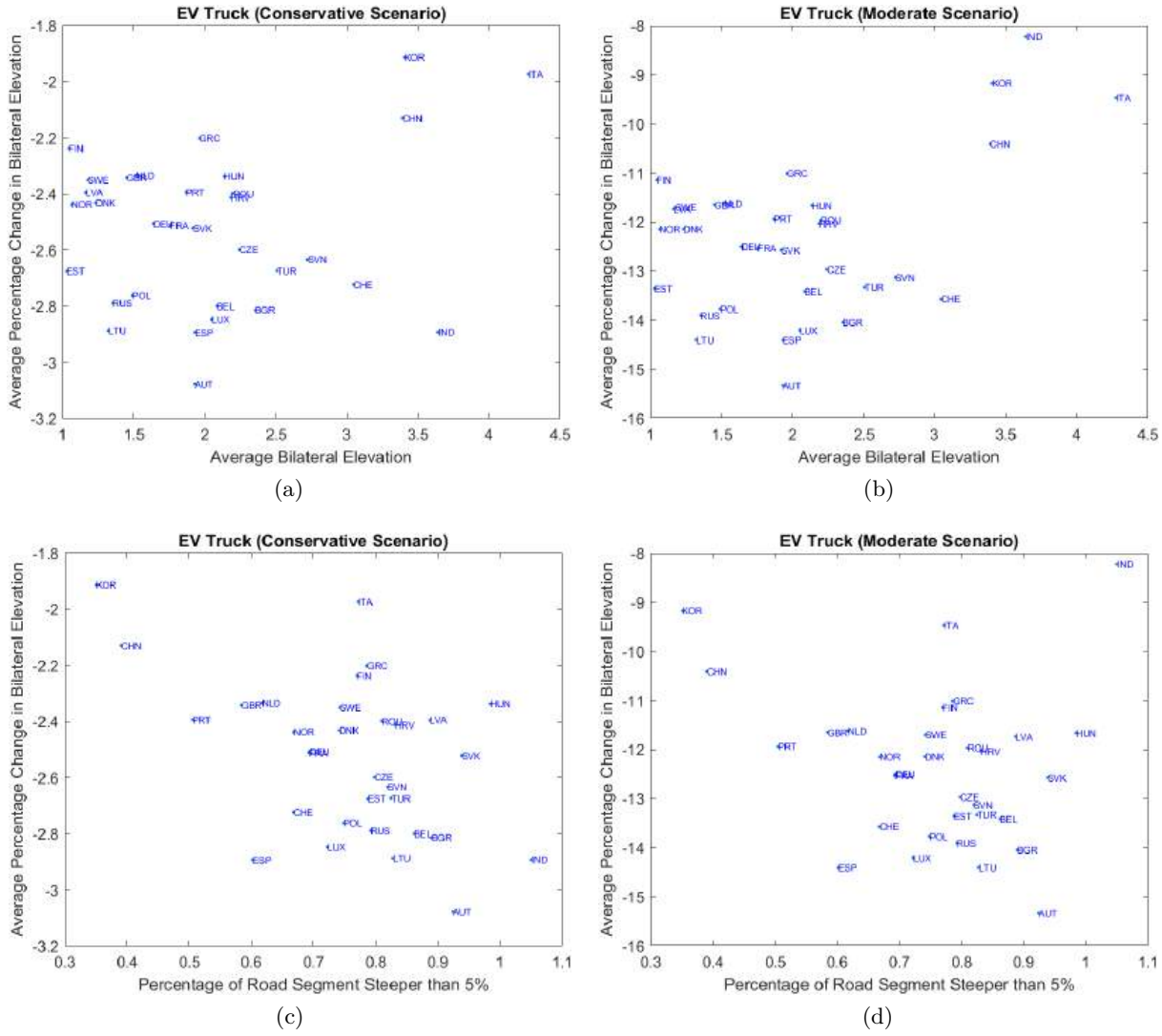

Figure 1.3: Average Percentage Change in EBE

Note: These figures depict each origin's average changes in EBE. Panels (a) and (b) illustrate that countries with higher average EBE experience greater reductions due to the adoption of EV trucks. Panels (c) and (d) reveal that countries with higher proportions of roads steeper than 5 percent observe larger decreases in bilateral elevations, as steeper roads enable RBS to recharge the battery more effectively. The conservative scenario uses the counterfactual fuel consumption in equation (1.20). The moderate scenario uses the counterfactual fuel consumption in equation (1.21).

modest, it yields significant outcomes. It results in an average reduction of 0.02 percent in trade costs and an average increase of 0.03 percent in real wages. The wage enhancements are particularly notable for regions with higher average EBE to the rest of the world. The effective recharging capability transforms mountainous areas into practical free charging stations, introducing a novel

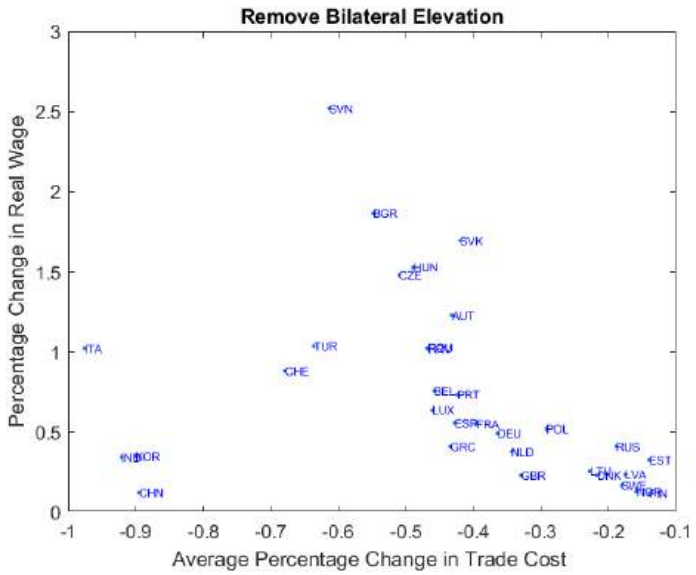

Figure 1.4: Counterfactual Results

Note: This figure shows the consequence if bilateral elevations are removed for all countries.

resource.

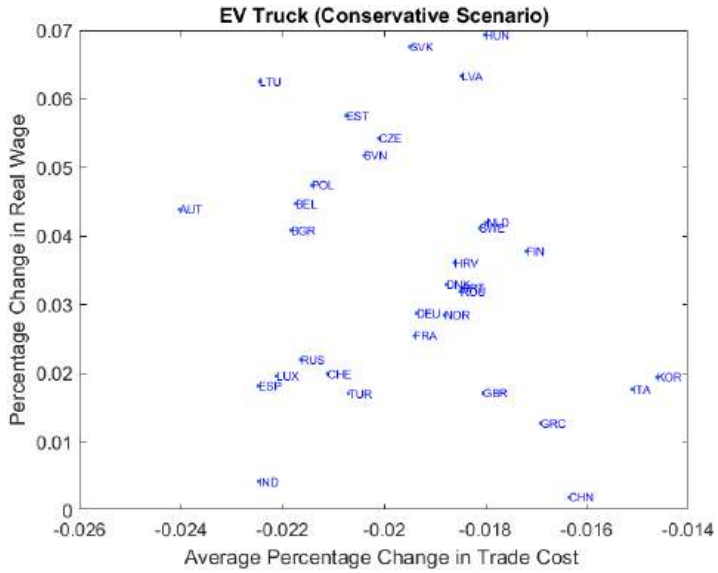

Figure 1.5: Counterfactual Results

Note: This figure illustrates a conservative estimate of wage gains resulting from the adoption of electric vehicle trucks. The scenario utilizes the counterfactual fuel consumption specified in equation (1.20).

Figure 1.6 illustrates the counterfactual outcomes if EV trucks with moderate Regenerative Braking Systems (RBS) become prevalent in transportation. When descending on a 6-8 percent

grade road, the efficient RBS could potentially recharge 20-40 percent of the electricity consumed from driving on flat roads. This would contribute to reducing trade costs by an average of 0.1 percent and increasing real wages by an average of 0.2 percent. Similar to the previous scenario, the benefits would be more pronounced for origins with higher average bilateral elevations to the rest of the world. To conclude, mountains that impeded trade in the past may be less of trade barriers; instead, charging stations where electric trucks can recharge. As electric trucks become more and more common and as RBS evolves, opportunities presented by downhill roads that allow for efficient battery recharging will be crucial.

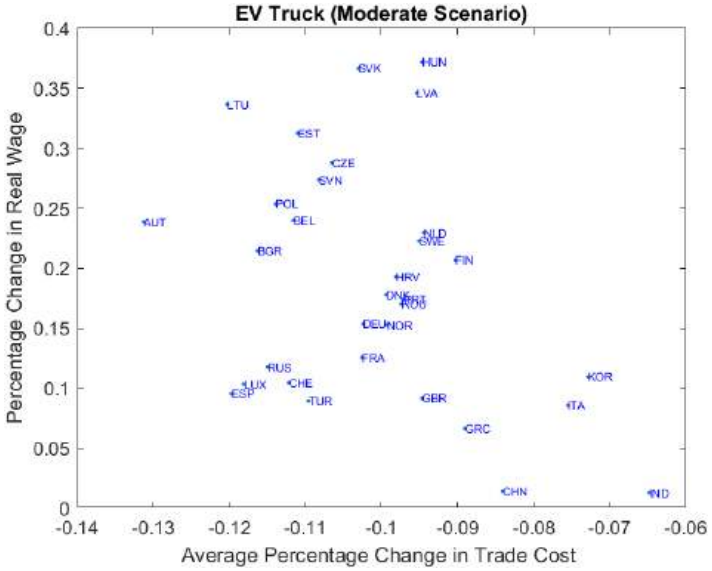

Figure 1.6: Counterfactual Results

Note: This figure illustrates a moderate estimate of wage gains resulting from the adoption of electric vehicle trucks. The scenario utilizes the counterfactual fuel consumption specified in equation (1.21).

1.7 Extensions and Robustness Checks

1.7.1 Extension: Landlocked Countries

Coastal countries have the advantage of utilizing maritime trade routes[20] to bypass mountainous regions, while landlocked countries do not have this option right away. Consequently, this

[20] Compared with the elevation difference between different areas on land, the elevation changes at different locations on the ocean are almost negligible.

section affirms that landlocked countries are more exposed to the effects of elevation changes as they face more significant obstacles on their trade routes.

Table 1.5 investigates the interaction between EBE and landlocked trading partners, revealing significant heterogeneous impacts of EBE across different regions worldwide, particularly emphasizing its importance for landlocked countries. The variable *Locked* is entered into the regression as a categorical variable, dividing the observed trade flow into three scenarios: Neither origin nor destination is landlocked; Either origin or destination is landlocked; Both origin and destination are landlocked. Columns (1)-(3) control for route distance, while columns (4)-(6) control for straight distance. Instrumental Variable (IV) results in column (3) indicate that if neither origin nor destination is landlocked, a one percent increase in EBE decreases trade value by 0.047 percent. This impact triples to 0.115 percent if the origin or destination is landlocked and increases over ninefold to 0.455 percent if both origin and destination are landlocked. These findings underscore the significance of bilateral elevation for landlocked country pairs. Comparing the coefficient on distance (-0.983) from the baseline IV result (column (4) of Table 1.4) with the coefficient on EBE (-0.455), it is evident that EBE constitutes a substantial component of trade costs for landlocked country pairs.

		(1)	**(2)**	**(3)**	**(4)**	**(5)**	**(6)**
CASE	**VARIABLES**	$\mathbf{log}(X_{ijt}^k)$	X_{ijt}^k	$\mathbf{log}(X_{ijt}^k)$	$\mathbf{log}(X_{ijt}^k)$	X_{ijt}^k	$\mathbf{log}(X_{ijt}^k)$
Neither O nor D is Landlocked	Locked*log($Elev_{ij}$)	-0.033***	-0.042	-0.047***	-0.063***	-0.059**	-0.075***
		(0.011)	(0.026)	(0.012)	(0.011)	(0.026)	(0.011)
Either O or D is Landlocked	Locked*log($Elev_{ij}$)	-0.084***	-0.243***	-0.115***	-0.134***	-0.256***	-0.166***
		(0.020)	(0.048)	(0.022)	(0.020)	(0.048)	(0.022)
Both O and D are Landlocked	Locked*log($Elev_{ij}$)	-0.398***	-0.375*	-0.455***	-0.398***	-0.309	-0.449***
		(0.054)	(0.192)	(0.057)	(0.053)	(0.188)	(0.056)
Model		OLS	PPML	IV	OLS	PPML	IV
Kleibergen-Paap F-Statistic				9186			9300

Standard errors in parentheses
**** p<0.01, ** p<0.05, * p<0.1*

Table 1.5: Impact of Effective Bilateral Elevation on the Landlocked Countries

Note: "O" stands for "origin," and "D" stands for "destination." "*Locked*" is entered into the regression as a categorical variable with three categories: neither origin nor destination is landlocked; either origin or destination is landlocked; and both origin and destination are landlocked. Columns (1)-(3) control for the route distance. Columns (4)-(6) control for the great-circle distance. Other controls, the sample, the period of study, and the clustered standard errors are identical to the baseline model.

Motivated by the insights from Table 1.5, I conduct new counterfactual analyses examining the impact of removing bilateral elevation and the adoption of EV trucks, allowing for heterogeneous coefficients for landlocked countries. The coefficients (-0.047, -0.155, and -0.455) in column (3) of Table 1.5 are utilized. Counterfactual results are depicted in Figures 1.7, 1.8, and 1.9. As the focus shifts to regional heterogeneity, both coefficients are assumed to be homogeneous across sectors.

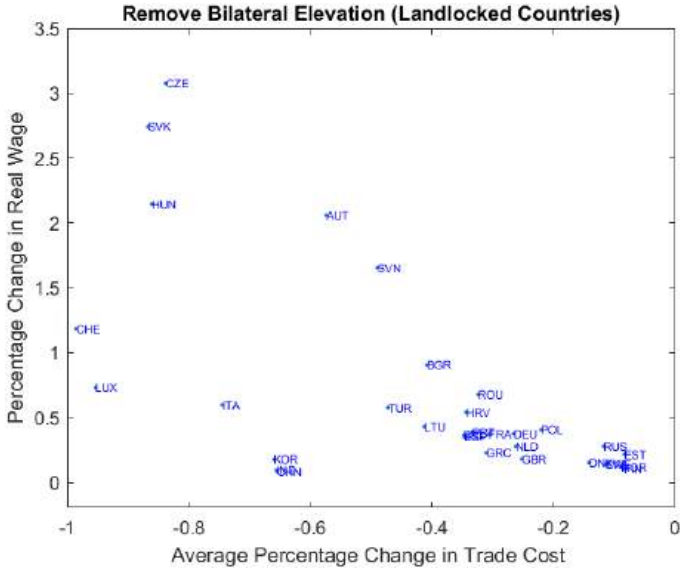

Figure 1.7: Counterfactual Results

Note: The figure shows the consequence if bilateral elevations were removed, assuming the impact of EBE is larger for landlocked countries. Coefficients on bilateral elevation from Column (3) of Table 1.5 are used.

Figure 1.7 illustrates the counterfactual change in real wages assuming heterogeneous coefficients on EBE for landlocked countries, showing distinct clusters of countries in the figure. Coastal countries are positioned near the y-axis ($y = 0$) due to minimal changes in trade costs. On average, coastal countries experience a slight reduction in trade costs (0.2 percent) and an increase in real wages of up to 1 percent. In contrast, landlocked countries are situated further from the y-axis, indicating a more significant reduction in trade costs (averaging around 0.8 percent) and an average rise in real wages of approximately 2 percent. The regional heterogeneity of EBE suggests its potential greater significance for intra-country trade, as regions within a country are more likely to be landlocked compared to the probability of entire countries being landlocked. However, exploring

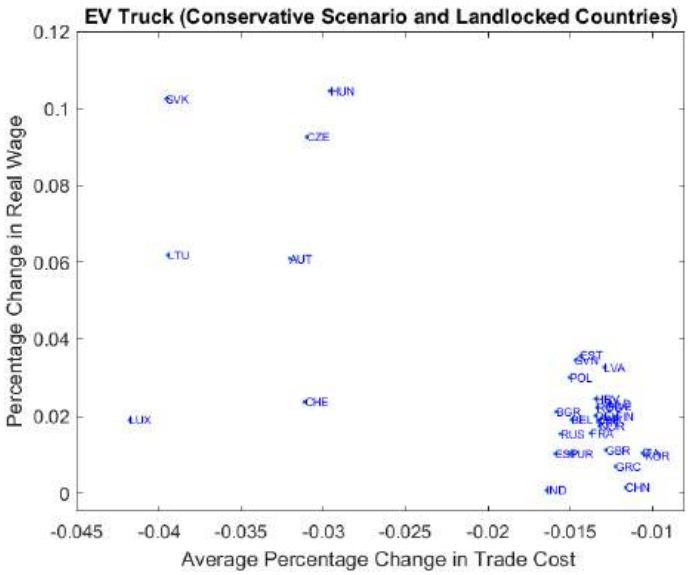

Figure 1.8: Counterfactual Results

Note: The figure shows the consequence if EV trucks with conservative RBS become a prevalent mode of transportation, assuming the impact of EBE is larger for landlocked countries. Coefficients on the bilateral elevation from Column (3) of Table 1.5 are used. The conservative scenario utilizes the counterfactual fuel consumption specified in equation (1.20).

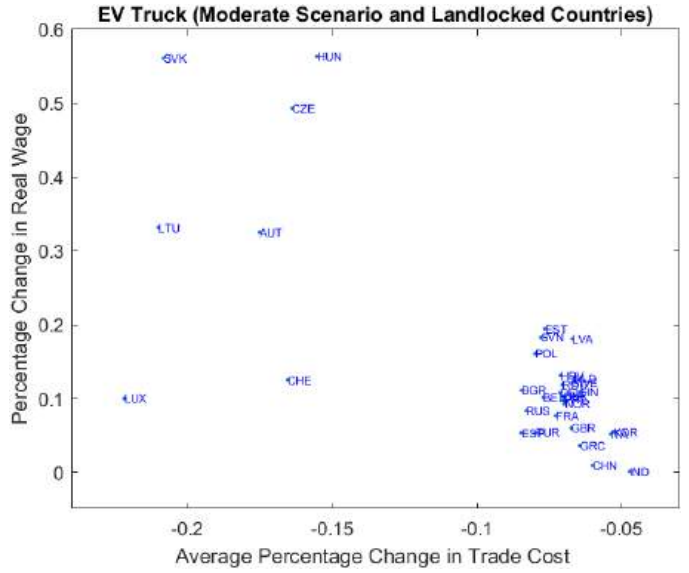

Figure 1.9: Counterfactual Results

Note: The figure shows the consequence if EV trucks with moderate RBS become a prevalent mode of transportation, assuming the impact of EBE is larger for landlocked countries. Coefficients on the bilateral elevation from Column (3) of Table 1.5 are used. The moderate scenario utilizes the counterfactual fuel consumption specified in equation (1.21).

the relationship between EBE and intra-country trade is beyond the scope of this paper.

Figure 1.8 presents the counterfactual results assuming widespread adoption of EV trucks with conservatively speculated Regenerative Braking Systems (RBS), revealing two distinct clusters. Coastal countries experience a minor reduction in trade costs (approximately -0.013 percent) and a slight increase in real wages (around 0.02 percent) on average. In contrast, landlocked countries witness a more noticeable reduction in trade costs (approximately -0.035 percent) and a more significant increase in real wages (around 0.06 percent) on average.

Figure 1.9 showcases the counterfactual results assuming widespread adoption of EV trucks with moderate RBS. Figure 1.9 magnifies Figure 1.8 because the magnitudes of changes are greater. Similar to Figure 1.9, two clusters are evident. Coastal countries experience a less substantial reduction in trade costs (approximately -0.07 percent) and a small increase in real wages (around 0.1 percent) on average. Conversely, landlocked countries witness a significant reduction in trade costs (approximately -0.018 percent) and a more pronounced increase in real wages (around 0.3 percent) on average. These counterfactual results suggest that EV trucks will have a more significant impact on landlocked countries.

1.7.2 Extension: Industry Heterogeneity

This section examines the heterogeneous impact of EBE across different industries. To achieve this, interaction terms between EBE and grouped industry dummies are included in the regression analysis. Panels (a) and (b) of Figure 1.10 depict the industry-specific effect of EBE, conditional on the distance of the shortest routes. Panel (a) employs Instrumental Variable (IV) estimation, instrumenting $Industry * log(BilateralElevation)$ by $Industry * log(IV)$, while Panel (b) utilizes Poisson Pseudo Maximum Likelihood (PPML) estimation. Both IV and PPML results reveal that bilateral elevation exerts varying effects on different industries. Detailed coefficients and standard errors are provided in Table . A similar set of regressions that control for great-circle distance instead of the route distance are examined for robustness checks, and the results are shown in Figure A.2.

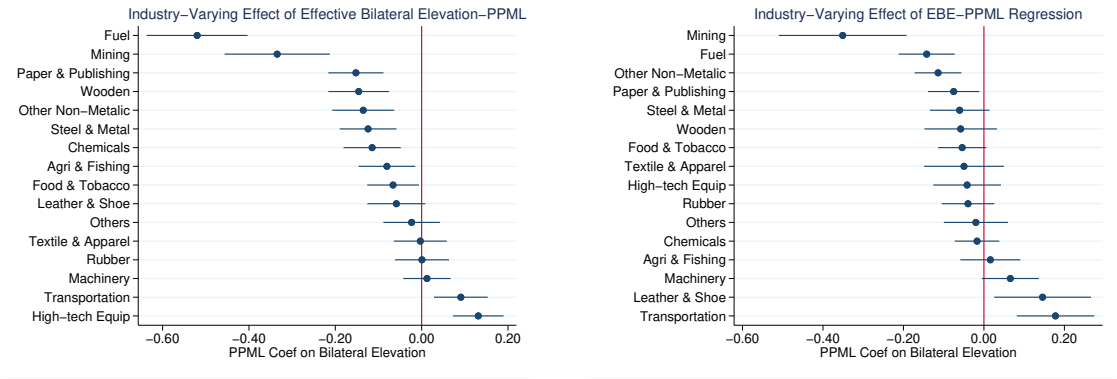

(a) IV (b) PPML

Figure 1.10: Industry-Varying Effect of Effective Bilateral Elevation

Note: Panels (a) and (b) control for the distance of the shortest route. Panel (a) uses IV. Panel (b) uses PPML. A similar set of regressions that control for great-circle distance is examined and included in Figure A.2. The coefficients and standard errors are in Table A.6 in the Appendix.

To explain the mechanism of industry heterogeneity, I calculate the heaviness index for each industry. The heaviness measure follows Coşar and Demir (2016) and is calculated as

$$heaviness_k = ln(\frac{wgt^k}{val^k}) \tag{1.22}$$

where wgt^k and val^k are the weight and value of total imports in each industry group k from the rest of the world to the UK in 2019.

Figure 1.11 depicts the industry-varying coefficients from Figure 1.10 plotted against the heaviness of each industry. It confirms a negative relationship between the coefficients on EBE and heaviness. Heavier products, such as fuel, mining products, glass, and concrete, are more significantly impacted by bilateral elevation. Conversely, lighter products, including leather products, transportation vehicles, and higher-tech machinery, are affected less by bilateral elevation. The majority of coefficients exhibit a negative trend, consistent with bilateral elevation imposing additional costs.

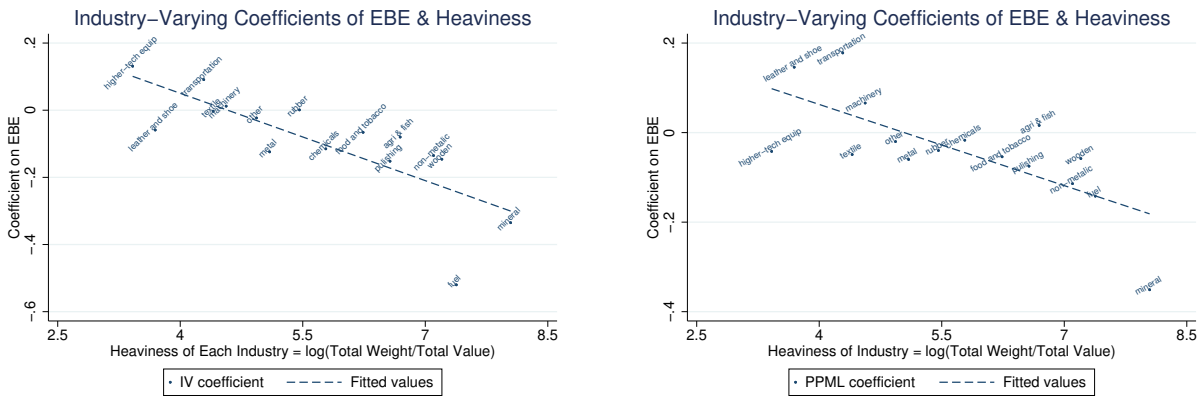

(a) IV

(b) PPML

Figure 1.11: Industry-varying Effect and Heaviness

Note: The figures plot industries' heaviness against their coefficients on EBE from IV (panel (a)) and PPML (panel (b)) regressions. The regressions control for route distance. They suggest that industries with cheaper but heavier products have more negative coefficients on EBE. The coefficients shown in these figures and their standard errors can be found in Table A.6.

Two industries stand out with positive and statistically significant IV coefficients in panel (a) of Figure 1.10: transportation vehicles and high-tech equipment industries.[21] These coefficients, which I refer to as problematic coefficients in this section, may arise due to the frequent utilization of air freight driven by large value-per-weight ratios. Notably, transportation and high-tech equipment industries exhibit among the lowest heaviness measures, indicating the lowest weight per value. Additionally, the high-tech equipment industry notably relies on air freight, ranking second among industries in terms of air freight usage in the US in 2019. Hence, it's plausible that these industries are minimally affected by bilateral elevation. Further robustness checks delve into the role of air freight in detail. Other possible explanations for the problematic coefficients are that the coefficients on distance and other controls do not vary across industries. Consequently, I conduct a full-gravity IV analysis, allowing every coefficient to vary across industries and instrumenting $Industry * log(BilateralElevation)$ by $Industry * log(IV)$. The full-gravity IV regression results

[21] Two additional grouped industries show positive coefficients in panel (a) of Figure 1.10, namely the rubber and machinery industries. However, both their magnitudes and significance levels are low.

are presented in Table A.7, where both problematic coefficients become statistically insignificant, while coefficients for other industries remain negative and significant.

1.7.3 Robustness Check: Air Freight

One way to avoid the mountains is to fly over them. One may worry about the endogeneity problem created by air freight because country pairs with significant EBE may be more likely to transport goods using airplanes. But, this may be one of the mechanisms by which EBE decreases trade. Firms aiming to minimize costs may resort to air transportation when it proves to be more economical in terms of both time and monetary expenses compared to trucks and trains. Air transportation tends to be more cost-effective than ground transportation when traversing routes with substantial changes in bilateral elevation. As a result, substantial levels of bilateral elevations can induce air freight usage, which drives up transportation costs and reduces trade.

To further investigate this issue, I collect data on US air freight usage for each industry from US Trade Online and calculate the portion of goods shipped by air freight in each industry using the following equation:

$$Portion = \frac{Import_{2019}^{Air,k}}{Import_{2019}^{k}} \tag{1.23}$$

where $Import_{2019}^{Air,k}$ is the total value imported in each industry k by the US via air in 2019. $Import_{2019}^{k}$ is the total value imported in each industry k by the US (via all modes of transportation) in 2019. The data and ranking are presented in Table 1.6. One may argue that US air freight does not represent the rest of the world. While I do not disagree with this statement, I argue that the ranking of the portion of goods imported by air in the US, as presented in Table 1.6, is still representative. For example, suppose the US imports more goods in industry X via air. In that case, it reveals some underlying properties of industry X that induce other countries to ship X via air more often. If the US barely imports goods in industry Y via air, it reveals some underlying properties that discourage other countries from shipping good Y via air. A 2009 report from the World Bank Group Weltbank (2009) surveyed the air freight industry in developing coun-

tries and found that top commodities transported by air varied by country but were predominantly concentrated in industries such as capital equipment, transport equipment, intermediate goods, refrigerated goods, and electronics. The US also imported these goods via air, as shown in Table 1.6. So, in this section, I use the ranking of the portion of goods imported by air in the US as a proxy for similar rankings in Eurasia.

Industry	**US Imports Shipped by Air Freight**	**Rank**
Chemicals	52.49%	1
Higher-Tech Equip	50.93%	2
Other	32.12%	3
Leather and Shoes	16.48%	4
Machinery	16.11%	5
Metal and Steel	15.99 %	6
Textile and Apparel	12.15%	7
Fishing and Agri	10.34%	8
Transportation	9.94%	9
Glass, Ceramic, Concrete	7.53%	10
Rubber	6.38%	11
Paper and Publishing	4.70 %	12
Food and Tobacco	3.02%	13
Fuel	1.46%	14
Wooden Products	0.97%	15
Mining, Quarrying and Oil	0.25%	16

Table 1.6: US Import-by-air Portion and Ranking in 2019

Note: This table shows the US portion of imports by air and the US ranking of the portion of the import by air for each grouped industry in 2019. The data come from US Trade Online. The portion is calculated by taking the import value by air freight and dividing it by the total import value for each industry. Before calculation, the values are converted from the Harmonized System (HS) 6-digit level to ISIC version 3.1 and then aggregated to the 16 industries.

Figure 1.12 shows the relationship between industry-varying coefficients on EBE and the US ranking of the portion of goods imported by air. Panel (a) plots the IV coefficients, and panel (b) PPML coefficients. Clear negative correlations in both panels suggest that industries with more negative and significant coefficients are least often transported via air. In Figure A.4, I use the US portion of goods imported by air, rather than the rankings, as the independent variable. The figures suggest that industries that heavily utilize air transportation for shipping tend to display coefficients on EBE that are closer to zero and exhibit lower levels of statistical significance.

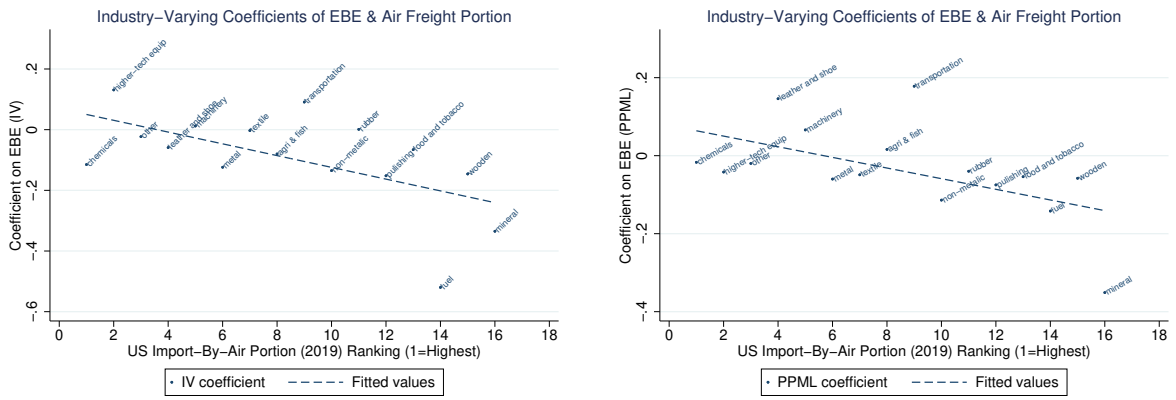

(a) IV

(b) PPML

Figure 1.12: Industry-varying Coefficients on Effective Bilateral Elevation and Ranking of US Import-by-air Portion

Note: These figures plot the US ranking of portions of goods imported via air (import-by-air portion ranking) against the coefficients on bilateral elevation for each grouped industry from OLS (panel a) and PPML (panel b) regressions. Clear negative correlations in both panels show that industries that use air freight less frequently have more negative coefficients on bilateral elevation.

The evidence presented in this section indicates that air freight usage may have influenced the estimated impact of EBE, particularly for industries with significant air freight activity. However, it's noteworthy that air freight is uncommon in industries dealing with lower-cost manufactured goods and raw materials. Hence, the reliance on air freight is unlikely to pose a significant challenge to the robustness of the estimates presented in the preceding sections.[22]

1.8 Conclusions

This paper introduces two metrics for bilateral elevation: physical bilateral elevation (PBE) and effective bilateral elevation (EBE). PBE quantifies the total elevation changes along the shortest route for a country pair, representing a physical terrain characteristic. In contrast, EBE measures the costs associated with vehicle travel over uphill and downhill terrain at the bilateral level.

[22] Additional robustness checks and extensions, including analyses on island countries, EBE from smaller intervals, EBE from higher speeds, and EBE using different fuel consumption data, are available in the Appendix

Notably, EBE is asymmetric, acknowledging that uphill travel incurs higher costs than downhill travel. EBE is the preferred measure of bilateral elevation in this study.

Through the use of gravity-estimating equations and IV analysis focused on a selection of Eurasian countries, this paper establishes that EBE constitutes a significant component of trade costs. Average EBE levels vary considerably, with inland countries exhibiting higher EBE values compared to coastal nations. On average, a one-percent increase in EBE is associated with a 0.046 percent decrease in trade. The impacts of EBE display substantial heterogeneity across industries and regions. This effect is more pronounced for industries with higher weight per value. Additionally, when both origin and destination countries are landlocked, a one-percent increase in EBE results in an average trade value reduction of 0.455 percent, surpassing the baseline coefficient by over nine times. This coefficient is not trivial compared to the coefficients on distance.

Subsequently, I employ a multi-sector Armington model to account for asymmetric trade costs incurred by bilateral elevations. The counterfactual analysis reveals that if bilateral elevations were removed or overlooked, trade costs would be underestimated by an average of 0.4 percent. I contend that we should not overlook bilateral elevations, particularly when examining countries located in hilly and mountainous regions.

Moreover, I examine the influence of regenerative braking systems (RBS) in electric vehicles on bilateral elevations. With the increasing prevalence of electric trucks and the growing efficiency of RBS, mountains may transition from being formidable trade barriers to serving as charging stations where trucks can conveniently recharge.

In summary, unlike the elevation level itself, both physical and effective bilateral elevations can decrease with the construction of new infrastructure and improvements in vehicle efficiency. Conversely, bilateral elevations can rise when hindrances exist, such as the obstruction of crucial infrastructure segments or features like tunnels. The development of better roads and advancements in vehicle technology has the potential to substantially reduce bilateral elevations, contributing to development in mountainous regions.

Chapter 2

Optimal Infrastructure Investment under a Two-Tier Government Structure in the Global Economy

2.1 Introduction

Highway infrastructure is typically the result of collaborative planning between central and local governments. In the United States, the Federal Highway Administration coordinates the planning and funding of the Interstate Highway System, while state transportation departments manage state highways. A similar division of responsibilities exists in Germany, where the federal government oversees the Autobahn network, and state governments manage the LandstraSSen (state roads). In China, the central government plans the national expressways, while provincial governments are responsible for provincial expressways. This two-tier government structure plays a crucial yet understudied role in shaping infrastructure development. Highways and tunnels are two crucial types of infrastructure. Although the economic benefits of highways, particularly in reducing trade costs, have been extensively studied, tunnels remain relatively underexplored by the literature despite their critical importance. Tunnels are essential for overcoming geographic obstacles and ensuring year-round connectivity but are more costly to build.

This paper examines how the interplay of centralization and decentralization influences the provision of highways and tunnels and the consequent effects on welfare and equality. I develop a quantitative spatial model where a benevolent national government, followed by self-interested provincial governments, optimally invests in highways and tunnels to maximize aggregated welfare within their jurisdictions. The model assumes that governments recognize that investments in

highways and tunnels on a particular road have differentiated impacts in reducing trade costs and promoting regional and international trade. However, the model also assumes that provincial governments focus only on their jurisdictions, disregarding the spillover benefits and costs their investments impose on other provinces. This paper finds that central and provincial planning leads to divergent infrastructure outcomes despite assuming identical welfare-maximizing objectives and complete information. A collaborative effort between national and provincial governments in infrastructure planning preserves much of the efficiency gains from centralized planning while allowing provincial governments to address local needs and mitigate inequality.

The spatial model features a set of locations connected by the transport network and mobile workers with heterogeneous preferences across locations. Locations are heterogeneous in productivity, residential land, elevation level, and geographic position. In each location, monopolistically competing firms produce an endogenous measure of differentiated varieties in the spirit of Krugman (1980). These goods are traded between locations, including the rest of the world (ROW), with transport costs influenced by distance and bilateral elevation. The latter is an asymmetric measure that reflects trucks' costs when going uphills and downhills from origins to destinations. Locations can engage in international trade through ports. Building on recent advances in spatial models, including Redding (2016) and Santamaria et al. (2020), I develop a framework that allows for optimal investment decisions by both national and provincial governments in a leader-follower manner, subject to endogenously determined budgets, which derives the solution to the planner's problem involving two tiers of government. The solution algorithm includes that, initially, the national government determines the total budget under a scenario with no infrastructure investment and allocates funds to provincial governments according to an exogenous plan. Subsequently, the national government optimally invests in highways and tunnels across all locations, subject to spatial equilibrium conditions. Provincial governments then solve their respective optimization problems, aiming to improve upon the preexisting national investments within their jurisdictions. Ultimately, locations receive investments from both national and provincial governments. The results indicate that a location is more likely to receive greater investment from its provincial government when it is

relatively more central to the provincial trade network than to the national network. For instance, consider Boulder, Colorado. As the home of the University of Colorado, Boulder plays a significant role in the state's economy and has a substantial population. However, it is less critical within the broader U.S. transportation network. Thus, the model predicts that Boulder would attract more infrastructure investment from the state of Colorado than from the federal government.

To quantify the implications of the two-tier government structure, the model is calibrated to 309 prefectures across 23 provinces in China, using data primarily from 2019. An additional region representing the rest of the world is included, and 25 of China's largest coastal ports serve as gates for international trade. China provides an interesting case study for the two-tier government structure. China's expressway system, comprising National and Provincial Expressways, has undergone a significant transformation. Between 2015 and 2017, the approval power for various transportation projects, including local highways, was delegated to provincial governments. Overall China's infrastructure is governed by a complex system where national and provincial governments share authority over highway construction projects.

The impact of highways and tunnels in reducing internal trade costs in China is estimated using gravity equations, using two novel shift-share instrumental variables (IVs). The first IV, for highways, is derived from historical courier routes and post stations from the Ming dynasty, arguing that the share of historical post stations predicts a region' s contemporary importance and centrality. The second IV, for tunnels exploits the fact that some rock types are easier to drill through and using the relative abundance of these types of rock to construct the IV for tunnels. Cost-mitigating effects of highways and tunnels are found. The results indicate that highways reduce the cost associated with distance, while tunnels decrease the cost of bilateral elevation. Results show that an increase in highway density by one standard deviation reduces the magnitude of the trade cost elasticity with respect to distance by about 10 percent (from -1.13 to -0.96). In addition, an increase in tunnel density by one standard deviation reduces the magnitude of the trade cost elasticity with respect to elevation by about 50 percent (from -0.015 to -0.007).

Two counterfactual analyses are conducted. The first counterfactual analysis compares the

efficiency and equality outcomes of the two-tier structure with those under complete centralization. The findings suggest that the two-tier structure promotes greater equality, lowering the Gini coefficient by 0.4 percent, Theil's index by 0.8 percent, the interquartile ratio (IQR) for real wages by 1.1 percent, and the IQR for highway density by 7.6 percent. This improvement stems from the provincial government's tendency to invest in central areas within their jurisdictions but possibly peripheral to the nation—regions that would likely be neglected under centralization. However, this reduction in inequality comes at the expense of efficiency, measured by the expected utility, as the national government perceives provincial reallocations as misallocations. Consequently, the two-tier system results in a 0.4 percent decrease in the expected utility relative to a fully centralized approach.

The second counterfactual analysis assesses the effects of complete decentralization in infrastructure investment, revealing that a fully decentralized scenario results in lower aggregate welfare and higher inequality compared to the two-tier structure. The expected utility decreases by 2.35 percent, while the Gini coefficient increases by 3.9 percent, Theil' s index increases by 8.5 percent, the interquartile ratio for real wage increases by 1.9 percent, and the interquartile ratio for highway density increases by 16 percent. Increased inequality metrics signify dampened inequality under decentralization. This outcome arises because provincial governments fail to internalize the spillover effects of their infrastructure investments in other provinces. This leads to underinvestment in critical trade routes connecting the western inland regions to the eastern coast. As a result, western landlocked provinces experience the most significant losses under decentralization, while coastal provinces benefit modestly due to their increased infrastructure investments and sustained access to international trade at relatively low costs.

This paper is related to four strands of literature. First, it is related to the literature on endogenous infrastructure investment. Balboni (2019) examines the dynamic effects of infrastructure investment in coastal Vietnam. Jannin and Sotura (2020) models how endogenous local public goods provided by local governments create spillovers across jurisdictional boundaries. Santamaria et al. (2020) considers how the central government in Germany endogenously chose highway invest-

ments before and after the country's division, while Felbermayr and Tarasov (2022) explores how multiple planners non-cooperatively decide on transport infrastructure, explaining the border effect in Europe (also see Chatterjee and Turnovsky (2012), Meurers and Moenius (2018) and Fajgelbaum and Schaal (2020)). This paper contributes to this strand by introducing a two-tier government structure to the endogenous infrastructure problem.

Second, this paper is related to the large literature on estimating the impact of infrastructure on trade. (See Faber (2014), Donaldson (2018), Asturias et al. (2019), Xu and Nakajima (2017), Jaworski and Kitchens (2019), Banerjee et al. (2020), Baum-Snow et al. (2020), Coşar et al. (2021), Gallen and Winston (2021), Loumeau (2023), Egger et al. (2023).) This paper contributes to this strand by investigating the impact of highways and tunnels on internal trade costs in China and introducing two novel instrumental variables to evaluate the impact of infrastructure. The first IV is based on historical courier routes from the Ming dynasty, and the second leverages the lithological distribution of China.[1]

Third, this paper is connected to the literature on the political economy of transport infrastructure. For instance, Brueckner and Selod (2006) examine how the socially optimal transport system contrasts with the one selected through the voting process, demonstrating that voting equilibria can lead to a transportation system that is slower and less costly than the social optimum. Glaeser and Ponzetto (2018) investigates how voters' perceptions of various transportation project costs can distort the types of projects chosen by politicians. Additionally, Fajgelbaum et al. (2023) analyzes how political preferences influenced the development of California's High-Speed Rail.[2] This paper contributes to this literature by exploring how the interaction between national and provincial governments affects infrastructure investment decisions.

Lastly, this paper is related to the research that utilizes spatial equilibrium models to analyze trade outcomes (see Redding (2016), Redding and Rossi-Hansberg (2017), Davis and Dingel (2019),

[1] Also see Limao and Venables (2001), Turner (2006), Möller and Zierer (2018), Duranton and Turner (2012), Duranton and Turner (2011), and Duranton et al. (2014), Banerjee et al. (2020).

[2] Also see Castells and Solé-Ollé (2005) who empirically estimated the main determinants of the allocation of infrastructure investment among Spanish regions.

Fajgelbaum and Schaal (2020), Allen and Arkolakis (2022), and Barwick et al. (2024)). This paper contributes to this literature by incorporating elevation as a location attribute, introducing bilateral elevation as an edge attribute, and allowing it to play a role in trade costs.

The rest of the paper is organized as follows: Section 2 introduces the background of China's highway system. Section 3 shows the stylized facts. Section 4 introduces the spatial equilibrium model, the government structure, and the solution algorithm. Section 5 details the calibration process. Section 6 presents the baseline and counterfactual results. Section 7 concludes.

2.2 Background

2.2.1 China's National and Provincial Expressway System

China's expressway network is one of the most extensive and well-developed in the world, comprising two major systems: the National Expressways (starting with "G," short for "Guodao," meaning "National Road" in Chinese) and the Provincial Expressways (starting with "S," short for "Shengdao," meaning provincial road in Chinese).

The National Expressway Network, also known as the National Trunk Highway System (NTHS), was conceived in the early 1990s. The network has been developed in phases. According to Xu and Nakajima (2017), "the first.....National Trunk Highway System(NTHS).....was intended to connect transport hubs, main ports, all cities with a population above one million, and most cities with populations above 500,000." NTHS, also known as the "7918 Network," established a clear blueprint and laid the foundation for a coordinated and standardized approach to highway construction nationwide. In the 2000s, more national highways are extended to remote areas.

The Provincial Expressway Network complements the national network by providing links within provinces and to neighboring regions. This network expanded significantly in the early 2000s, focusing on less densely populated and economically underdeveloped areas. Provincial expressways are designed to meet local needs, connecting provincial capitals, major cities, airports, and ports. Although the standards for provincial expressways are generally comparable to na-

tional expressways, the total length of provincial highways and tunnels is shorter as of 2019, as shown in Figure (2.1). This is primarily due to the later commencement of provincial expressway development. When the provincial expressway networks began to expand, a substantial national expressway network was already in place.

National expressways are marked with a red background and white text on their signs. Provincial expressways are marked with a yellow background and black text on their signs. Based on their alignment, expressways are categorized into vertical, horizontal, radial, ring, connecting, and parallel lines, each differentiated by different numerical codes. The numbering of China's National Expressways uses one-digit, two-digit, and four-digit Arabic numerals, distinct from the three-digit numbering of national primary roads. The numbering is composed of a letter identifier and Arabic numerals. Capital radial lines use one-digit numbers, such as G1; vertical and horizontal lines use two-digit numbers, such as G35; city ring lines use two or four-digit numbers, such as G9511; and parallel lines and connecting lines also use four-digit numbers. The naming and numbering principles of the provincial expressways generally align with those of the national. The letter identifier for provincial expressways is "S."

The development of highway infrastructure in China from 1990 to the present follows a staged leader-follower style. In this approach, the national government acts as the leader by first establishing a substantial national expressway network, beginning in the 1990s. By the time provincial expressway networks began to expand significantly in the 2000s and 2010s, this national framework was already well-established. In addition, the national government releases its highway construction plans approximately every 8 to 10 years, outlining objectives for the next decade and beyond. This timing ensures that provincial governments are fully aware of the national government's plan when designing their own highways. For example, the national highway plan published in 2005 set clear goals for 2010 and outlined broader objectives for the 20 years that followed. The 2013 plan laid out the roadmap for highway development from 2013 to 2030. Most recently, the 2022 national highway plan set goals from 2022 to 2035, continuing this strategic planning process.

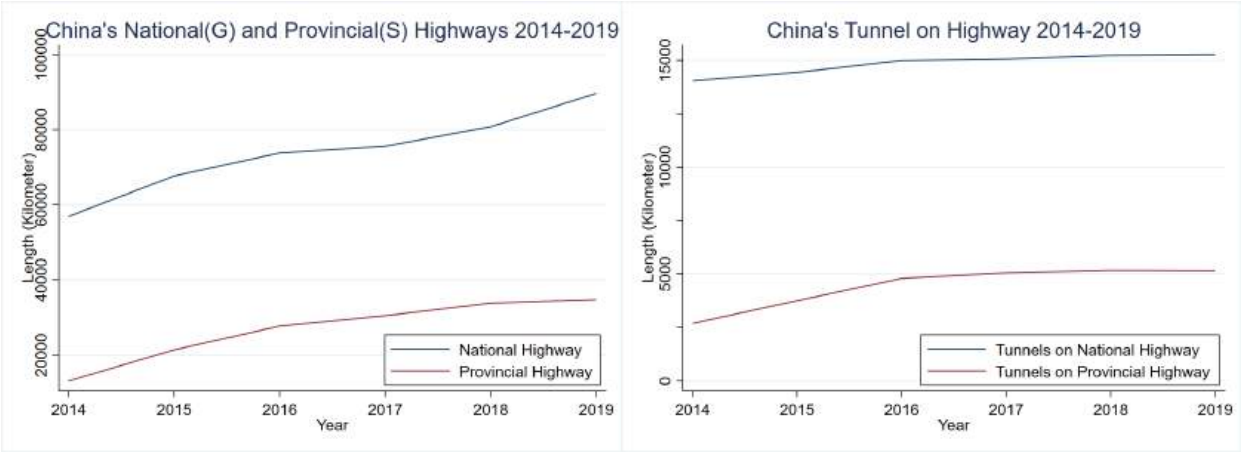

(a) Highways (b) Tunnels on Highways

Figure 2.1: China's Highways and Tunnels

Note: These figures show the length of highways and tunnels belonging to National (G) and Provincial (s) Expressway networks from 2014 to 2019.

2.2.2 Decentralization in Approval Authority of Infrastructure Projects

Since 2015, China has implemented significant reform in the approval processes for infrastructure projects. Three key documents issued by China's National Development and Reform Commission (NDRC) and State Council (SC) played a central role in these changes. The first document, NDRC (2015), significantly delegated approval authority for various transportation projects, including highways, to provincial governments. A subsequent document, SC (2016), further clarified that projects within the national highway network and national roads would be approved by provincial governments, provided that they adhere to the national plan. It also stipulated that local highway projects should be approved at the provincial level, while other road projects should be entrusted to local governments.

Building on these reforms, additional measures were introduced in NDRC (2017) to streamline the approval process further. By 2018, the NDRC had reduced its involvement in transportation project approvals by over 90 percent, retaining authority only for major projects requiring substantial public funds, resources, or complex coordination. Provincial governments were given the responsibility to approve the preliminary stages of highway construction, including the feasibility

reports, design, and construction bidding, as outlined in the "Guidelines for Preliminary Work on Expressway Construction Projects" by the Department of Transportation of Zhejiang Province. According to this document, the approval authority for provincial highway projects has been fully delegated to provincial governments. Specifically, it states that projects such as the reconstruction and expansion of the national expressway network, general national and provincial road construction, and similar infrastructure projects have been handed over to provincial governments for approval, with only a few exceptions. This delegation of authority allows provincial governments to plan and approve these highway projects within their jurisdictions.

2.3 Stylized Facts

This section presents five stylized facts illustrated in Figure (2.2), which not only offer interesting insights but also provide guidance for structuring the model. First, Panel (a) reveals a positive correlation between highway length in each prefecture and local income, measured by gross product per person. This correlation hints at potential two-way causality: on the one hand, infrastructure investments play a crucial role in driving welfare and economic growth; on the other, governments prioritize wealthier regions when allocating infrastructure investments.

Second, prefectures with higher average bilateral elevation to destinations across the country tend to exhibit higher tunnel-to-highway ratios, as depicted in Panel (b). Bilateral elevation, calculated as per equation (2.21), reflects the average change in elevation trucks must traverse when transporting goods from origin to destination. This observation suggests that tunnels are primarily constructed in regions where elevation significantly increases trade costs, indicating a strategic use of tunnels to mitigate these geographic barriers and reduce transportation costs associated with steep terrains.

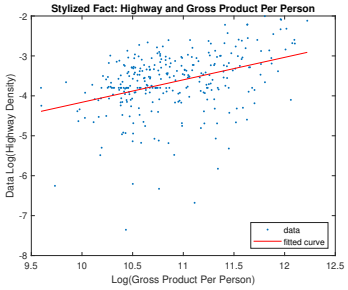

(a) Highway and Income

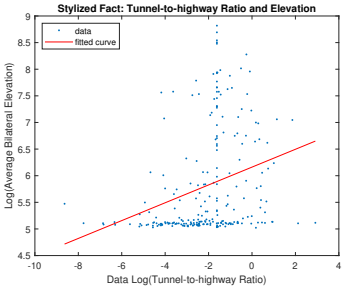

(b) Tunnel Highway and Elevation

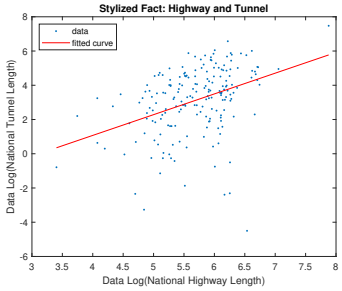

(c) National Highway and Tunnels

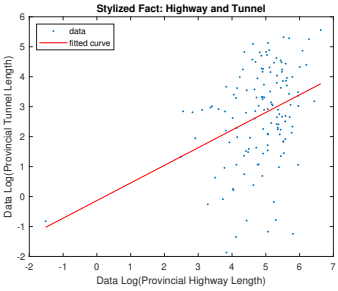

(d) Provincial Highway and Tunnels

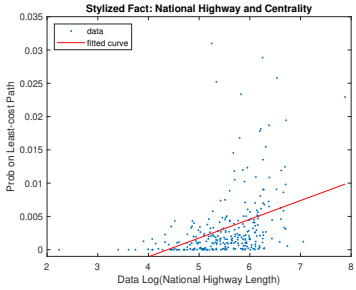

(e) National Highway and Centrality

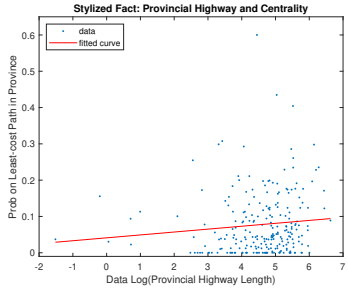

(f) Provincial Highway and Centrality

Figure 2.2: Stylized Facts

Note: These figures demonstrate several stylized facts that provide guidance for model assumptions. Data points are at the prefecture level. Panel (a) shows a positive correlation between highway density and gross product per person, a measure of income. Panel (b) shows a positive correlation between the tunnel-to-highway ratio and the average bilateral elevation to destinations. Panels (c) and (d) show positive correlations between the length of highways and tunnels for national expressways and provincial expressways. Panel (e) shows a positive correlation between national highways and centrality within the nation. Panel (f) shows a positive correlation between provincial highways and centrality within provinces.

Third, Panel (c) reveals a positive correlation between national highways and tunnels, while Panel (d) shows a similar correlation at the provincial level, underscoring the complementary relationship between highways and tunnels across both tiers of government. This suggests that highways and tunnels should be modeled as complementary goods, such that governments aiming to reduce trade costs will naturally invest in both types of infrastructure, especially in regions with substantial bilateral elevation relative to the rest of the country.

The fourth and fifth stylized facts emphasize that governments at both levels tend to prioritize infrastructure planning in regions that are central to their respective jurisdictions. Fourth, Panel (e) indicates that the length of national highways in prefectures is positively correlated with the likelihood of being on the least-cost path, a metric representing the geographic centrality of prefectures within China. These least-cost paths, calculated using Dijkstra's algorithm, minimize transportation costs due to distance and bilateral elevation, as specified in the transportation cost function in Equation (2.23). The probabilities reflect natural geographic centrality, assuming zero infrastructure investment.

Fifth, Panel (f) demonstrates that the length of provincial highways in prefectures is positively correlated with the likelihood of being on the least-cost path within each province. These probabilities, calculated similarly to those in Panel (e), are constrained to origin and destination pairs within the same province, capturing within-province geographic centrality. The last two facts hint at the model assumption that centrality should be a key determinant of infrastructure investment decisions. More central regions, whether in relation to the country or their respective provinces, are likely to attract greater investment in highways and tunnels because of their strategic importance in reducing trade costs for other regions.

2.4 Theory

2.4.1 A Spatial Equilibrium Model

The model follows Redding (2016) and Santamaria et al. (2020). There are $N + 1$ regions in the model, N regions within the country, and one additional region representing the rest of the world(ROW). Each location, $i, n \in N+1$, is endowed with exogenous land, H_n, exogenous elevation level, E_n, and exogenous productivity, A_n. There are L workers within the country. Workers are perfectly mobile across locations within the country with no migration costs and immobile across countries.

The assumption of perfectly mobile labor in China is a simplification, especially given that migration costs within China are well-documented and widely recognized by economists. By relying on this assumption, the model likely underestimates the true potential of the two-tier government structure to mitigate inequality. Introducing migration costs would create persistent wage disparities that cannot be easily mitigated by labor movements. As the national government continues to focus its investments on central regions, the resulting wage increases in those areas would be exacerbated, with fewer offsetting labor inflows to dampen the rise. However, under a two-tier system where provincial governments allocate more resources to peripheral areas, the redistribution of infrastructure investments could have a much greater impact on reducing inequality. Therefore, the model likely provides a lower bound for the two-tier government structure's ability to mitigate inequality. However, the author believes that relaxing the assumption of labor mobility would not change the direction of the findings.

In this model, workers either produce goods inelastically in their location of residence or are hired as construction workers for infrastructure. Each worker ω draws $b_n(\omega)$, an idiosyncratic preference parameter for each location, from a Fréchet distribution.

$$G_{b_n}(b) = prob(b_n \leq b) = e^{-B_n b^{-\epsilon}} \tag{2.1}$$

where ϵ is the shape parameter and B_n is the location parameter. The preference for the worker ω,

living in location n, depends on consumption $C_n(\omega)$, housing $H_n(\omega)$, and idiosyncratic preference shock for the location of residence $b_n(\omega)$.

$$U_n(\omega) = b_n(\omega)(\frac{C_n(\omega)}{\alpha})^{\alpha}(\frac{H_n(\omega)}{1-\alpha})^{1-\alpha} \tag{2.2}$$

where parameter α governs the share of tradable goods. The consumption index in location n, C_n, depends on endogenously-determined quantity M_i of differentiated varieties z.

$$C_n = \big[\sum_{i}^{N}\int_{0}^{M_i} c_{in}(z)^{\frac{\sigma-1}{\sigma}}dz\big]^{\frac{\sigma}{\sigma-1}} \tag{2.3}$$

where $\frac{\sigma-1}{\sigma}$ is the elasticity of substitution between goods. The production follows Krugman (1980) and is characterized by monopolistic competition. Each firm supplies a unique variety. Let $l_n(z)$ be the labor required to produce $q_n(z)$ units of the variety z in location n. $l_n(z)$ is given as:

$$l_n(z) = F + \frac{q_n(z)}{A_n} \tag{2.4}$$

The profit maximization price for variaty z, $p_n(z)$, at the factories' gate is:

$$p_n(z) = \frac{\sigma}{\sigma-1}\frac{w_n}{A_n} \tag{2.5}$$

where w_n is the wage in location n, and A_n is the productivity. Consumer price $p_{in}(z)$ of goods produced in i, and consumed in n is given as:

$$p_{in}(z) = p_i(z) * T_{in} = \frac{\sigma}{\sigma-1}\frac{w_i}{A_i}T_{in} \tag{2.6}$$

$T_{in} \geq 1$ is the iceberg transportation cost for shipping one unit of goods from i to n. Free entry drives profits to zero, which helps determine the optimal quantity, $y_n(z)$, that each firm produces.

$$y_n(z) = (1-\sigma)A_nF \tag{2.7}$$

where F is the fixed cost of production. In equilibrium, the optimal quantities, $y_n(z)$, will require $l_n(z)$ units of labor.

$$l_n(z) = \sigma F \tag{2.8}$$

Labor market clearing condition for each location suggests that the number of firms (and varieties), M_n, in each location is determined by local labor supply after infrastructure construction:

$$M_n = \frac{(1-\lambda)L_n}{\sigma F} \tag{2.9}$$

where λ is the share of construction workers in the labor force. Workers solve the utility maximization problem for optimal consumption, C_n^*, and housing, H_n^*, given budget v_n.

$$C_n^* = \alpha \frac{v_n}{P_n} \tag{2.10}$$

where P_n is the price index.

$$H_n^* = (1-\alpha)\frac{v_n}{r_n} \tag{2.11}$$

where r_n is the rent. The indirect utility of worker ω is:

$$U_n^*(\omega) = \frac{b_n(\omega)v_n}{P_n^\alpha r_n^{1-\alpha}} \tag{2.12}$$

The indirect utility is a transformation of $b_n(\omega)$, which has a Fréchet distribution.

$$G_n(U) = Pr(U_n^* \leq u) = e^{-\Phi_n u^{-\epsilon}} \tag{2.13}$$

where $\Phi_n = \frac{v_n}{P_n^\alpha r_n^{1-\alpha}}$. The expectation of the indirect utility, $\bar{U}$, of worker ω in n is the same across all locations and equals that for the nation as a whole. The expected utility is specified in equation (2.14). Although expected utility equalizes across regions, real wages generally differ. Whether calculated as nominal wages divided by prices or as total income divided by prices and rents, these measures of real income vary across regions. This variation arises because, in attractive regions —those with higher productivity, ample housing, better market access, and therefore lower prices —firms must offer higher real wages to attract workers, raising utility to offset workers' lower idiosyncratic preference for these areas, which would otherwise reduce utility. However, migration inflow to attractive locations is limited. The housing market serves as the congestion factor because the rent rises to prevent the overflow of people into any specific location.

$$\bar{U} = \Gamma(\frac{\epsilon-1}{\epsilon})\Big[\sum_{n\in N}(v_n/P_n^\alpha r_n^{1-\alpha})^\epsilon\Big]^{\frac{1}{\epsilon}} \tag{2.14}$$

where Γ is the gamma function. This is the objective function of the social planner's problem. Expenditure share is derived from CES expenditure function, equilibrium price p_{in}, and labor market clearing condition:

$$\pi_{in} = \frac{X_{in}}{X_n} = \frac{M_i p_{in}^{1-\sigma}}{\sum_{k \in N} M_k p_{kn}^{1-\sigma}} = \frac{(1-\lambda)L_i}{\sigma F}(\frac{\sigma}{\sigma-1}\frac{w_i}{A_i}T_{in})^{1-\sigma}P_n^{\sigma-1} \tag{2.15}$$

where $X_{in} = M_i p_{in}^{1-\sigma}$ is the expenditure on goods produced in i and consumed in n. X_n is the total expenditure in location n. The price index is defined as:

$$P_n^{1-\sigma} = \sum_k M_k p_{kn}^{1-\sigma} = \sum_k \frac{(1-\lambda)L_k}{\sigma F}(\frac{\sigma}{\sigma-1}\frac{w_k}{A_k}T_{kn})^{1-\sigma} \tag{2.16}$$

Similar to Redding (2016), the expenditure on land in each location is redistributed lump-sum to the workers residing there. Therefore, the before-tax income in location n is the following:

$$w_n L_n + (1-\alpha)v_n L_n = \frac{w_n L_n}{\alpha} \tag{2.17}$$

where $v_n = \frac{w_n}{\alpha}$. The national government imposes a flat tax on households' total income with tax rate $\tau < 1$. So, the aggregate income after-tax in location n is:

$$v_n L_n = (1-\tau)\frac{w_n L_n}{\alpha} \tag{2.18}$$

and the aggregate tax income is

$$\tau \sum_n \frac{w_n L_n}{\alpha} \tag{2.19}$$

The probability, $\pi_n(\omega)$, that a worker ω chooses location n is the probability that living in n gives the highest utility:

$$\begin{aligned}\pi_n(\omega) &= Pr(U_n(\omega) \geq max[U_k(\omega), \forall k \neq n.]) \\ &= \frac{(v_n/P_n^\alpha r_n^{1-\alpha})^\epsilon}{\sum_{k \in N}(v_k/P_k^\alpha r_k^{1-\alpha})^\epsilon}\end{aligned}$$

Therefore, labor supply in location n is:

$$L_n = \pi_n(\omega) * L = \frac{(v_n/P_n^\alpha r_n^{1-\alpha})^\epsilon}{\sum_{k \in N}(v_k/P_k^\alpha r_k^{1-\alpha})^\epsilon} L \tag{2.20}$$

The geography of the model contains $N+1$ locations and $N+1$ regions. One region contains one location, which is assumed to be the region's center. There are N regions in the nation and one additional region representing the rest of the world. Locations of two adjacent regions are connected by edges(links). Edges serve as roads, and goods can only be transported along edges between two adjacent locations. Figure (2.3) shows N locations and edges in the sample. The rest of the world is connected to the port regions, allowing the export and import of goods via ports. There are two edge-specific exogenous attributes, distance and effective bilateral elevation (EBE) following Sun (2023), assumed to be costly for goods transportation. Let $dist_{in}$ be the length of edges (distance) between two adjacent locations i, n. Distance is symmetric $dist_{in} = dist_{ni}$. Besides distance, this paper includes elevation as a location endowment and effective bilateral elevation as an edge attribute in order to evaluate the influence of tunnels. As shown in Equation (2.23), tunnels are assumed to mitigate the trade cost of EBE. EBE from location i to neighboring location n is denoted as $elev_{in}$ and defined as follows:

$$elev_{in} = \frac{|Elev_n - Elev_i| * w_{grade}}{dist_{in}} \tag{2.21}$$

where $w_{grade} > 0$ is the trucks' fuel-consumption ratio of driving on the road with a specific grade (slope). w_{grade} is greater than one for uphill roads and less than one for downhill roads, indicating that uphills are more costly than downhills. Therefore, EBE is asymmetric, $elev_{in} \neq elev_{ni}$. Specifically, if location i has a higher altitude than location n, traveling from n to i (ascending uphill) results in a larger EBE than the reverse direction, meaning $elev_{in} < elev_{ni}$. The bilateral elevation in this paper is simplified from Sun (2023) in that it only depends on the elevation level at the origin and destination and not on roads, as infrastructure is endogenous in this paper. In addition, note that distance and EBE only along the edge of two adjacent locations are relevant for this paper, as shown by the trade cost functions in Equations (2.23) and (2.25).

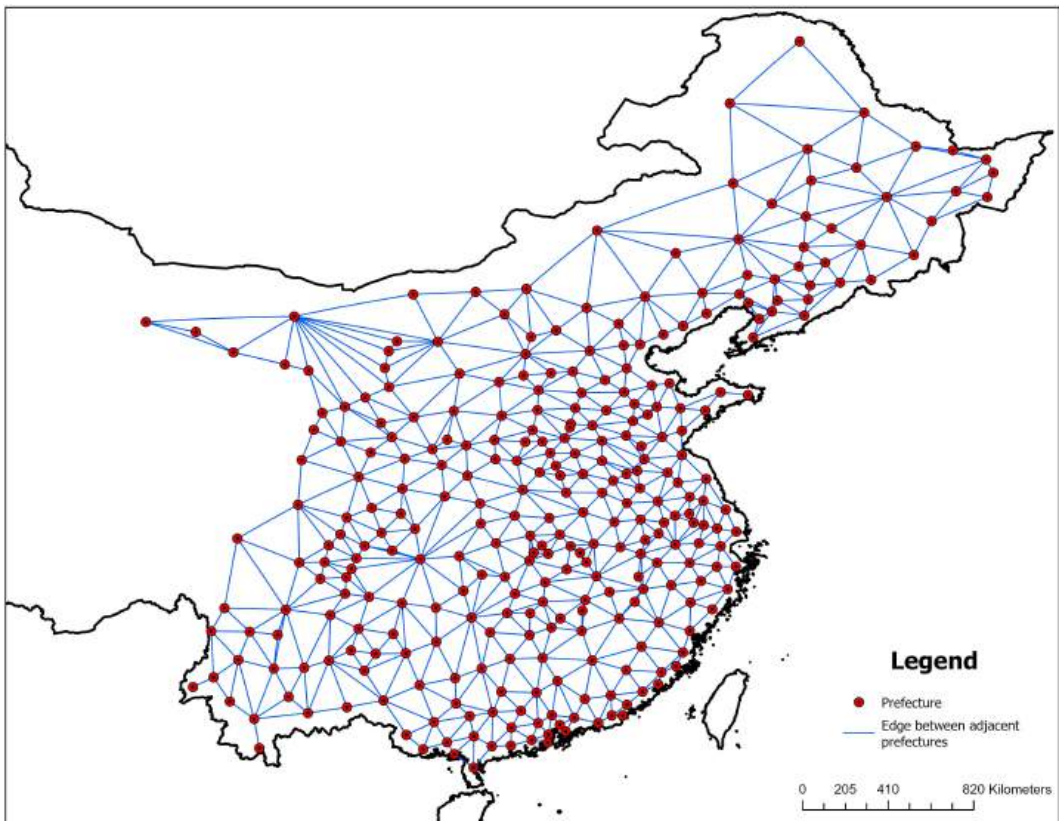

Figure 2.3: Locations and Edges

Note: This figure illustrates the distribution of locations and edges in the model. The locations are in the center of prefectures in China. Locations of adjacent prefectures are connected by edges.

The elevation measure used in this paper is related to Nunn and Puga (2012) and Hirte et al. (2020), who create measures to quantify the impact of geographical barriers to trade. Also, see Fajgelbaum and Schaal (2020), who evaluate the impact of mountains in optimal infrastructure networks in a quantitative spatial model.

Endogenously determined infrastructure (highways and tunnels) can be constructed in each region to mitigate the transportation cost from distance and elevation. Let ϕ_n^r and ϕ_n^t denote the length of highways and tunnels built in region n, respectively, measured in kilometers. Also, define highway and tunnel density in each region as $\rho_n^r = \frac{\phi_n^r}{area_n}$ and $\rho_n^t = \frac{\phi_n^t}{area_n}$, where $area_n$ is the area of region n. To build infrastructure, construction workers compensated at the local wage rate are hired by two tiers of government. The construction is funded by an endogenously raised

government income based on an exogenous flat-rate income tax. It is assumed that workers can build infrastructure in any region, not restricted to the worker's location of residence. In other words, local infrastructure is not required to be built by local workers.[3] For simplicity, it is further assumed that the same proportion of labor in each region is hired as construction workers.[4]

Let $\lambda < 1$ denote the share of construction workers in the labor force. λ will be determined endogenously after the optimal infrastructure. Each kilometer of highways and tunnels require c_n^r and c_n^t units of workers, respectively. Let L_n^{infra} denote the number of construction workers in each region.

$$L_n^{infra} = c_n^r * \phi_n^r + c_n^t * \phi_n^t = \lambda L_n \tag{2.22}$$

Construction workers are compensated at the local wage rate. The total government expenditure paid to construction workers is $G = \sum_n w_n * L_n^{infra} = \lambda \sum_n w_n * L_n$.

Trade cost is modeled as follows. Define adjacent-location-pair-specific costs as t_{in} for an adjacent location pair, i, n.

$$\begin{aligned} t_{in} = exp\left[\frac{1}{2} * \frac{(\beta_{dist} + \beta_{dist}^r \rho_i^r) * log(dist_{in})}{1-\sigma} + \frac{1}{2} * \frac{(\beta_{dist} + \beta_{dist}^r \rho_n^r) * log(dist_{in})}{1-\sigma}\right] \\ * exp\left[\frac{1}{2} * \frac{(\beta_{elev} + \beta_{elev}^t \rho_i^t) * log(elev_{in})}{1-\sigma} + \frac{1}{2} * \frac{(\beta_{elev} + \beta_{elev}^t \rho_n^t) * log(elev_{in})}{1-\sigma}\right] \end{aligned} \tag{2.23}$$

where $\rho_i^r = \frac{\phi_i^r}{area_i}$ and $\rho_i^t = \frac{\phi_i^t}{area_i}$ represent the highway and tunnel density(length per area). β_{dist} and β_{elev} are coefficients that governs the trade costs from distance and EBE, respectively. β_{dist}^r is the coefficient on the interaction term between distance and highways, which shows the trade cost mitigating effect of highways. Similarly, β_{elev}^t is the coefficient on the interaction term between EBE and tunnels which indicates the trade cost mitigating effects of tunnels. Equation (2.23) will be estimated using IV in Section (2.5) to evaluate the values of the coefficients. Equation (2.23) assumes three things: First, distance and bilateral elevation are costly for transportation, so that β_{dist} and β_{elev} are expected to be negative. Secondly, highway density mitigates the cost of distance,

[3] This assumption is trivial for most regions with abundant labor supply. It comes in handy when a region with a small population needs to borrow labor from other areas due to insufficient local labor supply. In this case, labor borrowing takes place implicitly when the model is solved as long as there is enough labor for the country as a whole.

[4] This simplifying assumption assumes that every region has a positive quantity of labor left to produce goods.

and tunnel density mitigates the cost of bilateral elevation so that β^r_{dist} and β^t_{elev} are expected to be positive. Third, the weight, $\frac{1}{2}$, assumes that infrastructure in the origin and destination has equal impacts in reducing trade costs along the connecting edge.

Next, for any two locations k and l that may not be adjacent, the cost of going from k to l is the product of the costs of traversing all edges on the least-cost path. These least-cost paths are determined using Dijkstra's algorithm, which accounts for the level of infrastructure investments. When infrastructure investments change, paths will be endogenously re-routed if the current path no longer represents the least-cost option. Define $\mathcal{I}^{in}_{kl}$ as the indicator function that shows whether the edge from i to n is on the least-cost path from k to l.

$$\mathcal{I}^{in}_{kl} = \begin{cases} 1 & \text{if edge from } i \text{ to } n \text{ is on the least-cost path between } k \text{ and } l \\ 0 & \text{if edge from } i \text{ to } n \text{ is not on the least-cost path between } k \text{ and } l \end{cases} \tag{2.24}$$

Lastly, the general form of trade costs from any origin k to any destination l is the following:

$$T_{kl} = \prod_{in \in \mathcal{L}} (t_{in} | \mathcal{I}^{in}_{kl} = 1) \quad \forall k, l \in N \tag{2.25}$$

where $\mathcal{L}$ is the set of all edges.

2.4.2 General Equilibrium

The following equations solve the spatial general equilibrium. Goods market clears:

$$w_n L_n = \sum_{n \in N} \pi_{in} w_n L_n = \sum_{n \in N} \frac{(1-\lambda) L_i}{\sigma F} (\frac{\sigma}{\sigma - 1} \frac{w_i}{A_i} T_{in})^{1-\sigma} P_n^{\sigma - 1} \; w_n L_n$$

Trade cost along the least-cost path:

$$\text{argmin} T_{k,l} = \prod_{in \in \mathcal{L}} (t_{in} | \mathcal{I}^{in}_{in} = 1)$$

Labor market clears:

$$L_n = \pi_n(\omega) * L = \frac{(v_n / P_n^{\alpha} r_n^{1-\alpha})^{\epsilon}}{\sum_{k \in N} (v_k / P_k^{\alpha} r_k^{1-\alpha})^{\epsilon}} L$$

where and $\sum_i L_i = L$. Price index:

$$P_n^{1-\sigma} = \sum_k \frac{(1-\lambda)L_k}{\sigma F}(\frac{\sigma}{\sigma-1}\frac{w_k}{A_k}T_{kn})^{1-\sigma}$$

Rent:

$$r_n = \frac{1-\alpha}{\alpha}\frac{w_n L_n}{H_n}$$

The four equations above solve the: $\{w_n, L_n, P_n, r_n\}$.

2.4.3 Government Structure

Infrastructure is determined by two tiers of government: the national government and the provincial government. The national government collects tax income and reallocates a portion to the provincial governments. Let Z denote the tax income the national government keeps for itself. Let $p \in \mathcal{P}$ denote the index for provinces. Let Z_p be the tax income allocated to the provincial government, p. While the total budget is endogenously solved, the budget allocation plan is exogenous and will be calibrated to match the observed provincial highway distribution in China in 2019. Keeping the reallocation plan exogenous is crucial in order to study its impact on the counterfactual analyses. Equation (2.26) shows that the total government income is split between two tiers of government.

$$Z + \sum_p Z_p = \tau \sum_n \frac{w_n L_n}{\alpha} \tag{2.26}$$

Let $\phi^r_{upper,n}$ be the investment on highways in location n from the national government. Let $\phi^r_{lower,n}$ be the provincial investment on highways in location n. Let $\phi^t_{upper,n}$, and $\phi^t_{lower,n}$ be the investments in tunnels from national and provincial governments, respectively. Let ϕ^r_n and ϕ^t_n be the total investment in highways and tunnels in location n. All investments are measured in kilometers.

$$\phi^r_n = \phi^r_{upper,n} + \phi^r_{lower,n} \tag{2.27}$$

$$\phi^t_n = \phi^t_{upper,n} + \phi^t_{lower,n} \tag{2.28}$$

With a budget of Z, the national government solves the following social planner's problem by maximizing the expected utility for the country:

$$\underset{(\phi^r_{upper,n},\phi^t_{upper,n})}{Max} \bar{U} = \Gamma(\frac{\epsilon-1}{\epsilon})\Big[\sum_{n\in N}(v_n/P_n^{\alpha}r_n^{1-\alpha})^{\epsilon}\Big]^{\frac{1}{\epsilon}} \tag{2.29}$$

subject to the budget constraint in Equation (2.30) and the construction worker labor supply constraint in Equation (2.31). In practice, the labor supply constraint is almost always non-binding. This is because the tax rate will be calibrated to be relatively small so that only a small fraction of workers are hired as construction workers. Moreover, the government's problem is implicitly subject to the equilibrium conditions of the spatial equilibrium model.

$$Z \geq \sum_{n\in N} w_n L_n^{infra} \tag{2.30}$$

$$\frac{\sum_{n\in N} L_n^{infra}}{\sum_{n\in N} L_n} \leq 1 \tag{2.31}$$

Unlike the national government, which takes care of the nation, provincial governments are self-interested. Provincial governments $p \in \mathcal{P}$ with budget Z_p improves upon the national government's equilibrium outcome by building infrastructures within their province. Without loss of generality, let p also denote the set of locations in the provincial government's jurisdiction. Let $n \in p \in N$ be the locations within province p of the country N. It is assumed that provincial governors maximize the expected utility of people only within their jurisdiction. The planner's problem for provincial governments is given as

$$\underset{(\phi^r_{lower,n},\phi^t_{lower,n})}{Max} \bar{U}_p = \Gamma(\frac{\epsilon-1}{\epsilon})\Big[\sum_{n}^{p}(v_n/P_n^{\alpha}r_n^{1-\alpha})^{\epsilon}\Big]^{\frac{1}{\epsilon}} \tag{2.32}$$

subject to the budget constraint and the labor supply constraint below.

$$Z_p \geq \sum_{n}^{p} w_n L_n^{infra} \quad \forall p \tag{2.33}$$

$$\frac{\sum_{n\in p} L_n^{infra}}{\sum_{n\in p} L_n} < 1 \quad \forall p \tag{2.34}$$

The problem of provincial government p is implicitly subject to the equilibrium conditions for locations within province p.

2.4.4 Solution Algorithm

Following the steps below, I solve the model for the optimal infrastructure investments of the national and provincial governments while adhering to their leader-follower relationship, as discussed in section 2.2.

(1) Starting with zero investment, the trade cost matrix is updated, and the spatial equilibrium is solved using an iterative procedure. This process yields initial wages. The government tax income is then calculated based on initial wages and then allocated to different governments.

(2) The National government starts with zero investments in infrastructure.

(3) The trade cost matrix is updated. Spatial equilibrium is solved using an iterative procedure. The expected utility in equilibrium is calculated.

(4) An interior-point algorithm is used to take a utility-maximizing step to obtain investment in highways $\phi^r_{upper,n}$, and tunnels $\phi^t_{upper,n}$.

(5) Go back to step 3 and repeat until convergence to a local optimum.

(6) Optimal investment from the national government $(\phi^{r*}_{upper,n}, \phi^{t*}_{upper,n})$ is found, and the national government's problem is solved.

(7) Provincial governments update the trade cost matrix with optimal investment of the national government and continue to improve upon them. Each provincial government solves for the optimal provincial investment, $(\phi^{r*}_{lower,n}, \phi^{t*}_{lower,n})$, following the same procedure in steps 3-5.

2.4.5 Model Predictions

Let's start by considering the Lagrangian of the national government's problem:

$$\begin{aligned}\mathcal{L} =&\Gamma(\frac{\epsilon-1}{\epsilon})\Big[\sum_{n\in N}(v_n/P_n^{\alpha}r_n^{1-\alpha})^{\epsilon}\Big]^{\frac{1}{\epsilon}}\\ &-\sum_{n}^{N}\mu_{n,1}\Big[w_nL_n-\sum_{i\in N}\frac{(1-\lambda)L_i}{\sigma F}(\frac{\sigma}{\sigma-1}\frac{w_i}{A_i}T_{in})^{1-\sigma}P_n^{\sigma-1}w_nL_n\Big]\\ &-\sum_{n}^{N}\mu_{n,2}\Big[\frac{(v_n/P_n^{\alpha}r_n^{1-\alpha})^{\epsilon}}{\sum_{k\in N}(v_k/P_k^{\alpha}r_k^{1-\alpha})^{\epsilon}}-\frac{L_n}{L}\Big]\\ &-\sum_{kl\in\mathcal{L}}\mu_{kl,3}\Big[\prod_{in\in\mathcal{L}}(t_{in}|\mathcal{I}_{kl}^{in}=1)-T_{kl}\Big]\\ &-\mu_4(\sum_{n\in N}w_n(c_n^r\phi_{upper,n}^r+c_n^t\phi_{upper,n}^t)-Z)\\ &-\mu_5(\frac{\sum_{n\in N}L_n^{infra}}{\sum_{n\in N}L_n}-1)\end{aligned}\tag{2.35}$$

where $\mu_{n,1}$, $\mu_{n,2}$, $\mu_{kl,3}$, μ_4 and μ_5 are the Lagrangian multipliers. In practice, the construction worker supply constraint is not binding, so $\mu_5 = 0$. The first-order condition with respect to $\phi_{upper,n}^r$ implies:

$$\begin{aligned}&\frac{\partial\mathcal{L}}{\partial\phi_{upper,m}^r}=0:\\ &\underbrace{\frac{\partial\bar{U}}{\partial\phi_{upper,m}^r}}_{\text{Direct Effect}}+\underbrace{\sum_n\sum_i\mu_{n,1}\frac{\partial x_{in}}{\partial\phi_{upper,m}^r}}_{\text{Wage Effect}}+\underbrace{\sum_n\sum_i\mu_{n,2}\frac{\partial\frac{L_n}{L}}{\partial\phi_{upper,m}^r}}_{\text{Labor Effect}}+\underbrace{\mu_3\frac{\partial T_{kl}}{\partial\phi_{upper,m}^r}}_{\text{Path Effect}}=\underbrace{\mu_4w_mc_m^r}_{MC}\end{aligned}\tag{2.36}$$

where $x_{in} = M_ip_{in}^{1-\sigma} = \frac{(1-\lambda)L_n}{\sigma F}(\frac{\sigma}{\sigma-1}\frac{w_i}{A_i}T_{in})^{1-\sigma}$ is the expenditure on goods produced in i and consumed in n. Equation (2.36) suggests that infrastructure affects local outcomes in four ways. First, through the direct effect, infrastructure lowers edge-specific trade costs, which reduces the consumer prices of goods and increases their utility. Second, there is the wage effect, in which wages are influenced by changes in trade flow. Thirdly, the labor effect influences households' residence choices, leading to labor reallocation. Fourthly, there is the path effect in which new infrastructure may redirect the least-cost paths.

For the purpose of simple intuitions, let's focus on the direct effect and assume that only the edge-specific cost is altered by infrastructure while labor, wage, rent, and paths are unaffected. Let

$U_n = v_n/P_n^{\alpha} r_n^{1-\alpha}$. The marginal utility from investment on highways is:

$$\frac{\partial \bar{U}}{\partial \phi^r_{upper,m}} = \frac{1}{2} C_1 C_2 * \sum_i^N x_{in} * \left[\sum_x^V \mathcal{I}_{kl}^{xm} \frac{\beta^r_{dist} log(dist)_{xm}}{area_m} + \sum_x^V \mathcal{I}_{kl}^{mx} \frac{\beta^r_{dist} log(dist)_{mx}}{area_m} \right] \tag{2.37}$$

where $C_1 = -\alpha(\bar{U})^{-1} \sum_n U_n^{\epsilon} P_n^{\sigma-1}$ and $C_2 = \frac{1}{1-\sigma}$. $\mathcal{I}_{kl}^{xm} = 1$ if edge xm is on the least-cost path from k to l. $\mathcal{I}_{kl}^{xm}$ can be viewed as a measure of geographic centrality because location m is more likely to be on one of the least-cost paths if the location is central. V is the set of all locations near m. Derivation of the marginal utility can be found in Appendix B.1.1. Similarly, one can derive the marginal utility with respect to investment in tunnels.

$$\frac{\partial \bar{U}}{\partial \phi^t_{upper,m}} = \frac{1}{2} C_1 C_2 * \sum_i^N x_{in} * \left[\sum_x^V \mathcal{I}_{in}^{xm} \frac{\beta^t_{elev} log(elev_{xm})}{area_m} + \sum_x^V \mathcal{I}_{in}^{mx} \frac{\beta^t_{elev} log(elev_{mx})}{area_m} \right] \tag{2.38}$$

Equations (2.37) and (2.38) show that the marginal return of infrastructure investment in location m is positively affected by three factors. First, greater trade flow, x_{in}, that passes through location m increases the return. Note that trade flows originating from m and terminating at m are two special cases that pass through m. Second, the return correlates positively with nationwide centrality, measured by $\mathcal{I}_{kl}^{mx}$ $\forall x \in V$. Lastly, higher trade costs, $dist_{xm}$ and $elev_{xm}$, also increase the return. Thus, the model predicts that infrastructure investment in m will be higher for three cases: if it is a crucial importer/exporter, if it is central to the country, and if distances or bilateral elevations to other regions are significant.

Next, let's consider the relative marginal utility per dollar between highways and tunnels.

$$\begin{aligned}
&\frac{MU^r_{upper,m}/MC^r}{MU^t_{upper,m}/MC^t} \\
&= \frac{\frac{1}{2} C_1 C_2 * \sum_n x_{in} * \left[\sum_x^V \mathcal{I}_{in}^{xm} \frac{\beta^r_{dist} log(dist)_{xm}}{area_m} + \sum_x^V \mathcal{I}_{in}^{mx} \frac{\beta^r_{dist} log(dist)_{mx}}{area_m} \right]}{\frac{1}{2} C_1 C_2 * \sum_n x_{in} * \left[\sum_x^V \mathcal{I}_{in}^{xm} \frac{\beta^t_{elev} log(elev_{xm})}{area_m} + \sum_x^V \mathcal{I}_{in}^{mx} \frac{\beta^t_{elev} log(elev_{mx})}{area_m} \right]} * \frac{w_n c^t_m}{w_n c^r_m} \\
&= \frac{\sum_x^V \mathcal{I}_{in}^{xm} \beta^r_{dist} log(dist_{xm}) + \sum_x^V \mathcal{I}_{in}^{mx} \beta^r_{dist} log(dist)_{mx}}{\sum_x^V \mathcal{I}_{in}^{xm} \beta^t_{elev} log(elev_{xm}) + \sum_x^V \mathcal{I}_{in}^{mx} \beta^t_{elev} log(elev_{mx})} * \frac{c^t_m}{c^r_m}
\end{aligned} \tag{2.39}$$

Equation (2.39) reveals the intuition behind the tunnel-highway ratio. It shows that the return on tunnels is greater relative to highways if bilateral elevation imposes a greater trade cost relative to

distance. Consequently, the model predicts that regions with particularly pronounced elevation-related trade costs will exhibit a higher tunnel-to-highway ratio in infrastructure development.

To gain insights into the distinction between national and provincial infrastructure planning, let's solve the marginal utility of highways and tunnels for provincial governments. Unlike the national government, provincial governments optimize solely based on the welfare of locations within their own province.

$$\frac{\partial \bar{U}_p}{\partial \phi^r_{lower,m}} = \frac{1}{2} C_1 C_2 * \sum_n^p x_{in} * \left[\sum_x^{V' \in p} \mathcal{I}^{xm}_{in} \frac{\beta^r_{dist} log(dist)_{xm}}{area_m} + \sum_x^{V' \in p} \mathcal{I}^{mx}_{in} \frac{\beta^r_{dist} log(dist)_{mx}}{area_m} \right] \tag{2.40}$$

$$\frac{\partial \bar{U}_p}{\partial \phi^t_{lower,m}} = \frac{1}{2} C_1^{'} C_2 * \sum_n^p x_{in} * \left[\sum_x^{V' \in p} \mathcal{I}^{xm}_{in} \frac{\beta^t_{elev} log(elev_{xm})}{area_m} + \sum_x^{V' \in p} \mathcal{I}^{mx}_{in} \frac{\beta^t_{elev} log(elev_{mx})}{area_m} \right] \tag{2.41}$$

where $C_1^{'} = -\alpha(\bar{U}_p)^{-1} \sum_n^p U_n^{\epsilon} P_n^{\sigma-1}$, where $\bar{U}_p$ is the expected utility within province p, $\bar{U}_p = \Gamma(\frac{\epsilon-1}{\epsilon}) \left[\sum_n^p (v_n / P_n^{\alpha} r_n^{1-\alpha})^{\epsilon} \right]^{\frac{1}{\epsilon}}$. V' is the set of all locations adjacent to x and within province p. A key distinction in the provincial governments' solution arises from the altered centrality measure, $\sum_x^{V' \in p} \mathcal{I}^{mx}_{in}$, where only origins and destinations within the province are taken into account. As a result, provincial infrastructure investments are more strongly tied to a region's centrality within the province rather than the broader national network. This localized centrality drives provincial governments to prioritize investments that enhance intra-provincial connectivity and welfare.

To understand the difference in investment priorities between the two tiers of government, consider the relative marginal returns on provincial versus national highways.

$$\frac{MU^r_{lower,m}}{MU^r_{upper,m}} = \frac{C_1^{'} * \sum_n^p x_{in} * \sum_x^{V' \in p} \mathcal{I}^{xm}_{in} \left[\frac{\beta^r_{dist} log(dist_{xm})}{area_m} \right]}{C_1 * \sum_n^N x_{in} * \sum_x^V \mathcal{I}^{xm}_{in} \left[\frac{\beta^r_{dist} log(dist_{xm})}{area_m} \right]} \tag{2.42}$$

Equation (2.42) illustrates that regions that are relatively central within their province but peripheral to the nation, experience a higher marginal return on provincial infrastructure investments. Conversely, regions that hold central importance at the national level but are peripheral within the province exhibit a greater marginal return on national infrastructure investments. Define the

provincial-to-national centrality ratio for region m as follows:

$$\mathcal{R}_m = \frac{\sum_x^{V' \in p} \mathcal{I}_{kl}^{xm}}{\sum_x^{V} \mathcal{I}_{in}^{xm}}; \quad \forall k, l \in p; \quad \forall i, n \in N \tag{2.43}$$

Equation (2.42) predicts that the ratio of provincial to national highways in region m is positively correlated with the centrality ratio $\mathcal{R}_m$.

2.5 Calibration

2.5.1 Method

The model is calibrated to 309 prefectures in 23 provinces in China using data mainly from 2019. Island provinces and prefectures are dropped because they are not connected to the rest of the country via highways. Furthermore, three western provinces of China: Xinjiang, Tibet, and Qinghai, are dropped due to the irregular sizes of prefectures and missing data problems. Direct-administered municipalities (Beijing City, Tianjin City, Shanghai City, and Chongqing City) are cities with provincial administrative power that do not officially belong to any provinces. In this paper, they are merged into nearby provinces so that the nearby provincial governments will choose the infrastructure for those municipalities. Beijing and Tianjin are merged into Hebei Province. Chongqing is merged into Sichuan Province, and Shanghai is merged into Jiangsu Province. In addition, a region representing the rest of the world is included. Data on China's expressway and tunnel network from 2014 to 2019 come from OpenStreetMap. Prefecture-level economic variables are available in Prefecture Statistical Yearbooks.

In terms of parameters in the model, some are well-studied by the literature and have been borrowed to this paper. The shape parameter of Fréchet distribution: ϵ is assumed to be three. The location parameter of Fréchet is assumed to be one. Trade elasticity is assumed to be seven. Other parameters are specific to this paper. The share of tradable goods in total expenditure, α, takes the value of 0.7. It is calibrated using data from the 2014 World Input-output Table (WIOT) by taking China's final domestic demand for tradable goods and dividing it by China's total final domestic demand. The prefectures' adjacency matrix (AM) of China is computed by supplying the

prefecture-polygon shape file into the Near function in ArcGIS. The productivity A_i and housing H_i are solved using wage and labor supply after inverting the model, following Redding and Rossi-Hansberg (2017). China's nominal GDP per capita and total employment in 2019 are used to solve the problem of productivity and housing. Both variables are sourced from China's prefecture yearbooks.

The tax rate determines the government's budget, and it is calculated by dividing China's total investment in toll roads (including highways, tolled primary roads, tolled secondary roads, tunnels, and bridges) up to 2019 by China's nominal GDP in 2019.[5] The resulting calibrated tax rate is approximately 9.6 percent. Of the total tax income, two-thirds is allocated to the national government, reflecting the proportion of national expressways in 2019. The remaining one-third is distributed among 23 provinces, proportional to their share of provincial highways in the total highway network. Each province's allocation is further determined by the proportion of provincial highways within that province relative to the total length of provincial highways nationwide in 2019. Table (B.2) in the Appendix lists the share of the remaining budget allocated to each province in the sample. For simplicity, the labor requirement for infrastructure construction is assumed to be uniform across regions and is calibrated to match real-world investment costs using the following formulas:

$$c^r = \frac{\frac{c^r_{data}}{Y_{data}} * Y_{model}}{w_{model}} \tag{2.44}$$

$$c^t = \frac{c^t_{data}}{c^r_{data}} * c^r \tag{2.45}$$

where c^r is the labor cost of highway per kilometer in the model. c^t is the labor cost of the tunnel per kilometer in the model. c^r_{data} is the observed average monetary cost of highways per kilometer, which was 61,778.6 thousand Chinese Yuan(CNY) in 2019. This value is calculated by finding the quotient between the total length of highways in the year 2019 and the cumulative infrastructure

[5] As of 2019, China had invested 8,823 billion CNY in highway construction, 400 billion CNY in tolled primary roads, 42.5 billion CNY in tolled secondary roads, 219 billion CNY in tolled bridges, and 23.6 billion CNY in tolled tunnels. China's nominal GDP in 2019 was 99,086.5 billion CNY. These figures are sourced from the 2019 National Toll Road Statistics Bulletin of China.

investment spending till 2019. Y_{data} is the nominal GDP of China in 2019. Y_{model} and w_{model} are the total value of production and the average nominal wage, respectively, predicted by the model under zero infrastructure investment. c^t_{data} is the observed average monetary cost of tolled tunnels per kilometer, which was 189,072.2 thousand CNY, calculated similarly as c^t_{data}.

Trade costs of distance and elevation. The following regressions are estimated using IVs to recover the trade cost of distance and bilateral elevation in China.

$$\begin{aligned} log(X_{ij}) = \beta_0 + \beta_{dist} * log(dist_{ij}) + \beta_1 * log(dist_{ij}) * \frac{1}{2}(\frac{hwy_i}{area_i} + \frac{hwy_j}{area_j}) \\ + \beta_{elev} * log(elev_{ij}) + \beta_2 * log(elev_{ij}) * \frac{1}{2}(\frac{tnnl_i}{area_i} + \frac{tnnl_j}{area_j}) + \delta_i + \delta_j + \epsilon \end{aligned} \tag{2.46}$$

where the dependent variable is the logarithm of trade value from the origin prefecture i to the destination prefecture j in 2017. Data comes from China's Multi-region input-output (MRIO) tables (Zheng et al. (2022)). δ_i and δ_j capture the origin and destination fixed effects. ϵ is the error term. hwy_i and $tnnl_i$ are the lengths of highways and tunnels, respectively, in the origin in the unit of 1000 kilometers. $area_i$ is the area of prefecture i in the unit of 10,000 square kilometers. The term $\frac{1}{2}(\frac{hwy_i}{area_i} + \frac{hwy_j}{area_j})$ measures the average highway density between the origin and the destination. This term interacts with the distance variable, allowing the average highway density to impose a mitigating impact on the trade cost of distance. The mitigation impact is captured by the coefficient, β_1, while β_{dist} governs the trade cost of distance. Similarly, β_{elev} governs the trade cost of bilateral elevation. The term $\frac{1}{2}(\frac{tnnl_i}{area_i} + \frac{tnnl_j}{area_j})$ measures the average tunnel density in origin and destination. It interacts with the elevation variable, allowing tunnels to mitigate the trade cost of elevation. This reduction is captured by the coefficient β_2.

Equation (2.46) is estimated using IV. Two instrumental variables are introduced in section 2.5.2 to address the widely recognized endogenous problem of infrastructure. The interaction term between distance and highway density is instrumented by $log(dist_{ij}) * (Z_i^{ming,g} + Z_j^{ming,g})$, in which $Z_i^{ming,g}$ stems from the historical courier routes and post stations from the Ming dynasty era. It is designed to instrument for China's highways. Additionally, the interaction term between tunnel density and elevation is instrumented by $log(elev_{ij}) * (Z_i^{lithological} + Z_j^{lithological})$, in which $Z_i^{lithological}$

stems from lithological distributions and instruments for tunnels.

Table 2.1 shows the IV regression results from estimating Equation (2.46). The coefficients of distance and bilateral elevation are both negative and consistent with the trade cost. The coefficients of the interaction terms are positive, indicating that the highways and tunnels reduce trade costs of distance and bilateral elevation. The result shows that effective bilateral elevation is indeed a component of trade cost in China along with distance. A one percent increase in bilateral elevation decreases trade by 0.015 percent. On the other hand, the impact of a one percent increase in the distance is a 1.284 percent decrease in trade. The magnitude of the coefficients are aligned with those in Sun (2023). Results suggest a cost-mitigating effect of highways and tunnels. It is found that highway density mitigates the cost from distance, while tunnel density mitigates the cost of bilateral elevation. An increase in highway density by one standard deviation reduces the magnitude of the trade cost elasticity with respect to distance by about 0.171, from -1.284 to -1.113, indicating that highways reduce the trade cost from distance. In addition, an increase in tunnel density by one standard deviation reduces the magnitude of the trade cost elasticity with respect to elevation by about 0.008 from -0.015 to -0.007, indicating that tunnels help mitigate the trade cost from elevation substantially.[6]

The first stage regression results of Equation (2.46) are shown in Table (2.2). Coefficients from the first stage are positive and statistically significant at conventional levels, indicating that the proposed instruments are positively correlated with the variables being instrumented. Origin and destination fixed effects are controlled in the first-stage regressions.

Rest of the world. The model includes one region representing the rest of the world, with economic parameters calibrated to be proportional to China's relative size. For instance, employment in the rest of the world is set as China's total employment multiplied by the ratio of China's population to the global population. The wage level in the rest of the world is calibrated based on China's GDP per capita relative to the world's GDP per capita in 2019. The 25 coastal ports with the highest container throughput in 2019 are selected, and these ports are made adjacent

[6] The standard deviation of highway density is 0.146, and that of tunnel density is 0.057.

VARIABLES	$\ln(X_{ij})$
$\ln(dist_{ij})$	-1.284***
	(0.074)
$\ln(elev_{ij})$	-0.015***
	(0.005)
$\ln(dist_{ij})$ * hwy_{ij}	1.174***
	(0.254)
$\ln(elev_{ij})$ * $tnnl_{ij}$	0.141*
	(0.077)
Observations	73,432
Model	IV
Origin FE	Yes
Destination FE	Yes
Min Eigenvalue	324.2
Durbin P-value	0.001

Standard errors in parentheses

*** p<0.01, ** p<0.05, * p<0.1

Table 2.1: Regression results

Note: This table summarizes the result from estimating Equation (2.46) with IVs, in order to estimate the trade costs from distance and effective bilateral elevation and the cost-mitigating effects of highways and tunnels. Variables $dist_{ij}$ and $elev_{ij}$ are the great circle distance and effective bilateral elevation between prefectures i and j. Variable $hwy_{ij} = \frac{1}{2}(\frac{hwy_i}{area_i} + \frac{hwy_j}{area_j})$ is the average highway density between i and j. $tnnl_{ij} = \frac{1}{2}(\frac{tnnl_i}{area_i} + \frac{tnnl_j}{area_j})$ is the average tunnel density between i and j. Highways and tunnels are measured in kilometers, while the area is measured in ten square kilometers. The dependent variable is the logarithm of trade value from prefecture i to prefecture j in China in 2017. Trade data comes from China's Multi-region input-output tables. Origin and Destination fixed effects are included.

	(1)	(2)
VARIABLES	$ln(dist_{ij}) * (hwy_{ij})$	$ln(elev_{ij}) * (tnnl_{ij})$
$ln(dist_{ij}) * (\text{hwy IV}_{ij})$	0.00027***	
	(0.00000)	
$ln(elev_{ij}) * (\text{tnnl IV}_{ij})$		0.07070***
		(0.00028)
Observations	73,441	73,441
Model	OLS	OLS
Origin FE	Yes	Yes
Destination FE	Yes	Yes

Standard errors in parentheses

*** p<0.01, ** p<0.05, * p<0.1

Table 2.2: First Stage Regression Results for Equation (2.46)

Note: This table summarizes the result from the first stage regression for the IV estimation in Equation (2.46). Variables $dist_{ij}$ and $elev_{ij}$ are the great circle distance and effective bilateral elevation, respectively, between prefectures i and j. Variable $hwy_{ij} = \frac{1}{2}(\frac{hwy_i}{area_i} + \frac{hwy_j}{area_j})$ is the average highway density between i and j. $tnnl_{ij} = \frac{1}{2}(\frac{tnnl_i}{area_i} + \frac{tnnl_j}{area_j})$ is the average tunnel density between i and j. hwy IV_{ij} is the average of hwy IV_i and hwy IV_j which is used as an instrument for highway density, hwy_{ij}. Similarly, tnnl IV_{ij} is the average of tnnl IV_i and tnnl IV_j. The instrument for highways stems from the Ming Courier routes and post stations. The instrument for tunnels stems from the lithological distribution in China. Origin and Destination fixed effects are included.

to the rest of the world, allowing international trade. Table (B.1) in the Appendix lists the selected ports and their container throughput. In 2019, Shanghai ports alone accounted for 26 percent of China's total trade value (exports and imports) (SMOPS (2020)). Consequently, the 25 selected ports handled the vast majority of China's international trade. I make a simplifying assumption that the distance and bilateral elevation from the ports to the rest of the world are assumed to be one. This assumption is made to focus on how governments mitigate internal trade costs rather than international ones. Since goods must still be transported to the ports for export, and internal trade involves significant costs, this simplification does not significantly alter the patterns of internal trade or the distribution of internal infrastructure. Additionally, infrastructure investment in the rest of the world is excluded, and international immigration is not considered in the model.

2.5.2 Instrumental Variables

This section introduces two shift-share instrumental variables. Section (2.5.2.1) proposes an instrument for highways in China using the Ming Dynasty's Courier routes and post stations. Section (2.5.2.2) introduces an instrument for tunnels in China using lithological distributions of unconsolidated sediments.

2.5.2.1 Ming Courier Routes

The first instrument stems from the Chinese Ming dynasty's historical courier routes and post stations. During the Ming Dynasty (1368–1644), China developed an extensive courier system known as the "Ming Imperial Post" for better communication and administration across the empire. This system featured a network of relay stations, or "post stations," where couriers could change horses and rest, ensuring the efficient transmission of official documents and orders. Major routes connected the capital, Beijing, with key cities in all directions, like Nanjing, Hangzhou, Datong, and Xi' an. Notably, many of the crucial cities during the Ming Dynasty continued to remain critical. Using this dataset to study China's infrastructure has been recommended by previous literature (see Egger et al. (2023).) The data comes from Harvard Dataverse, and this paper utilizes version

V6. An illustration of the data is shown in Figure 2.4.

Figure 2.4: Chinese Ming Dynasty's Courier Routes and Post Stations

Note: This figure shows the Chinese Ming Dynasty's courier routes and post stations. Data comes from Harvard Dataverse. Version V6 is utilized.

The instrument is introduced as follows. Let $Z_{it}^{ming,g}$ be the IV representing the length of highways predicted by post stations on Ming courier routes,

$$Z_{it}^{ming,g} = \frac{\#\text{ of Stations}_i}{\Sigma_i \#\text{ of Stations}_i} * \text{Highway Length}_t^g \tag{2.47}$$

where i stands for prefecture, t stands for year, and g stands for national highways. $\#$ of Stations$_i$ is the number of post stations in prefecture i. Highway Length$_t^g$ is the total length of national highways in year t. $Z_{it}^{ming,g}$ is used as an instrument for China's highway density at the prefecture level in equation (2.46). It is highly relevant to China's highways in each prefecture because routes and post-stations in the Ming dynasty predicted each prefecture's economic importance and centrality, which also determined the highway distribution today. The exclusion restriction requires that the historical courier routes in the Ming dynasty affect contemporary trade only because they predicted contemporary highway density. The author believes that the exclusion restriction is not likely to fail.

2.5.2.2 Lithology

The second instrument considers the world lithological distribution. Lithological distribution refers to the spatial arrangement and composition of different rock types on the Earth's surface and subsurface. An area's lithology encompasses the rocks' physical characteristics, including their mineral content, grain size, texture, and structural features. These factors are crucial in understanding the geological history of an area but also have significant implications for various engineering projects, including tunnel construction. For instance, weak rocks that are prone to failure require more extensive support systems while digging tunnels. Porous rocks may require complex drainage systems and waterproofing measures because porous rocks have minute spaces or holes through which liquid may pass. Hard rocks can cause excessive wear on tunnel-boring machines. Therefore, lithology is highly relevant for tunnel construction. Table (2.3) summarizes the various types of rocks found on Earth and their various problems for tunnel construction.[7] Figure (2.5) shows the lithological distribution of China. The data is sourced from Hartmann and Moosdorf (2012) and available on Esri.

Due to their inherent hardness, some rocks in Table (2.3) are challenging to construct tunnels. Siliciclastic sedimentary rocks, pyroclastics, volcanic rocks (acid, intermediate, and basic), plutonic rocks (acid, intermediate, and basic), and metamorphics are all examples of these hard rocks. Additionally, materials like ice and glaciers are problematic because they are meltable, leading to unstable foundations and water ingress. Water-soluble rocks, such as mixed sedimentary, carbonate sedimentary, and evaporites, present challenges due to their potential to dissolve when exposed to water.

[7] see literature in mechanical engineering: Zhang (2004), Turner (2006), Kurian (2013), Bandara and Gunaratne (2018)

Abbreviation	Name	Problems
su	Unconsolidated sediments	Few problems found
ss	Siliciclastic sedimentary rocks	Hard
py	Pyroclastics	Hard
sm	Mixed sedimentary rocks	Water-soluble
sc	Carbonate sedimentary rocks	Water-soluble
ev	Evaporites	Water-soluble
va	Acid volcanic rocks	Hard
vi	Intermediate volcanic rocks	Hard
vb	Basic volcanic rocks	Hard
pa	Acid plutonic rocks	Hard
pi	Intermediate plutonic rocks	Hard
pb	Basic plutonic rocks	Hard
mt	Metamorphics	Hard
ig	Ice and Glaciers	Meltable

Table 2.3: Level-1 Lithology Types and Problems for Tunnels Construction

Note: This table summarizes the level-1 lithology types and their associated challenges for tunnel construction. The rock type names and abbreviations are sourced from Hartmann and Moosdorf (2012), and the general challenges posed by each rock type are based on mechanical engineering literature. It is important to note that while the challenges listed generally apply to subcategories within each rock type, the severity of these challenges can vary across different subcategories.

Unconsolidated sediment is a sediment that is loosely arranged or unstratified, or whose particles are not cemented together, found either at the surface or at depth. They are usually young, from the Cenozoic age. Examples of unconsolidated sediments are sands, mud, swamp deposits, dunes, loess, and beach sands. Compared to the 13 other types of rocks, unconsolidated sediments have few problems and are the easiest to work on when drilling tunnels.

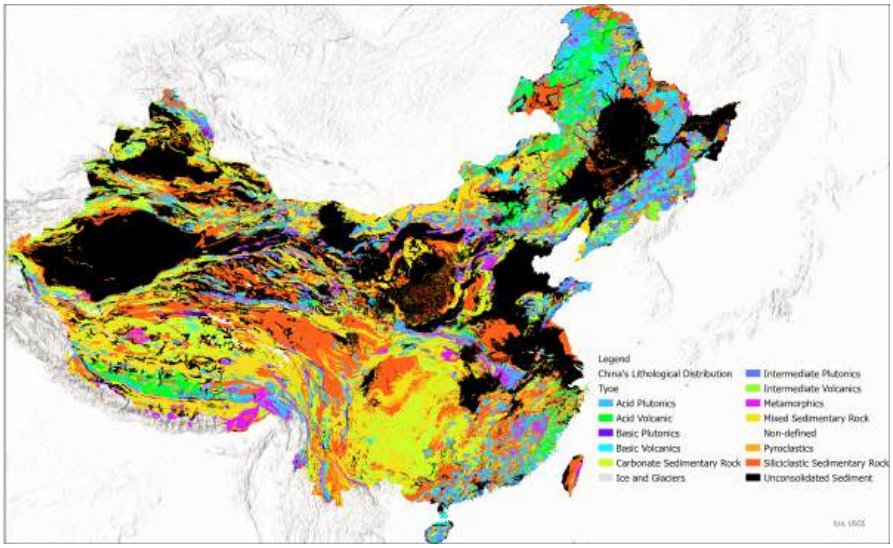

Figure 2.5: Lithological Distribution of China

Note: This figure depicts the lithological distribution of level-1 lithology types listed in Table (2.3). The map is sourced from Hartmann and Moosdorf (2012). The unconsolidated sediments are colored in black.

Unconsolidated sediments in China, depicted in black in Figure (2.5), are primarily concentrated in the North China Plain, the Yangtze River Delta, the Tarim Basin in Xinjiang, the Songliao Basin in northeast China and the Loess Plateau in central-north China. These regions have a wide range of climatical conditions and precipitation patterns. The North China Plain and the Yangtze River Delta experience a temperate monsoon climate characterized by hot, humid summers and cold, dry winters, with annual precipitation ranging from 600 to 1,500 mm, mostly concentrated in the summer months. In contrast, the Tarim Basin, situated in Xinjiang, has an arid desert climate with very low precipitation, often less than 100 mm per year, making it one of the driest regions in China. The Songliao Basin in the northeast experiences a temperate continental climate, with cold winters, warm summers, and moderate rainfall between 400 and 800 mm annually. The Loess Plateau, known for its semi-arid climate, receives about 400 to 600 mm of rainfall annually. While it's true that unconsolidated sediments are sometimes associated with river valleys and agriculture, this correlation does not universally apply. For example, the Loess Plateau in northern China does not have a rich water network compared to other regions. In addition, while the lower

Yangtze River Delta is predominantly composed of unconsolidated sediments, the upper sections of the Yangtze River Basin feature a variety of other geological formations, such as sedimentary rocks and mountainous terrains. In the upper reaches, the Yangtze River flows through regions with significant sedimentary rock formations and rugged highlands, including areas with ancient volcanic rocks and metamorphic terrain. Similarly, the majority of the Pearl River Basin does not predominantly consist of unconsolidated sediments.

Given the relative ease of drilling tunnels in unconsolidated sediment, the abundance of this type of rock will be used to construct the instrumental variable for tunnels. Let $Z_{it}^{Lithology}$ be the shift-share IV representing the length of highway tunnels predicted by the share of the area of unconsolidated sediments(SU). I estimate the following using OLS to predict tunnel shares in 2014 using shares of unconsolidated sediments(SU).

$$\text{Tunnel Share}_{i,2014} = \alpha_0 + \alpha_1 * \frac{\text{Area of SU}_i}{\Sigma_i \text{Area of SU}_i} + \epsilon_i \tag{2.48}$$

where i stands for prefectures and $\text{Tunnel Share}_{i,2014}$ is the share of the length of highway tunnels in prefecture i in 2014 with respect to the total length of highway tunnels in the same year. Next, the lithological instrumental variable for tunnels is calculated below:

$$Z_{it}^{Lithological} = \widehat{\text{Tunnel Share}}_{i,2014} * \text{Tunnel Length}_t \tag{2.49}$$

where $\widehat{\text{Tunnel Share}}_{i,2014}$ is the predicted tunnel share from equation (2.48) and Tunnel Length_t is the total length of highway tunnels in China in year t. The exclusion restriction for the lithological IV requires that the tunnel shares predicted by the share of unconsolidated sediments affect trade only because they predict the easiness of tunnel constructions. The author believes that the exclusion restriction holds.

2.5.3 Calibration Fit

Table (2.4) shows the mean and standard deviation for highways and tunnels in the data and predicted by the baseline model. As unmatched moments, the means and standard deviation of

highways and tunnels predicted by the model do not align perfectly with the data. Note that the baseline model predicts more highways but fewer tunnels than the data. Also, it predicts a more average distribution (smaller standard deviations).

Variables	moment	Data	Baseline Model
Hwy Length	Mean	372.5	358.1
	SD	221.4	350.0
Ntnl Hwy Length	Mean	285.8	267.5
	SD	238.6	325.5
Prvn Hwy Length	Mean	110.9	90.6
	SD	120.5	183.9
Tnnl Length	Mean	73.0	9.4
	SD	149.3	11.4
Ntnl Tnnl Length	Mean	49.1	6.7
	SD	130.2	10.7
Prvn Tnnl Length	Mean	16.6	2.8
	SD	36.9	5.7

Table 2.4: Calibration Fit: Infrastructure Length in Data and Baseline Result

Note: This table summarizes the mean and standard deviation of the infrastructure length in 2019 and predicted by the baseline model. The unit for length is 1 kilometer. The variables from top to bottom are highway length, national highway length, provincial highway length, tunnel length, national tunnel length, and provincial tunnel length. Only tunnels on highways are included in the sample.

Despite the discrepancy, the model successfully replicates the six stylized facts outlined in Section (2.3), as shown in panels (a)-(f) of Figure (B.2). These results highlight the model's accuracy in capturing key relationships: the positive correlation between infrastructure and income, the role of elevation in determining tunnel investment, the complementarity between highways and tunnels at national and provincial levels, and the role of centrality within jurisdiction in determining optimal investment. In addition, Figure(2.6) illustrates an excellent fit between the predicted and actual

values for two targeted variables, wage and labor.

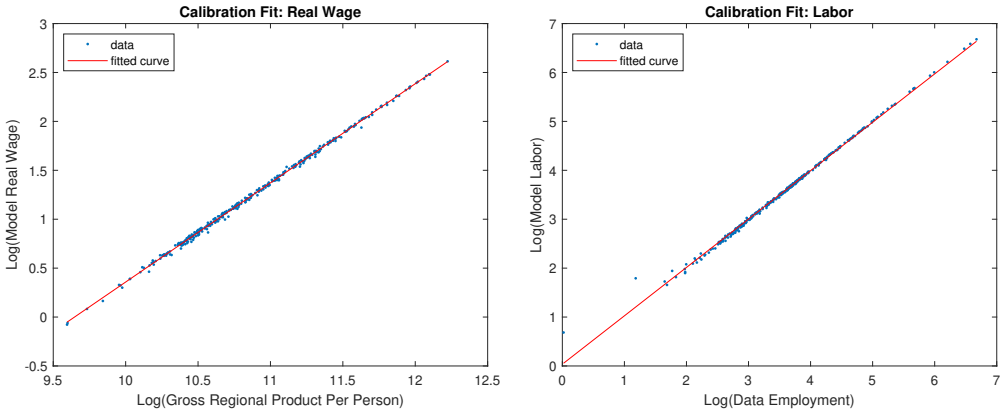

(a) Real Wage (b) Labor

Figure 2.6: Calibration Fit: Targeted Moments

Note: These figures show the calibration fit for the targeted moments. It can be seen in Panel (a) that the model predicted real wage aligns with the gross regional product per person in the data. In Panel (b), the model predicted labor is in line with the number of employed people in the data. Data points are at prefecture level. Data on income and employment are sourced from prefecture yearbooks, 2019.

Figure(2.7) compares the predicted and actual values for three un-targeted moments: trade value, length of highway, and tunnel. Positive relations in Figure(2.7) confirm that the model generates similar values as in the data.

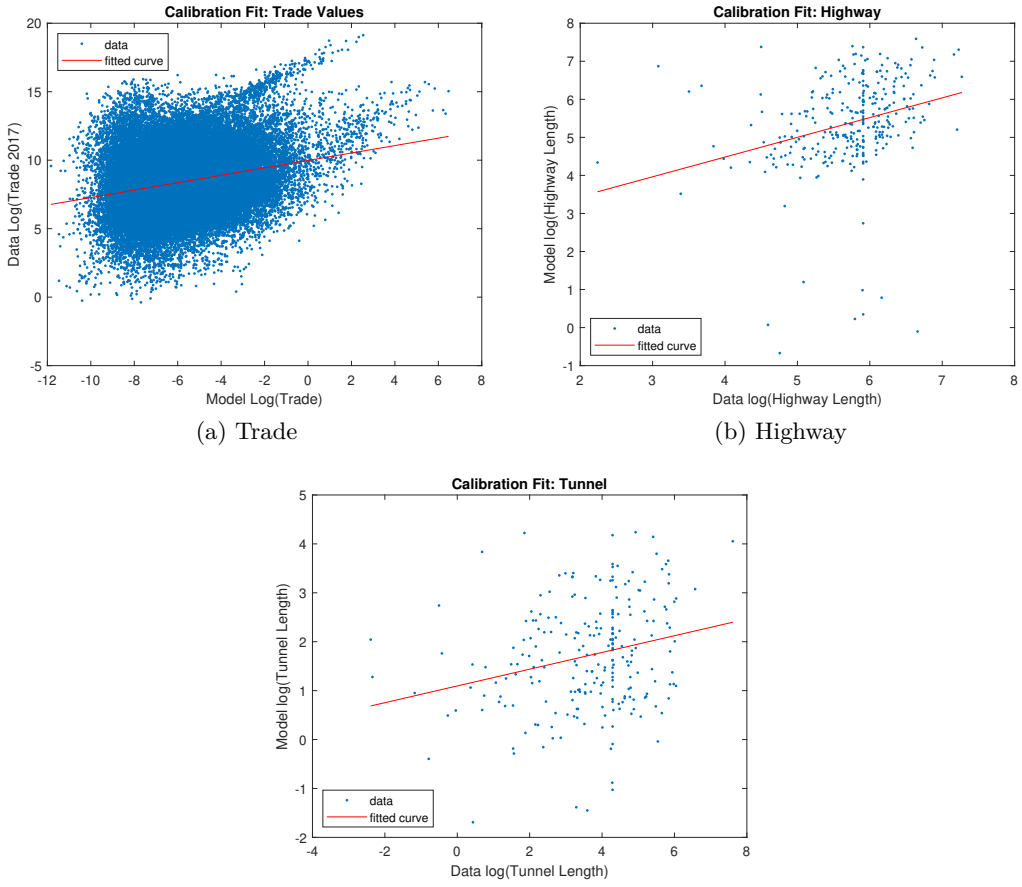

(a) Trade

(b) Highway

(c) Tunnel

Figure 2.7: Calibration Fit: Un-targeted Moments

Note: These figures show the calibration fit for the untargeted moments. Specifically, the trade value (a), the length of highway (b), and the length of tunnel (c) are in line with the corresponding values in the data. Data on trade value comes from China's city (prefecture) level multi-regional input-output table, sourced from Zheng et al. (2022). Data on highways and tunnels are sourced from Open Street Maps.

2.6 Baseline Results and Counterfactual Analysis

2.6.1 Baseline Results

In the baseline setup, both national and provincial governments jointly determine infrastructure investments. Figure (2.8) presents the resulting baseline infrastructure distributions. The total highway network, depicted in panel (a), is predominantly shaped by the centrally-planned national highway shown in panel (c). This highlights how centralized governments prioritize infrastructure investment in more central regions, allocating fewer resources to peripheral areas. Panel (b) illus-

trates the baseline model' s predicted distribution of tunnels. The patterns observed for tunnels in panels (b), (d), and (e) closely mirror those of highways, underscoring the complementary relationship between highways and tunnels discussed in section (2.4). In essence, regions with more highways also tend to have more tunnels.

The infrastructure distribution based on the data is presented in Figure (B.7) in the Appendix. The optimal lengths of highways and tunnels by provinces in the baseline scenario are detailed in Tables (B.5), (B.6), and (B.7), also found in the Appendix. These tables compare the infrastructure allocation across provinces in the baseline model, distinguishing between national and provincial highways and tunnels.

2.6.2 Counterfactual Analyses

Two counterfactual scenarios are examined. First, I analyze the impact of complete centralization, where the national government exclusively determines optimal infrastructure investments. In this scenario, provincial governments are prohibited from investing, and their budget is reallocated to the national government. Second, I explore the effects of a fully decentralized structure, in which each provincial government independently optimizes infrastructure investments within its jurisdiction, and the national government does not intervene. In this decentralized case, each province receives a share of the total budget proportional to its actual share of provincial highways in 2019. In both scenarios, other parameters, such as the tax rate, are fixed.

Although the expected utility equalizes across regions, real wages vary.[8] This difference arises because, in attractive regions—those with higher productivity, ample housing, better market access, and therefore lower prices—firms must offer higher and higher real wages to attract more workers with lower and lower idiosyncratic preferences. While higher wages boost utility, lower idiosyncratic preferences diminish it. Furthermore, the influx of residents to these desirable areas drives up rent, offsetting the gains in utility. Consequently, when factoring in wages, rents, and

[8] Whether it is the nominal wage divided by the price or the total income divided by price and rent, these measures of real income generally differ across regions.

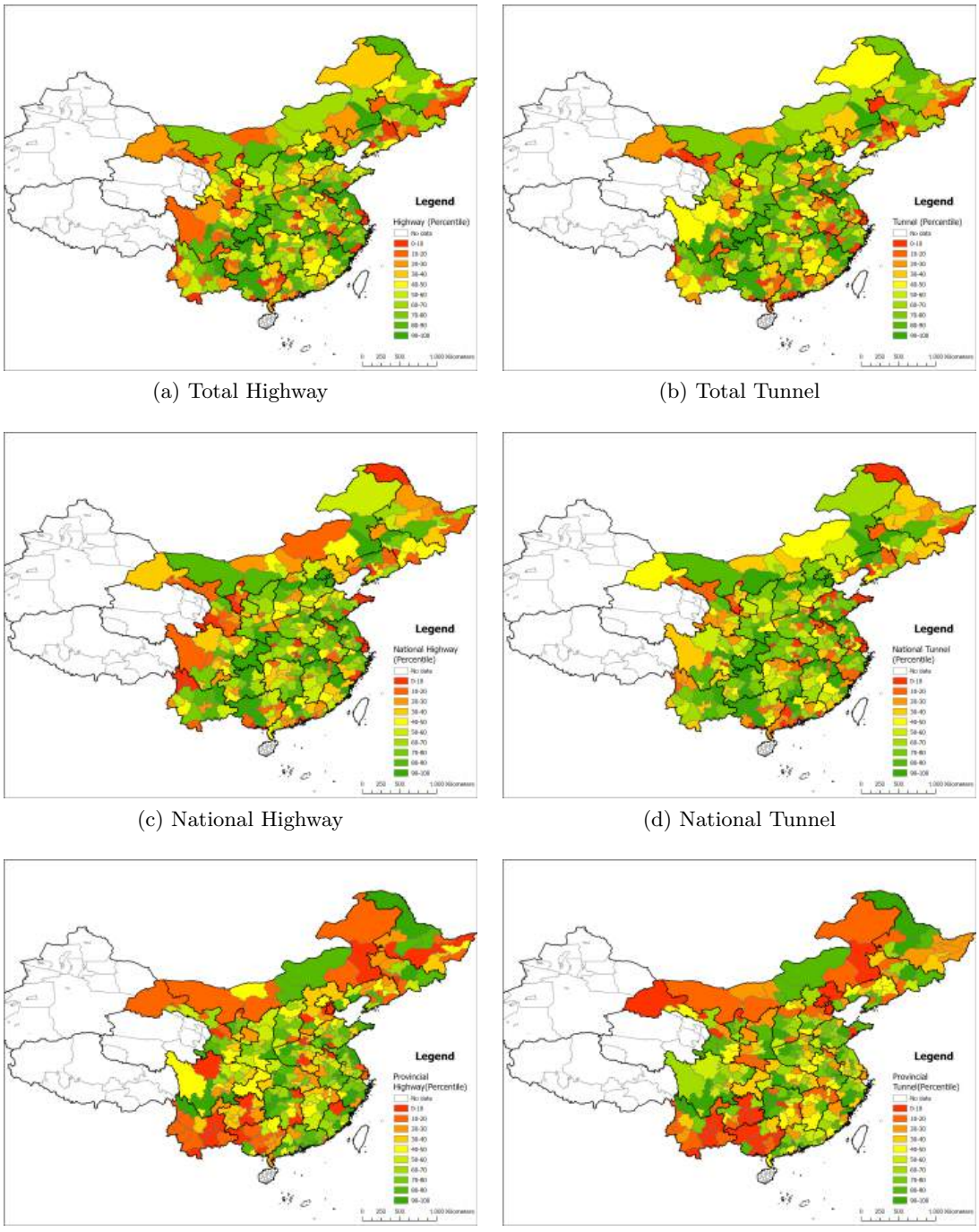

(a) Total Highway

(b) Total Tunnel

(c) National Highway

(d) National Tunnel

(e) Provincial Highway

(f) Provincial Tunnel

Figure 2.8: Baseline Results

Note: This figure displays the distribution of highways and tunnels in predicted by the baseline model, broken down by total, national, and provincial investments. Panel (a) shows the distribution of the total highway. Panel (b) illustrates the total tunnels. Panel (c) focuses on the highways constructed by the national government. Panel (d) depicts tunnels constructed by the national government. Panel (e) represents the highways developed by provincial governments. Panel (f) shows tunnels constructed by provincial governments.

personal taste, a worker in an attractive region has a different real wage but achieves the same

expected utility as a worker in a less attractive location, with both equaling the national expected utility. I use the real wage—calculated as nominal wage divided by the price index—to measure a region' s ability to attract workers and as a proxy for the level of regional development. I will analyze spatial inequality in development by examining the disparities in real wages and highway density across regions.

The expected utility is identical across regions in equilibrium and is used as a measure of welfare in this paper, as in Redding (2016). Note that the change in the expected utility can be interpreted similarly to the equivalence variation. Appendix (B.1.2) defines the equivalence variation (EV) as the change in real wages in the baseline setting that would achieve the same utility level after a counterfactual change in infrastructure investments. Then, the EV margin is defined to represent the average percentage change in real wage that must be compensated (if positive) or charged (if negative) in the baseline scenarios for consumers to be indifferent between the respective counterfactual scenario and the baseline scenario. Then, it is concluded that the change in the expected utility is identical to the change in EV margin.

Counterfactual Analysis One. Under full centralization, the welfare increases for the country as a whole. This is confirmed by a positive change in the expected utility of 0.4 percent in Table (2.6). Interpreting the change in the expected utility as the EV margin, the 0.4 percent increase suggests that consumers in the baseline scenario would need to be compensated by 0.4 percent of their real wage to be indifferent between the baseline and fully centralized scenario. The real wages aggregated at the provincial level are presented in columns (1)-(4) of Table (2.5): The average real wages at the province level increase across all provinces. The welfare gains are driven by the national government's ability to account for the spillover effects of infrastructure.

However, alongside the rise in overall welfare, inequality across space also increases. Four metrics are used to measure inequality across space as shown in Table (2.7). Among the four metrics, three of which compare real wages across space, such as the Gini coefficient, Theil's index, and interquartile ratio (IQR) in real wages. The IQR is calculated as the value in the 75th percentile divided by the value in the 25th percentile. In addition, the IQR in highway density compares

infrastructure development across space.

The Gini and Theil indices, along with the interquartile ratios in real wages and highway density, all rise compared to the baseline, indicating that centralization leads to more unequal outcomes. This suggests that the two-tier government structure in the baseline scenario is more effective in reducing inequality than complete centralization. Specifically, the Gini coefficient increases by 0.4 percent, Theil's index by 0.8 percent, the interquartile ratio for real wages by 1.1 percent, and for highway density by 7.6 percent.

The two-tier government structure mitigates inequality through the following mechanism: while the national government prioritizes infrastructure investments in regions that are central to the entire country, provincial governments tend to focus on regions that are central to their own provinces. Large metropolitan areas, such as Los Angeles in the USA or Hangzhou in China, are simultaneously central to both the country and their respective state or province. However, there are regions that, while central to their state or province, are peripheral to the country. Examples include Des Moines, the capital and largest city of Iowa, and Lanzhou, the capital of Gansu Province in China. The model predicts that it is optimal for the government of Iowa and Gansu province to invest heavily in their state/province capital. This additional provincial investment boosts local wages, helping to reduce regional inequality. However, from the perspective of a centralized planner who focuses on maximizing national utility, such investments would be seen as a misallocation of resources. Therefore, under a fully centralized system, these areas would receive less investment as they are less crucial to national connectivity. The metric $\mathcal{R}_m$ was introduced in Section (2.4) to represent the province-to-country relative centrality ratio for prefecture m. This measure can be calculated using the probability of being on the least-cost paths as follows:

$$\mathcal{R}_m \equiv \frac{\frac{\sum_{k,l \in p} \mathcal{I}_{kl}^m}{p^2}}{\frac{\sum_{i,n \in N} \mathcal{I}_{in}^m}{N^2}} \quad , m \in p \tag{2.50}$$

where m, k and l are locations in province p. i and n are locations in the country N. Let p also denote the total number of locations in province p. $\mathcal{I}_{kl}^m = 1$ if location m is on the least-cost path between k and l, and 0 otherwise. p^2 and N^2 calculates the total number of paths in province

p and country N. The numerator in Equation (2.50) represents the probability of a prefecture being on the least-cost path between locations within its province, while the denominator captures the probability of being on the least-cost path between locations across the entire country. Panels (a) and (b) of Figure (B.4) illustrate that prefectures receiving greater investment under fully centralized planning are those with lower $\mathcal{R}$ values, meaning they are relatively more central on a national scale rather than just within their province. This highlights the national government's tendency to prioritize regions that enhance country-wide connectivity over those that are central only within provincial boundaries.

Figure (B.3) in the Appendix displays the counterfactual outcomes at the prefecture level. While most regions experience gains under centralization, some prefectures suffer losses, highlighted in red in Panel (a) of Figure (B.3). The primary mechanism behind these losses is detailed in Panel (d) of Figure (B.4), which demonstrates that the losing regions generally have a low probability of being on the least-cost path. Consequently, these regions receive minimal infrastructure investment from the national government under centralized planning, which leads to a decrease in real wages. Panels (b) and (c) of Figure (B.4) demonstrate a positive correlation between change in infrastructure and change in the real wage. These regional disparities further explain the pattern of labor migration. Panel (a) of Figure (B.4) shows that labor tends to reallocate to the places where wages rise.

	(1)	(2)	(3)	(4)	(5)	(6)	(7)	(8)
Provinces	W	L	HWY	TNNL	W	L	HWY	TNNL
Hebei	0.78	0.25	-10.62	3.28	1.01	4.92	-38.42	-38.92
Shanxi	0.36	-0.30	-16.54	-12.90	-2.22	1.32	-23.34	-12.99
Inner Mongolia	0.31	-0.37	-22.76	-22.84	-3.89	-0.74	-65.82	-66.98
Liaoning	0.76	0.14	-23.15	-10.75	0.61	4.16	-60.05	-68.19
Jilin	0.51	-0.05	-19.56	-13.27	-10.16	-7.18	-32.19	-37.29
Heilongjiang	0.38	-0.45	-46.29	-39.79	-11.51	-9.12	-13.27	-10.98
Jiangsu	0.74	0.20	-28.25	-20.82	-0.51	3.27	-76.97	-75.31
Zhejiang	0.66	0.05	-38.66	-39.94	0.67	4.63	-34.63	-28.48
Anhui	0.03	-0.42	-30.03	-36.26	-1.54	1.78	-39.19	-48.45
Fujian	0.67	0.08	-25.69	-6.88	1.24	5.21	-39.17	-55.75
Jiangxi	0.86	0.31	0.41	3.07	-3.84	-0.29	-31.99	-32.03
Shandong	0.64	0.09	-31.93	-28.99	-1.43	1.55	-49.18	-53.19
Henan	0.33	-0.15	-23.68	-34.68	-6.12	-2.88	-13.46	-5.33
Hubei	0.63	0.10	-35.30	-40.41	-6.56	-3.57	-36.33	-23.98
Hunan	0.39	-0.38	-39.35	-34.42	-4.86	-1.67	-20.55	-22.19
Guangdong	0.80	0.17	-49.37	-46.13	1.32	5.16	-47.07	-46.92
Guangxi	0.70	0.16	-5.36	-0.51	-0.70	2.97	-63.99	-77.29
Sichuan	0.39	-0.28	-38.11	-35.79	-8.43	-5.67	-15.48	-23.64
Guizhou	0.76	0.25	-6.25	0.90	-7.88	-4.89	-50.06	-51.44
Yunnan	0.65	0.12	-14.81	-16.58	-16.84	-15.88	-84.22	-88.32
Shaanxi	0.36	-0.33	-24.04	-26.79	-9.12	-6.75	-79.81	-80.51
Gansu	0.22	-0.75	-23.37	-20.62	-21.04	-17.99	-80.30	-87.12
Ningxia	0.40	-0.41	-36.02	-18.44	-4.78	-2.02	1.75	-6.35

Table 2.5: Counterfactual Results at Province Level

Note: This table shows the counterfactual results at the province level from counterfactual analysis one (columns 2-5), in which only the national government makes decisions, and counterfactual analysis two (columns 6-9), in which only provincial governments make decisions. The variables shown in the table are the average percentage change in real wage (W) weighted by population, the percentage change in labor (L), the percentage change in highway length(HWY), and the percentage change in tunnel length(TNNL).

Metric	Counterfactual 1	Counterfactual 2
Change in Expected Utility	0.40 %	-2.35 %

Table 2.6: Change in Welfare in Counterfactual Analyses

Note: This table shows the percentage change in the expected utility in counterfactual scenarios compared to the baseline, which is used to measure overall welfare following Redding (2016). Counterfactual analysis one raises the expected utility compared to the baseline scenario. Counterfactual analysis two yields lower expected utility than the baseline scenario.

Counterfactual Analysis Two. The results from the second counterfactual analysis, which explores complete decentralization, are aggregated at the provincial level and presented in columns (5)-(8) of Table (2.5). In this scenario, overall welfare declines relative to the baseline, as shown by a -2.35 percent change in expected utility. Interpreted as an EV margin, this suggests that consumers in the baseline would need to forfeit 2.35 percent of their real wage to be indifferent between the baseline and the decentralized scenario. Furthermore, all inequality metrics rise, as shown in Table (2.7): the Gini coefficient increases by 3.9 percent, Theil' s index by 8.5 percent, the interquartile ratio for real wage by 1.9 percent, and for highway density by 16 percent. These shifts reflect deepened inequality under decentralization.

Figure (B.5) in the Appendix illustrates the counterfactual outcomes at the prefecture level. Coastal provinces such as Hebei, Liaoning, Zhejiang, Fujian, and Guangdong experience gains in average real wages, while other provinces see wage declines, underscoring the uneven distribution of benefits in a decentralized structure. Generally, western inland provinces experience sharper declines in real wages. On the contrary, eastern provinces face milder decreases, and the coastal provinces experience small gains.

These provincial-level outcomes are driven by three main mechanisms. First, access to global markets via coastal ports plays a crucial role. In the baseline scenario, the national government ensures sufficient infrastructure along the least-cost paths connecting the eastern coast to the western inland, enabling the inland regions to trade with the rest of the world at relatively low

costs. Under decentralization, this national coordination is lost, leading to underinvestment in infrastructure along key national trade routes. As a result, western inland provinces face a more substantial increase in trade costs, limiting their ability to engage in international trade and causing a considerable decline in real wages.

Metric	**Baseline**	**Counterfactual 1**	**Counterfactual 2**
Gini Index	0.2987	0.2998	0.3103
Theil Index	0.1449	0.1461	0.1572
Wage IQR	2.1709	2.1939	2.2115
Hwy Density IQR	4.1333	4.4489	4.7902

Table 2.7: Inequality Metrics under Baseline and Counterfactual Scenarios

Note: This table shows the four metrics of inequality across space for the baseline scenario, counterfactual one (national government decisions), and counterfactual two (provincial governments' decisions). The metrics are the Gini coefficient, Theil's index, the interquartile ratio (IQR) in the real wage, and the IQR in highway density. IQR is calculated as the value in the 75th percentile divided by the value in the 25th percentile. The baseline scenario yields the lowest values (least inequality) in all metrics.

Second, under decentralization, provincial governments neglect the spillover effects of infrastructure, as their investments are focused solely on regions within their own borders. They prioritize areas that are central to the province rather than those benefiting neighboring regions. As shown in Panel (d) of Figure (B.6), the change in real wages at the prefecture level is positively correlated with a region's centrality within its province. Consequently, as demonstrated in Panels (a), (b) and (c), regions experiencing a decline in infrastructure investment also saw decreases in real wages, further fueling migration away from those areas. To explain the distribution of gains and losses, Panels (c) and (d) of Figure (B.4) highlight a positive relationship between provincial infrastructure investment and province-to-country relative centrality. This indicates that regions more central to a province but less central to the country receive disproportionately more investment under this

counterfactual. The failure of provincial governments to internalize the spillover effects of their infrastructure decisions exacerbates these imbalances, leading to a significant national welfare decline under decentralization, as reflected by the negative change in expected utility.

Third, national governments tend to underinvest in geographic peripheries, including non-port prefectures along the coast, such as those in Guangdong, Fujian, Zhejiang, Hebei, and Liaoning. Decentralization reallocates more of the budget to all provinces, allowing for greater investment in the peripheries. Consequently, additional investment and sustained low-cost access to international markets allow coastal provinces to benefit under decentralization.

2.7 Conclusion

This paper develops a quantitative spatial equilibrium model to analyze the provision of infrastructure under a two-tier government structure, where a benevolent national government and self-interested provincial governments invest in highways and tunnels to maximize welfare within their respective jurisdictions. The study examines how the interplay between centralization and decentralization shapes infrastructure investment decisions and their effects on welfare and equality. The findings suggest that collaborative planning between national and provincial governments preserves much of the efficiency gains from centralized planning while also enabling provincial governments to address local needs and reduce inequality. Despite having complete information and identical welfare-maximizing objectives, national and provincial governments often pursue divergent infrastructure strategies: the national government prioritizes investments that enhance country-wide connectivity, while the provincial governments focus on improving intra-provincial infrastructure and local welfare. I demonstrate that multi-level government planning across varying scopes can be leveraged to promote spatial equality. Additionally, I show that a two-tier government structure can lead to more equitable outcomes, even when equality is not an objective.

This paper opens several promising directions for future research in public policy using spatial models. First, incorporating varied objective functions to capture the distinct goals of local governments could offer new insights into policy outcomes. Second, exploring scenarios where

governments operate with incomplete information on location and network attributes may yield different predictions for efficiency and equity. Lastly, allowing for more complex interactions—whether through competition or collaboration—between different levels of government could help us better understand the consequences of government interactions.

Chapter 3

Tariffs and Mergers: The Impact of the US-China Trade War on China's Domestic M&A

3.1 Introduction

The escalating trade war between the United States and China in 2018 significantly altered the landscape of Chinese mergers and acquisitions (M&A). As trade tensions intensified through successive rounds of tariffs, export controls, and investment restrictions, Chinese firms faced mounting uncertainty, higher operational costs, and increasing disruptions to their supply chains. While much attention has focused on the impact of trade disputes on the global supply chain and cross-border M&A, the repercussions on domestic M&A activity within China are equally profound. In response to the US-China trade war, Chinese firms exhibited a noticeable decline in M&A activity, driven by growing economic uncertainty, weakened business confidence, and reduced access to global markets and capital. Additionally, international and domestic supply chain disruptions forced firms to reconsider their expansion strategies, leading to shifts in deal composition and sectoral consolidation.

Mergers and acquisitions (M&A) play a crucial role in shaping corporate strategies, market structures, and overall economic growth. They serve as a key mechanism for firms to achieve expansion. Companies can increase their market power through horizontal M&As and secure their supply chain through vertical M&As, which then boost productivity and profitability. Supply chain resilience is another critical motivation, particularly in times of heightened trade uncertainty. Firms may use M&A to secure upstream suppliers or downstream distributors, mitigating risks associated

with disrupted trade flows and tariff-induced cost increases. In the context of the US-China trade war, understanding the impact on M&A is particularly important because it reveals how Chinese and multinational firms are adapting to rising trade barriers and external shocks.

This paper investigates the following questions: How has the US-China trade war influenced domestic M&A patterns in China, particularly in tariff-targeted sectors? Did rising protectionism and external shocks lead firms to adopt a more cautious approach to expansion?

Using firm-level M&A data, trade policy announcements, and sectoral performance indicators, this study examines the relationship between trade war escalations and domestic M&A decision-making. The findings suggest that, despite the overall drop in M&A deals, industries facing higher tariff rates were more likely to experience a relative increase in mergers and acquisitions. This effect was particularly strong in sectors with tighter vertical relationships, suggesting that companies in these industries sought to consolidate supply chains in response to economic uncertainties and market changes caused by the trade war.

3.2 Literature Review

First, we contribute to an underexplored literature that studies how firms mitigate risk through vertical integration. Williamson (1971) was among the first to emphasize the role of vertical integration in managing uncertainty. In his framework, uncertainty arises from incomplete contracts between firms rather than external factors. The impact of external risk on firms' merger decisions has remained largely overlooked for a long time. Recent studies have shown that acquiring firms use vertical mergers as an external risk-mitigation strategy Bakshi et al. (2023); Ersahin et al. (2024); Garfinkel and Hankins (2011). In contrast to these studies, we examine both the demand and supply sides of vertical mergers. Furthermore, we aim to develop a theoretical framework that incorporates firms' endogenous decisions, including contract formation and integration, highlighting the role of vertical integration in maintaining supply chain resilience.

Second, We expand the understanding of the impact of the US-China trade war, with a particular focus on firm decision-making within supply chains under the trade reshuffling. A large

and growing literature examines the impact of the 2018 tariff increase on economic activity in China (Chor and Li (2024),Benguria et al. (2022)). Some recent work has shifted attention toward supply chain disruptions and reallocation resulting from the trade war (Handley et al. (2025); Grossman et al. (2024); Fajgelbaum et al. (2024))[1] . To our knowledge, our paper is the first to provide empirical evidence connecting trade war escalation and vertical mergers through supply chain resilience. This provides a new insight into how firms respond to and reorganize in the face of unexpected external shocks.

Third, a growing body of literature examines firms' endogenous adjustments to production networks. Recent studies develop frameworks in which industry-level firms decide whether to switch customers and suppliers (Acemoglu and Azar (2020); Kopytov et al. (2024)). Much of this research also explores how relationship-specific firms shape their networks (Elliott et al. (2022); Acemoglu and Tahbaz-Salehi (2025); Boehm and Oberfield (2020)). Grossman et al. (2023) introduces a model where firms endogenously invest in resilience to mitigate supply chain risks, identifying optimal firm-level resilience strategies. Our study contributes to this literature by examining mergers and acquisitions (M&A) as a novel form of endogenous adjustment to trade shocks.

3.3 Data

Our vertical merger data are sourced from PitchBook, a comprehensive financial data and research platform that provides detailed information on global mergers and acquisitions (M&A). This dataset has several advantages. First, the definition of M&A in PitchBook aligns with the criteria applied in this study —namely, that the acquiring firm gains effective control over the target firm, thereby stabilizing the supply chain. According to PitchBook, an investment qualifies as M&A only when the acquirer obtains a majority (larger than 50%) of equity shares in the target company. Second, PitchBook is recognized for its rigorous data validation procedures. Each transaction is carefully reviewed to verify its details before being included. Lerner et al. (2024)

[1] Also see Qiu et al. (2019), Bown (2021), Fajgelbaum and Khandelwal (2022), Jiang et al. (2023), Huang et al. (2023), Jiao et al. (2024), Alessandria et al. (2025).

further validates the high quality of PitchBook data. Finally, its coverage of private firms enables a broader analysis of M&A activity, extending beyond transactions involving only public firms. Table (**??**) summarizes the data.

Variable	**Mean**	**SD**	**Min**	**Max**
Deal Year			2011	2024
Vertical 1%	0.54	0.50	0.00	1.00
Vertical 5%	0.30	0.46	0.00	1.00
Horizontal	0.22	0.41	0.00	1.00
Tariff Exposure	0.69	0.89	0.00	2.38
Observations	4862			

Table 3.1: Summary Statistics

Note: Data comes from PitchBook. Vertical 1%: vertical M&A dummy if input-output share is greater than 1%. Vertical 5%: vertical M&A dummy if input-output share is greater than 5%. Horizontal: horizontal M&A dummy if input and output have identical primary industry code (comparable to ISIC 4). Tariff Exposure: output sector's exposure to Trump's tariff (see Bown (2021)).

Our objective is to systematically construct vertical merger deals between 2011 and 2024, focusing on acquisitions where the acquired firms are based in China while the investing firms operate globally. Specifically, we extract key deal characteristics, including the names of acquired firms, deal size, transaction dates, names of investing firms, and firm locations. Additionally, we incorporate several industry classification measures, such as primary industry code, primary industry group, and primary industry sector, for both acquired and investing firms to more accurately identify vertical mergers.

The study employs a multi-regional input-output (MRIO) table for China' s prefectures in 2017, as constructed by Zheng et al. (2022). The MRIO table captures the inter-industry linkages across different regions, allowing for the identification of vertical M&A deals by measuring the input-output trade shares between industries. This data enables the classification of vertical acquisitions based on whether the acquiring and target firms belong to the same supply chain.

we also incorporate tariff data from Bown (2021), which documents the tariffs imposed after the 2018 US-China trade war. This data is used to measure the tariff exposure of different industries, capturing the impact of trade protectionism on M&A activity. The tariff exposure variable reflects

the extent to which the target industry's output was affected by the tariffs introduced during the trade conflict.

3.4 Results

This section presents industry-level descriptive evidence on M&A in China after the 2018 US-China trade war.

Figure (3.1) shows the number of M&A deals over time in which a Chinese or foreign firm acquired a Chinese firm. The figure illustrates the trend in M&A activity, highlighting fluctuations in deal volume across different years. It is noticeable that the number of M&A dropped significantly around 2018 when the US-China trade war took place.

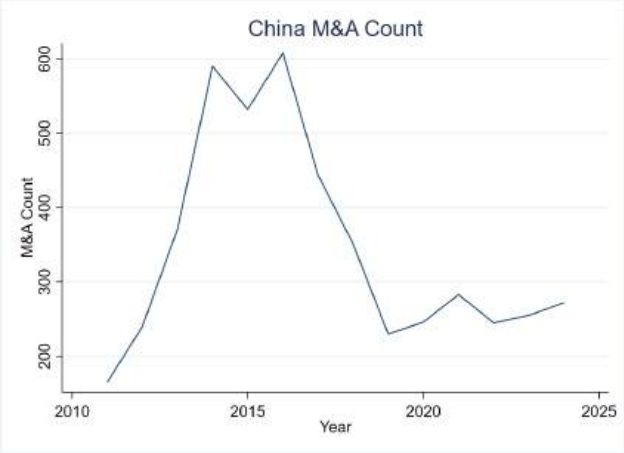

Figure 3.1: China M&A Count

Note: This figure shows the number of M&A deals over time in which a Chinese or foreign firm acquired a Chinese firm. Data is sourced from Pitchbook.

Figure (3.2) shows the share of vertical and horizontal M&A deals over time. The figure highlights the relative prevalence of vertical versus horizontal acquisitions across different years. Vertical M&A refers to deals where the acquiring company and the target company belong to the same supply chain, identified by an input-output share greater than 1% or 5%, following the definition by Fan and Goyal (2006). For example, the trade share from mining to chemical manufacturing is 12% in China based on the 2017 input-output table. So, an acquisition between

firms in these industries is classified as vertical.

Horizontal M&A, on the other hand, involves deals where the acquiring and target companies belong to the same industry category, using the most refined industry level provided by PitchBook, an industry classification level similar to ISIC 4-digit codes.

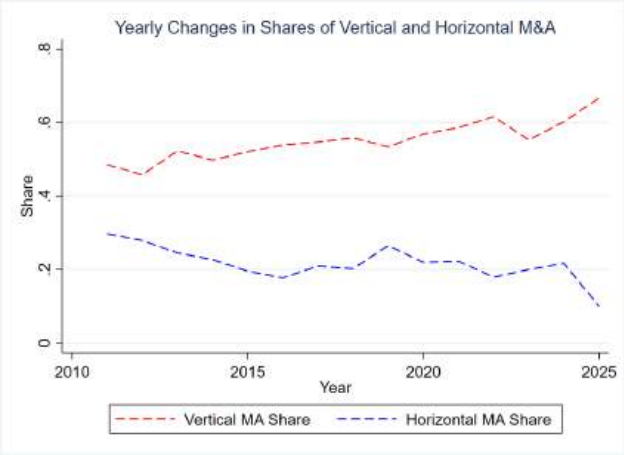

Figure 3.2: Share of Vertical and Horizontal M&A in China

Note: This figure shows the share of vertical and horizontal M&A deals over time in which a Chinese or foreign firm acquired a Chinese firm. Data is sourced from Pitchbook.

Figure 3.3 presents the count of vertical and horizontal M&A transactions in China from 2011 to 2024. The vertical M&A shown in this figure is defined as deals where the trade value between industries exceeds 5%. The data indicate a general decline in M&A activity over time, with both vertical and horizontal deals experiencing similar downward trends, suggesting that the overall reduction in M&A was not specific to either type.

Figure (3.4) categorizes M&A deals by the origin of the acquiring firms. Subfigure (a) shows the total count of M&A deals in China over time, with deals categorized by the origin of the acquiring firms. "Chinese Acquirers" refers to M&As where the acquiring firm is Chinese, while "Foreign Acquirers" refers to M&As where the acquiring firm is foreign, acquiring a Chinese firm. This subfigure illustrates that the total M&A count has dropped for both types of acquirers.

Subfigure (b) depicts the change in M&A activity over time, again categorized by the origin of the acquiring firms. It highlights that M&A deals have decreased for both Chinese and foreign

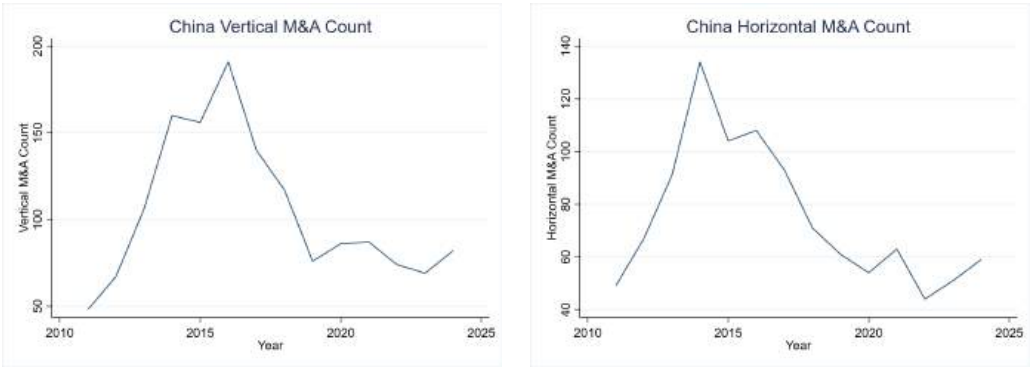

(a) Count (b) Percent Change

Figure 3.3: China Vertical and Horizontal M&A Count

Note: This figure displays the number of vertical (defined as deals where the trade value between industries exceeds 5%) and horizontal M&A transactions in China from 2011 to 2024. Both types of M&A exhibit a declining trend, indicating a broad decrease in acquisition activity rather than a shift in preference between vertical and horizontal deals.

acquirers. However, the drop in 2018 is more significant for Chinese acquirers compared to foreign ones.

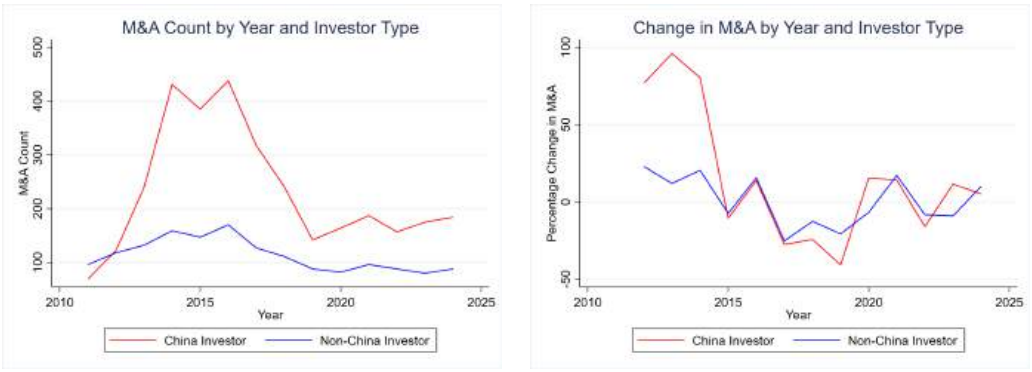

(a) Count (b) Percent Change

Figure 3.4: China M&A Count and Change by Origin of Acquirers

Note: Subfigure (a) shows the total count of M&A deals in China over time, categorized by the origin of the acquiring firms (Chinese vs. Foreign). Subfigure (b) depicts the percent change in M&A activity over time. Noticeable drops in 2018 can be observed in both subfigures, especially for Chinese acquirers. Data is sourced from PitchBook.

Following Chor and Li (2024), we construct the Bartik shift-share design to measure the industry-level exposure to the 2018 US-China Trade War tariff in equation (3.1).

$$\Delta Tariff_k = \frac{1}{N_{p,k}} \sum_{p \in k} \frac{X_p^{US}}{X_p} \sum_t \Delta Tariff_{pt} \tag{3.1}$$

where p is the industry at ISIC 4-digit level. k stands for 19 grouped industries. X_p^{US} is China's export to the US. X_p is China's total export. Tariff exposure at ISIC 4-digit level is further consolidated into 19 grouped industries k by taking the group average. $N_{p,k}$ is the number of p in each grouped industry k.

Table (**??**) summarizes the grouped industries and their tariff exposure. Tariff exposure varies substantially across industries. The most affected sectors include electronics machinery (2.38), general machinery (2.10), textiles (1.72), and chemicals (1.14). In contrast, many service sectors such as finance and healthcare experienced no direct tariff exposure.

Grouped Industry	**Tariff Exposure**
Machinery (electronics)	2.38
Machinery (general)	2.10
Textile	1.72
Chemical	1.14
Computer	1.07
Agriculture	0.46
Oil and gas	0.39
Mining	0.27
Entertainment	0.25
Leasing and commercial	0.07
Transport Service	0.00
Health care	0.00
Construction	0.00
Electricity and heat	0.00
Accommodation	0.00
Software and tech	0.00
Finance	0.00
Metal products	0.00
Wholesale and retail	0.00

Table 3.2: Tariff Exposure by Grouped Industry

Note: Tariff exposure represents the average tariff increase faced by each grouped industry due to the 2018 US-China trade war. The exposure is computed according to equation (3.1).

Figure 3.5 presents the relationship between tariff exposure and the change in vertical and

horizontal M&A share by industry following the 2018 trade war between China and the United States. The figure consists of three subfigures that display how industries with varying levels of tariff exposure experienced changes in M&A activity post-2018.

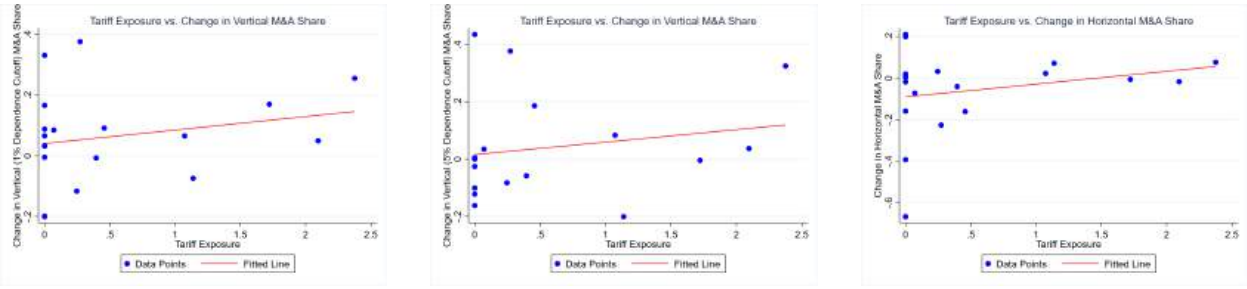

(a) Vertical 1% (b) Vertical 5% (c) Horizontal

Figure 3.5: Vertical, Horizontal M&A and Tariff Exposure by Industry

Note: The X-axis in all subfigures represents the tariff exposure by industry, while the Y-axis shows the change in vertical and horizontal M&A share after the 2018 trade war. The figures illustrate how tariff exposure is correlated with M&A activity in both vertical and horizontal mergers across different industries.

Subfigure (a) shows the change in the vertical M&A share for industries with a tariff exposure threshold of 1%. This subfigure reveals that industries heavily targeted by tariffs, such as those with a higher vertical integration within the supply chain, experienced notable changes in M&A activity. The pattern in this subfigure suggests that industries exposed to tariffs saw an increase in the concentration of M&A deals, particularly those with strong vertical linkages.

Subfigure (b) presents the change in the vertical M&A share for industries exposed to tariffs above the 5% threshold. Similar to subfigure (a), the industries targeted by higher tariff rates saw a significant shift in M&A activity, with vertical deals dominating in certain sectors. The heightened tariff exposure at this level appears to further influence M&A patterns, signaling the responsiveness of industries to tariff shocks.

Subfigure (c) illustrates the change in horizontal M&A share by industry. Unlike the vertical M&A deals, horizontal deals involve companies within the same industry category. The change in horizontal M&A activity following the tariff imposition is also depicted, showcasing how tariffs

affected not just vertical but also horizontal mergers.

Together, the three subfigures underscore the dominant role of tariff exposure in driving both vertical and horizontal M&A activity. The findings suggest that industries facing higher tariff rates were more likely to experience an increase in mergers and acquisitions, particularly in sectors with stronger vertical relationships, indicating that companies in these industries sought to consolidate in response to the economic uncertainties and market changes caused by the trade war.

3.5 Conclusion

The 2018 US-China trade war had a profound impact on China' s M&A landscape, reshaping both the volume and composition of deals. The overall decline in M&A activity reflects the broad uncertainty and caution that firms exercised in response to rising protectionism. The more substantial drop in deals by Chinese acquirers compared to foreign ones highlights the disproportionate impact of the trade war on domestic firms, which were more directly exposed to tariff pressures and supply chain disruptions.

The increased prevalence of vertical M&A deals in tariff-exposed industries reveals a strategic shift in firms' expansion behavior. As tariffs disrupted supply chains, companies sought to mitigate risks by acquiring suppliers or distributors, strengthening their vertical integration. This consolidation strategy helped firms secure greater control over their supply chains, improving resilience against external shocks.

Additionally, the analysis shows that industries with higher tariff exposure were more likely to engage in M&A activity, both vertically and horizontally. This finding underscores how firms in trade-sensitive sectors responded to the trade war not by retreating but by actively restructuring through mergers and acquisitions. Such responses reflect a strategic adaptation to the new trade environment, as companies sought to safeguard their market position and reduce dependence on vulnerable external suppliers.

Overall, the findings indicate that while the US-China trade war reduced the total number of M&A deals, it simultaneously spurred increased consolidation in heavily affected industries. The

dominance of vertical M&A in tariff-exposed sectors highlights the strategic role of deal-making in navigating trade-induced uncertainties, with firms using M&A as a tool to bolster resilience and secure competitive advantages in a volatile global trade landscape.

The findings suggest that M&A decisions are not solely driven by cost considerations, but also by the strategic value of supply chain stability. In these industries, vertical integration acts as a stronger link against input volatility, thereby sustaining M&A incentives despite rising costs. We identify two distinct channels through which tariffs affect vertical mergers: the Cost Pressure Effect and the Supply Chain Defense Effect. The Cost Pressure Effect implies that, after the trade war, firms broadly encountered tighter financial constraints, making it more difficult to afford the substantial fixed costs required for M&A transactions. As a result, overall merger activity declined. Supply Chain Defense Effect shows in industries more exposed to the tariff shock, the drop in M&A activity is less pronounced. This suggests that for these firms, vertical integration serves as a mechanism to stabilize input supply and maintain production reliability, even as M&A becomes costlier.

Bibliography

Acemoglu, Daron and Pablo D Azar (2020) "Endogenous production networks," *Econometrica*, 88 (1), 33–82.

Acemoglu, Daron and Alireza Tahbaz-Salehi (2025) "The Macroeconomics of Supply Chain Disruptions," *Review of Economic Studies*, 92 (2), 656–695.

Agnosteva, Delina E, James E Anderson, and Yoto V Yotov (2019) "Intra-national trade costs: Assaying regional frictions," *European Economic Review*, 112, 32–50.

Alder, Simon et al. (2015) "Chinese roads in India: The effect of transport infrastructure on economic development," in *2015 Meeting Papers*, 1447, Society for Economic Dynamics.

Alessandria, George, Shafaat Yar Khan, Armen Khederlarian, Kim J Ruhl, and Joseph B Steinberg (2025) "Trade war and peace: US-China trade and tariff risk from 2015–2050," *Journal of International Economics*, 104066.

Allen, Treb and Costas Arkolakis (2014) "Trade and the Topography of the Spatial Economy," *The Quarterly Journal of Economics*, 129 (3), 1085–1140.

——— (2022) "The welfare effects of transportation infrastructure improvements," *The Review of Economic Studies*, 89 (6), 2911–2957.

Anderson, James E (1979) "A theoretical foundation for the gravity equation," *The American economic review*, 69 (1), 106–116.

Anderson, James E and Eric Van Wincoop (2003) "Gravity with gravitas: A solution to the border puzzle," *American economic review*, 93 (1), 170–192.

——— (2004) "Trade costs," *Journal of Economic literature*, 42 (3), 691–751.

Anderson, James E and Yoto V Yotov (2020) "Short run gravity," *Journal of International Economics*, 126, 103341.

Anderson, James, Mykyta Vesselovsky, Yoto Yotov et al. (2014) "Gravity with Scale Economies,"Technical report, LeBow College of Business, Drexel University.

Asturias, Jose, Manuel García-Santana, and Roberto Ramos (2019) "Competition and the welfare gains from transportation infrastructure: Evidence from the Golden Quadrilateral of India," *Journal of the European Economic Association*, 17 (6), 1881–1940.

Autor, David, David Dorn, and Gordon Hanson (2011) "The China syndrome: Local labor market effects of import competition in the US," in *International Trade and Investment program meeting.*

Bakshi, Nitin, Robert Swinney, and Ali Kaan Tuna (2023) "Building supply chain resilience through vertical control," *Available at SSRN.*

Balboni, Clare Alexandra (2019) *In harm's way? infrastructure investments and the persistence of coastal cities*, Ph.D. dissertation, London School of Economics and Political Science.

Bandara, Nishantha and Manjriker Gunaratne (2018) *Geotechnical Aspects of Pavement Engineering*: Momentum Press.

Banerjee, Abhijit, Esther Duflo, and Nancy Qian (2020) "On the road: Access to transportation infrastructure and economic growth in China," *Journal of Development Economics*, 145, 102442.

Baniya, Suprabha, Nadia Rocha, and Michele Ruta (2020) "Trade effects of the New Silk Road: A gravity analysis," *Journal of Development Economics*, 146, 102467.

Barwick, Panle Jia, Shanjun Li, Andrew Waxman, Jing Wu, and Tianli Xia (2024) "Efficiency and equity impacts of urban transportation policies with equilibrium sorting," *American Economic Review*, 114 (10), 3161–3205.

Baum-Snow, Nathaniel, J Vernon Henderson, Matthew A Turner, Qinghua Zhang, and Loren Brandt (2020) "Does investment in national highways help or hurt hinterland city growth?" *Journal of Urban Economics*, 115, 103124.

Benguria, Felipe, Jaerim Choi, Deborah L Swenson, and Mingzhi Jimmy Xu (2022) "Anxiety or pain? The impact of tariffs and uncertainty on Chinese firms in the trade war," *Journal of International Economics*, 137, 103608.

Bertoli, Simone, Michaël Goujon, and Olivier Santoni (2016) "The CERDI-seadistance database."

Bird, Julia, Mathilde Lebrand, and Anthony J Venables (2020) "The Belt and Road Initiative: Reshaping Economic Geography in Central Asia?" *Journal of Development Economics*, 144, 102441.

Boehm, Johannes and Ezra Oberfield (2020) "Misallocation in the Market for Inputs: Enforcement and the Organization of Production," *The Quarterly Journal of Economics*, 135 (4), 2007–2058.

Borchert, Ingo and Yoto V Yotov (2017) "Distance, globalization, and international trade," *Economics letters*, 153, 32–38.

Bordeu, Olivia (2023) "Commuting infrastructure in fragmented cities," *Job Market Paper, University of Chicago Booth School of Business*, 6.

Boriboonsomsin, Kanok and Matthew Barth (2009) "Impacts of road grade on fuel consumption and carbon dioxide emissions evidenced by use of advanced navigation systems," *Transportation Research Record*, 2139 (1), 21–30.

Bown, Chad P (2021) "The US–China trade war and Phase One agreement," *Journal of Policy Modeling*, 43 (4), 805–843.

Brueckner, Jan K and Harris Selod (2006) "The political economy of urban transport-system choice," *Journal of Public Economics*, 90 (6-7), 983–1005.

Caliendo, Lorenzo and Fernando Parro (2015) "Estimates of the Trade and Welfare Effects of NAFTA," *The Review of Economic Studies*, 82 (1), 1–44.

Campbell, Douglas L (2010) "History, culture, and trade: a dynamic gravity approach,"Technical report, EERI Research Paper Series.

Castells, Antoni and Albert Solé-Ollé (2005) "The regional allocation of infrastructure investment: The role of equity, efficiency and political factors," *European Economic Review*, 49 (5), 1165–1205.

Chatterjee, Santanu and Stephen J Turnovsky (2012) "Infrastructure and inequality," *European Economic Review*, 56 (8), 1730–1745.

Chen, Maggie Xiaoyang and Chuanhao Lin (2020) "Geographic connectivity and cross-border investment: The Belts, Roads and Skies," *Journal of Development Economics*, 146, 102469.

Chen, Natalie and Dennis Novy (2012) "On the measurement of trade costs: direct vs. indirect approaches to quantifying standards and technical regulations," *World Trade Review*, 11 (3), 401–414.

——— (2021) "Gravity and Heterogeneous Trade Cost Elasticitiesď y."

Chor, Davin and Bingjing Li (2024) "Illuminating the effects of the US-China tariff war on China ' s economy," *Journal of International Economics*, 150, 103926.

Cohen, Joel E and Christopher Small (1998) "Hypsographic demography: the distribution of human population by altitude," *Proceedings of the National Academy of Sciences*, 95 (24), 14009–14014.

Combes, Pierre-Philippe and Miren Lafourcade (2005) "Transport costs: measures, determinants, and regional policy implications for France," *Journal of economic geography*, 5 (3), 319–349.

Coşar, A Kerem and Banu Demir (2016) "Domestic road infrastructure and international trade: Evidence from Turkey," *Journal of Development Economics*, 118, 232–244.

Coşar, A Kerem, Banu Demir, Devaki Ghose, and Nathaniel Young (2021) "Road Capacity, Domestic Trade and Regional Outcomes,"Technical report, National Bureau of Economic Research.

Coşar, A Kerem and Pablo D Fajgelbaum (2016) "Internal geography, international trade, and regional specialization," *American Economic Journal: Microeconomics*, 8 (1), 24–56.

Coughlin, Cletus C and Dennis Novy (2013) "Is the international border effect larger than the domestic border effect? Evidence from US trade," *CESifo Economic Studies*, 59 (2), 249–276.

——— (2016) "Estimating border effects: The impact of spatial aggregation," *International Economic Review*.

Dakhlia, Sami, Boubacar Diallo, and Akram Temimi (2021) "Financial inclusion and ethnic development: Evidence from satellite light density at night," *Journal of Behavioral and Experimental Finance*, 29, 100455.

Davis, Donald R and Jonathan I Dingel (2019) "A spatial knowledge economy," *American Economic Review*, 109 (1), 153–170.

De Soyres, François, Alen Mulabdic, Siobhan Murray, Nadia Rocha, and Michele Ruta (2019) "How much will the Belt and Road Initiative reduce trade costs?" *International Economics*, 159, 151–164.

Dix-Carneiro, Rafael and Brian K Kovak (2017) "Trade liberalization and regional dynamics," *American Economic Review*, 107 (10), 2908–46.

Donaldson, Dave (2018) "Railroads of the Raj: Estimating the impact of transportation infrastructure," *American Economic Review*, 108 (4-5), 899–934.

Donaldson, Dave and Adam Storeygard (2016) "The view from above: Applications of satellite data in economics," *Journal of Economic Perspectives*, 30 (4), 171–98.

DTZP (2019) "高速公路建设项目前期工作指南 (Guidelines for Preliminary Work on Expressway Construction Projects)," *Department of Transportation of Zhejiang Province*.

Ducruet, César, Réka Juhász, Dávid Krisztián Nagy, and Claudia Steinwender (2020) "All aboard: The effects of port development,"Technical report, National Bureau of Economic Research.

Duranton, Gilles, Peter M Morrow, and Matthew A Turner (2014) "Roads and Trade: Evidence from the US," *Review of Economic Studies*, 81 (2), 681–724.

Duranton, Gilles and Matthew A Turner (2011) "The fundamental law of road congestion: Evidence from US cities," *American Economic Review*, 101 (6), 2616–2652.

——— (2012) "Urban growth and transportation," *Review of Economic Studies*, 79 (4), 1407–1440.

Eaton, Jonathan and Samuel Kortum (2002) "Technology, geography, and trade," *Econometrica*, 70 (5), 1741–1779.

Egger, P, M Larch, and Y Yotov (2020) "Gravity-model estimation with time-interval data: Revisiting the impact of free trade agreements (CESifo Working Paper No 8553)."

Egger, Peter H, Gabriel Loumeau, and Nicole Loumeau (2023) "China's dazzling transport-infrastructure growth: Measurement and effects," *Journal of International Economics*, 142, 103734.

Elliott, Matthew, Benjamin Golub, and Matthew V Leduc (2022) "Supply network formation and fragility," *American Economic Review*, 112 (8), 2701–2747.

Ersahin, Nuri, Mariassunta Giannetti, and Ruidi Huang (2024) "Supply chain risk: Changes in supplier composition and vertical integration," *Journal of International Economics*, 147, 103854.

Faber, Benjamin (2014) "Trade integration, market size, and industrialization: evidence from China's National Trunk Highway System," *Review of Economic Studies*, 81 (3), 1046–1070.

Fajgelbaum, Pablo D, Cecile Gaubert, Nicole Gorton, Eduardo Morales, and Edouard Schaal (2023) "Political Preferences and the Spatial Distribution of Infrastructure: Evidence from California's High-Speed Rail,"Technical report, National Bureau of Economic Research.

Fajgelbaum, Pablo D and Amit K Khandelwal (2022) "The economic impacts of the US–China trade war," *Annual Review of Economics*, 14 (1), 205–228.

Fajgelbaum, Pablo D and Edouard Schaal (2020) "Optimal transport networks in spatial equilibrium," *Econometrica*, 88 (4), 1411–1452.

Fajgelbaum, Pablo, Pinelopi Goldberg, Patrick Kennedy, Amit Khandelwal, and Daria Taglioni (2024) "The US-China trade war and global reallocations," *American Economic Review: Insights*, 6 (2), 295–312.

Fan, Joseph PH and Vidhan K Goyal (2006) "On the patterns and wealth effects of vertical mergers," *The Journal of Business*, 79 (2), 877–902.

Faria, Marta V, Gonçalo O Duarte, Roberto A Varella, Tiago L Farias, and Patricia C Baptista (2019) "How do road grade, road type and driving aggressiveness impact vehicle fuel consumption? Assessing potential fuel savings in Lisbon, Portugal," *Transportation Research Part D: Transport and Environment*, 72, 148–161.

Felbermayr, Gabriel J and Alexander Tarasov (2022) "Trade and the spatial distribution of transport infrastructure," *Journal of Urban Economics*, 130, 103473.

Feyrer, James (2019) "Trade and income—exploiting time series in geography," *American Economic Journal: Applied Economics*, 11 (4), 1–35.

——— (2021) "Distance, trade, and income—The 1967 to 1975 closing of the Suez Canal as a natural experiment," *Journal of Development Economics*, 153, 102708.

Fretz, Stephan, Raphaël Parchet, and Frédéric Robert-Nicoud (2022) "Highways, market access and spatial sorting," *The Economic Journal*, 132 (643), 1011–1036.

Gallen, Trevor S and Clifford Winston (2021) "Transportation capital and its effects on the US economy: A general equilibrium approach," *Journal of Macroeconomics*, 69, 103334.

Gan, Nectar (2020) "For 200 years, these villagers lived 2,600 feet up a remote cliff. Now they're in a housing estate," *CNN*.

Garfinkel, Jon A and Kristine Watson Hankins (2011) "The role of risk management in mergers and merger waves," *Journal of Financial Economics*, 101 (3), 515–532.

Glaeser, Edward L and Giacomo AM Ponzetto (2018) "The political economy of transportation investment," *Economics of Transportation*, 13, 4–26.

Grossman, Gene M, Elhanan Helpman, and Stephen J Redding (2024) "When tariffs disrupt global supply chains," *American Economic Review*, 114 (4), 988–1029.

Grossman, Gene M, Elhanan Helpman, and Alejandro Sabal (2023) "Resilience in vertical supply chains."

Halpern, Benjamin S, Melanie Frazier, John Potapenko et al. (2015) "Spatial and temporal changes in cumulative human impacts on the world's ocean," *Nature communications*, 6 (1), 1–7.

Han, Tianlong, Biao Zeng, and Yijie Tong (2021) "Theoretical study on energy recovery rate of regenerative braking for hybrid mining trucks with different parameters," *Journal of Energy Storage*, 42, 103127.

Handley, Kyle, Fariha Kamal, and Ryan Monarch (2025) "Rising import tariffs, falling exports: When modern supply chains meet old-style protectionism," *American Economic Journal: Applied Economics*, 17 (1), 208–238.

Hartmann, Jens and Nils Moosdorf (2012) "The new global lithological map database GLiM: A representation of rock properties at the Earth surface," *Geochemistry, Geophysics, Geosystems*, 13 (12).

Head, Keith and Thierry Mayer (2014) "Gravity equations: Workhorse, toolkit, and cookbook," in *Handbook of international economics*, 4, 131–195: Elsevier.

Head, Keith and John Ries (2001) "Increasing returns versus national product differentiation as an explanation for the pattern of US-Canada trade," *American Economic Review*, 91 (4), 858–876.

Heerman, Kari ER and Ian M Sheldon (2018) "Gravity and comparative advantage: Estimation of trade elasticities for the agricultural sector,"Technical report, National Bureau of Economic Research.

Henderson, Daniel J and Daniel L Millimet (2008) "Is gravity linear?" *Journal of Applied Econometrics*, 23 (2), 137–172.

Hillberry, Russell and David Hummels (2008) "Trade responses to geographic frictions: A decomposition using micro-data," *European Economic Review*, 52 (3), 527–550.

Hirte, Georg, Christian Lessmann, and André Seidel (2020) "International trade, geographic heterogeneity and interregional inequality," *European Economic Review*, 127, 103427.

Hooker, John N (1988) "Optimal driving for single-vehicle fuel economy," *Transportation Research Part A: General*, 22 (3), 183–201.

Huang, Yi, Chen Lin, Sibo Liu, and Heiwai Tang (2023) "Trade networks and firm value: Evidence from the US-China trade war," *Journal of International Economics*, 145, 103811.

Hummels, David (1999) "Toward a geography of trade costs,"Technical report.

——— (2007) "Transportation costs and international trade in the second era of globalization," *Journal of Economic perspectives*, 21 (3), 131–154.

Hummels, David and Georg Schaur (2012) "Time as a trade barrier,"Technical report, National Bureau of Economic Research.

Jacks, David S, Christopher M Meissner, and Dennis Novy (2008) "Trade Costs, 1870-2000," *American Economic Review*, 98 (2), 529–34.

Jannin, Nicolas and Aurélie Sotura (2020) "This Town Ain't Big Enough? Quantifying Public Good Spillovers."

Jaworski, Taylor and Carl T Kitchens (2019) "National policy for regional development: Historical evidence from Appalachian highways," *Review of Economics and Statistics*, 101 (5), 777–790.

Jiang, Lingduo, Yi Lu, Hong Song, and Guofeng Zhang (2023) "Responses of exporters to trade protectionism: Inferences from the US-China trade war," *Journal of International Economics*, 140, 103687.

Jiao, Yang, Zhikuo Liu, Zhiwei Tian, and Xiaxin Wang (2024) "The impacts of the US trade war on Chinese exporters," *Review of Economics and Statistics*, 106 (6), 1576–1587.

Khalifa, Sherif (2016) "Trust, landscape, and economic development," *Journal of Economic Development*, 41 (1), 19.

Kopytov, Alexandr, Bineet Mishra, Kristoffer Nimark, and Mathieu Taschereau-Dumouchel (2024) "Endogenous production networks under supply chain uncertainty," *Econometrica*, 92 (5), 1621–1659.

Kovak, Brian K (2013) "Regional effects of trade reform: What is the correct measure of liberalization?" *American Economic Review*, 103 (5), 1960–76.

Krugman, Paul (1980) "Scale economies, product differentiation, and the pattern of trade," *The American Economic Review*, 70 (5), 950–959.

Kudamatsu, Masayuki (2018) "GIS for credible identification strategies in economics research," *CESifo Economic Studies*, 64 (2), 327–338.

Kunt, Mehmet Akif (2020) "Advisor Based Modelling of Regenerative Braking Performance of Electric Vehicles at Different Road Slopes," *International Journal of Automotive Science And Technology*, 4 (2), 98–104.

Kurian, Nainan (2013) *An introduction to modern techniques in geotechnical and foundation engineering*: Alpha Science International.

Lerner, Josh, Junxi Liu, Jacob Moscona, and David Y Yang (2024) "Appropriate entrepreneurship? The rise of China and the developing world."

Li, Xiangjie, Xiangwen Zhang, and Yangxiong Wang (2022) "Regenerative braking control strategies with fixed ratio and variable ratio braking forces optimization distribution for electric vehicles during downhill process," *International journal of automotive technology*, 23 (3), 667–681.

Li, Xuebo, Jian Ma, Xuan Zhao, Lu Wang et al. (2023) "Study on Braking Energy Recovery Control Strategy for Four-Axle Battery Electric Heavy-Duty Trucks," *International Journal of Energy Research*, 2023.

Liesbet, HOOGHE and Marks Gary (2003) "Unraveling the central state, but how? Types of multi-level governance," *American political science review*, 97 (2), 233–243.

Limao, Nuno and Anthony J Venables (2001) "Infrastructure, geographical disadvantage, transport costs, and trade," *The world bank economic review*, 15 (3), 451–479.

Liu, Zhentao and Jinlong Liu (2021) "Effect of altitude conditions on combustion and performance of a turbocharged direct-injection diesel engine," *Proceedings of the Institution of Mechanical Engineers, Part D: Journal of Automobile Engineering*, 09544070211026204.

Lopp, Sean, Eric Wood, and Adam Duran (2015) "Evaluating the impact of road grade on simulated commercial vehicle fuel economy using real-world drive cycles,"Technical report, National Renewable Energy Lab.(NREL), Golden, CO (United States).

Loumeau, Gabriel (2023) "Regional Borders, Commuting and Transport Network Integration," *Review of Economics and Statistics*, 1–45.

Marsden, Greg, Antonio Ferreira, Ian Bache, Matthew Flinders, and Ian Bartle (2014) "Muddling through with climate change targets: a multi-level governance perspective on the transport sector," *Climate policy*, 14 (5), 617–636.

Martincus, Christian Volpe, Jerónimo Carballo, and Ana Cusolito (2017) "Roads, exports and employment: Evidence from a developing country," *Journal of Development Economics*, 125, 21–39.

Meijer, Johan R, Mark AJ Huijbregts, Kees CGJ Schotten, and Aafke M Schipper (2018) "Global patterns of current and future road infrastructure," *Environmental Research Letters*, 13 (6), 064006.

Meurers, Martin and Johannes Moenius (2018) "Optimal public investment in economic centers and the periphery."

Möller, Joachim and Marcus Zierer (2018) "Autobahns and jobs: A regional study using historical instrumental variables," *Journal of Urban Economics*, 103, 18–33.

MOPU, Ministerio de Obras Públicas (1990) "Recomendaciones para la evolución económica, coste-beneficio de estudios y proyectos de carreteras.."

Morshed, AKM and Santanu Chatterjee, "Infrastructure Provision and Macroeconomic Performance."

Mulet, Sandrine, Marie-Hélène Rio, Hélène Etienne et al. (2021) "The new CNES-CLS18 global mean dynamic topography," *Ocean Science*, 17 (3), 789–808.

NDRC (2015) ''国家发展改革委关于下放部分交通项目审批权和简化审批程序的通知 (Notice from the National Development and Reform Commission on Delegating Approval Authority for Some Transportation Projects and Simplifying Approval Procedures)," *National Development and Reform Commission of China*.

——— (2017) ''国家发展改革委关于进一步下放政府投资交通项目审批权的通知 (Notice on Further Delegating the Approval Authority for Government Investment in Transportation Projects)," *National Development and Reform Commission of China*.

NHK, Documentary (2010) ''登天之路：西藏开山大运输."

Nitsch, Volker (2000) "National borders and international trade: evidence from the European Union," *Canadian Journal of Economics/Revue canadienne d'économique*, 33 (4), 1091–1105.

Novy, Dennis (2013) "Gravity redux: measuring international trade costs with panel data," *Economic inquiry*, 51 (1), 101–121.

Novy, Dennis and Alan M Taylor (2020) "Trade and uncertainty," *Review of Economics and Statistics*, 102 (4), 749–765.

Nunn, Nathan and Diego Puga (2012) "Ruggedness: The blessing of bad geography in Africa," *Review of Economics and Statistics*, 94 (1), 20–36.

Posada-Henao, John Jairo, Iván Sarmiento-Ordosgoitia, and Alexánder A Correa-Espinal (2022) "Effects of Road Slope and Vehicle Weight on Truck Fuel Consumption," *Sustainability*, 15 (1), 724.

Qiu, Larry D, Chaoqun Zhan, and Xing Wei (2019) "An analysis of the China–US trade war through the lens of the trade literature," *Economic and Political Studies*, 7 (2), 148–168.

Redding, Stephen J (2016) "Goods trade, factor mobility and welfare," *Journal of International Economics*, 101, 148–167.

Redding, Stephen J and Esteban Rossi-Hansberg (2017) "Quantitative spatial economics," *Annual Review of Economics*, 9, 21–58.

Redding, Stephen J and Matthew A Turner (2015) "Transportation costs and the spatial organization of economic activity," *Handbook of regional and urban economics*, 5, 1339–1398.

Redding, Stephen and Anthony J Venables (2004) "Economic geography and international inequality," *Journal of international Economics*, 62 (1), 53–82.

Samuelson, Paul A (1954) "The transfer problem and transport costs, II: Analysis of effects of trade impediments," *The Economic Journal*, 64 (254), 264–289.

Santamaria, Marta et al. (2020) *Reshaping Infrastructure: Evidence from the division of Germany*: University of Warwick, Centre for Competitive Advantage in the Global ⋯.

SC (2016) ''政府核准的投资项目目录 (2016 年本)(Catalog of Government-Approved Investment Projects (2016 Edition)),'' *State Council of China*.

Silva, JMC Santos and Silvana Tenreyro (2006) "The log of gravity," *The Review of Economics and statistics*, 88 (4), 641–658.

Simonovska, Ina and Michael E Waugh (2014) "Trade models, trade elasticities, and the gains from trade,"Technical report, National Bureau of Economic Research.

SMOPS (2020) "2019 年上海口岸主要数据统计表 (2019 Main Statistical Data of Shanghai Port)."

Sotelo, Sebastian (2020) "Domestic trade frictions and agriculture," *Journal of Political Economy*, 128 (7), 2690–2738.

Storeygard, Adam (2016) "Farther on down the road: transport costs, trade and urban growth in sub-Saharan Africa," *The Review of economic studies*, 83 (3), 1263–1295.

Sun, Weizhao (2023) *The Earth Is Not Flat: Bilateral Elevation as a Component of Trade Costs*, Ph.D. dissertation, University of Colorado, Boulder.

Szedlmayer, Michael and Chol-Bum M Kweon (2016) "Effect of altitude conditions on combustion and performance of a multi-cylinder turbocharged direct-injection diesel engine,"Technical report, SAE Technical Paper.

Topalova, Petia (2010) "Factor immobility and regional impacts of trade liberalization: Evidence on poverty from India," *American Economic Journal: Applied Economics*, 2 (4), 1–41.

Turner, John P (2006) *Rock-socketed shafts for highway structure foundations*, 360: Transportation Research Board.

Veeneman, Wijnand and Corinne Mulley (2018) "Multi-level governance in public transport: Governmental layering and its influence on public transport service solutions," *Research in Transportation Economics*, 69, 430–437.

Wang, Xin, Yunshan Ge, Linxiao Yu, and Xiangyu Feng (2013) "Effects of altitude on the thermal efficiency of a heavy-duty diesel engine," *Energy*, 59, 543–548.

Weltbank (2009) *Air Freight: A Market Study with Implications for Landlocked Countries*.

Williamson, Oliver E (1971) "The vertical integration of production: market failure considerations," *The American Economic Review*, 61 (2), 112–123.

Wolf, Nikolaus (2009) "Was Germany ever united? Evidence from intra-and international trade, 1885–1933," *The Journal of Economic History*, 69 (3), 846–881.

Wrona, Jens (2018) "Border effects without borders: What divides Japan's internal trade?" *International Economic Review*, 59 (3), 1209–1262.

Xu, Hangtian and Kentaro Nakajima (2017) "Highways and industrial development in the peripheral regions of China," *Papers in Regional Science*, 96 (2), 325–356.

Zhang, Lianyang (2004) *Drilled shafts in rock: analysis and design*: CRC press.

Zhang, Wei, Jue Yang, Wenming Zhang, and Fei Ma (2019) "Research on regenerative braking of pure electric mining dump truck," *World Electric Vehicle Journal*, 10 (2), 39.

Zheng, Heran, Johannes Többen, Erik Dietzenbacher, Daniel Moran, Jing Meng, Daoping Wang, and Dabo Guan (2022) "Entropy-based Chinese city-level MRIO table framework," *Economic Systems Research*, 34 (4), 519–544.

Appendix A

Appendix of Chapter One

A.1 Model

A.1.1 Derivation

There are S countries in the world. There is a representative consumer in each country $i \in S$. Also, there are K sectors and L_i amount of identical labor in each country. Workers are immobile across countries but mobile across sectors that inelastically supply labor. Each sector $k \in K$ in country $i \in S$ is represented by a single firm with exogenous productivity A_i^k. Without loss of generality, let sector subscript $k \in K$ also denote the representative firms. The quantity produced by each firm $k \in K$ while employing L_i^k labor is

$$q_i^k = A_i^k L_i^k \tag{A.1}$$

Assuming perfect competition, the price equals the marginal cost. This implies that the firm-gate price for each sector is given by cost c_i^k and productivity A_i^k.

$$p_i^k = \frac{c_i^k}{A_i^k} \tag{A.2}$$

where c_i^k is the cost of producing goods in sector k in country i.

$$c_i^k = w_i^{\gamma_i^k} \prod_l P_i^{l\eta_i^{lk}} \tag{A.3}$$

γ_i^k is the share of value-added and η_i^{lk} is the share of goods in industry l produced in country i used as intermediate goods in sector k.

There are iceberg trade costs τ_{ij}^k such that for each unit of good in sector k to arrive at destination country $j \in S$, τ_{ij}^k unit must be shipped from firm k in origin country i. τ_{ij}^k depends on sector k, indicating that different sectors face different levels of trade costs. The price in destination j of consuming the one unit of good in sector k from origin i is

$$p_{ij}^k = \tau_{ij}^k \frac{c_i^k}{A_i^k} \tag{A.4}$$

Note that

$$\frac{p_{ij}^k}{p_i^k} = \tau_{ij}^k$$

Moreover, τ_{ij} has the following properties. There are two components of τ_{ij}, distance and bilateral elevation. I assume that distance is symmetric. But, I do not assume bilateral elevation is symmetric.

$$\tau_{ij} = f(dist_{ij}, elev_{ij}) \quad where \;\; dist_{ij} = dist_{ji}; \;\; elev_{ij} \neq elev_{ji} \tag{A.5}$$

In each country, there is a representative consumer who maximizes the following CES preferences:

$$U_j = (\sum_{i \in S} \sum_{k \in K} {a_{ij}^k}^{\frac{1}{\sigma}} {q_{ij}^k}^{\frac{(\sigma-1)}{\sigma}})^{\frac{\sigma}{\sigma-1}} \tag{A.6}$$

subject to the following budget constraint:

$$\sum_{i \in S} \sum_{k \in K} q_{ij}^k p_{ij}^k \leq Y_j \tag{A.7}$$

where Y_j is the income of country j. First order condition yield that

$$(\sum_{i \in S} \sum_{k \in K} {a_{ij}^k}^{\frac{1}{\sigma}} {q_{ij}^k}^{\frac{\sigma-1}{\sigma}})^{\frac{1}{\sigma-1}} {a_{ij}^k}^{\frac{1}{\sigma}} {q_{ij}^k}^{-\frac{1}{\sigma}} = \lambda p_{ij}^k \tag{A.8}$$

where λ is the Lagrangian multiplier. The FOC yields that for each country i and i' and for each industry k and k':

$$\frac{{a_{ij}^k}^{\frac{1}{\sigma}} {q_{ij}^k}^{-\frac{1}{\sigma}}}{{a_{i'j}^{k'}}^{\frac{1}{\sigma}} {q_{i'j}^{k'}}^{-\frac{1}{\sigma}}} = \frac{p_{ij}^k}{p_{i'j}^{k'}} \tag{A.9}$$

Rearrange, multiply both sides by $p^k_{i'j}$, and sum over all countries and industries yield:

$$\sum_{i'\in S}\sum_{k'\in K} q^{k'}_{i'j}p^{k'}_{i'j} = \frac{1}{a^k_{ij}} q^k_{ij}{p^k_{ij}}^{\sigma} \sum_{i'\in S}\sum_{k'\in K} a^k_{i'j}{p^k_{i'j}}^{1-\sigma} \tag{A.10}$$

The left-hand side is equivalent to total production Y_j. Define the Dixit-Stiglitz price index by

$$\begin{aligned} P^k_j &\equiv (\sum_{i'\in S} a^k_{i'j}{p^k_{i'j}}^{1-\sigma})^{\frac{1}{1-\sigma}} \\ &= (\sum_{i'\in S} a^k_{i'j}(\tau^k_{ij}\frac{c^k_i}{A^k_i})^{1-\sigma})^{\frac{1}{1-\sigma}} \\ &= (\sum_{i'\in S} a^k_{i'j}{A^k_{i'}}^{\sigma-1}(\tau^k_{i'j}c^k_{i'})^{1-\sigma})^{\frac{1}{1-\sigma}} \end{aligned} \tag{A.11}$$

Country-level price index can be derived from P^k_j

$$P_j = \prod_{k\in K} (\frac{P^k_j}{\mu^k_j})^{\mu^k_j} \tag{A.12}$$

where μ^k_i is the consumption share of country i in industry k.

Define the trade value of the sector from country i to country j by $X^k_{ij} \equiv q^k_{ij}p^k_{ij}$. Rearranging the previous equation and multiplying both sides by p^k_{ij} yields the following gravity equation:

$$X^k_{ij} = a^k_{ij}{p^k_{ij}}^{1-\sigma}Y^k_j P^{\sigma-1}_j \tag{A.13}$$

Plug in the expression for p^k_{ij} gives:

$$X^k_{ij} = a^k_{ij}(\tau^k_{ij}\frac{c^k_i}{A^k_i})^{1-\sigma}Y^k_j P^{\sigma-1}_j \tag{A.14}$$

The trade share of country j with respect to country i in sector k, λ^k_{ij}, is the proportion of goods in sector k shipped to country j from country i relative to the total amount of k shipped to country j.

$$\lambda^k_{ij} \equiv \frac{X^k_{ij}}{\sum_{i'\in S} X^k_{i'j}} = \frac{a^k_{ij}(\tau^k_{ij}\frac{c^k_i}{A^k_i})^{1-\sigma}}{\sum_{i'\in S} a^k_{i'j}(\tau^k_{i'j}\frac{c^k_{i'}}{A^k_{i'}})^{1-\sigma}} \tag{A.15}$$

Trade balance includes the trade deficit, D_i.

$$\sum_{j\in S}\sum_{k\in K} X^k_{ij} - D_i = \sum_{j\in S}\sum_{k\in K} X^k_{ji} \tag{A.16}$$

Or equivalently

$$\sum_{i\in S}\sum_{k\in K}\lambda_{ij}^{k}Y_{j}^{k}-D_{i}=\sum_{i\in S}\sum_{k\in K}\lambda_{ji}^{k}Y_{i}^{k} \tag{A.17}$$

The total expenditure on goods from sector k in country i is:

$$Y_{i}^{k}=\sum_{l}\eta_{i}^{kl}\sum_{j}\lambda_{ji}^{l}Y_{j}^{l}+\mu_{i}^{k}I_{i} \tag{A.18}$$

where I_i represent final absorption in country i.

$$I_{i}=w_{i}L_{i}+D_{i} \tag{A.19}$$

A.1.2 Solution

The model is solved using hat-algebra. For any variable a, a' is the counterfactual value of a moving from policy τ to τ'. $\hat{a}=\frac{a'}{a}$ is the relative change in a after the policy. The equations below define the equilibrium.

$$\hat{c}_{i}^{k}=\hat{w}_{i}{}^{\gamma_{i}^{k}}\prod_{l}\hat{P}_{i}^{l}{}^{\eta_{i}^{lk}} \tag{A.20}$$

$$\hat{P}_{j}^{k}=\big(\sum_{i\in S}\lambda_{ij}^{k}(\hat{\tau}_{i}^{k}\hat{c}_{i}^{k})^{1-\sigma}\big)^{\frac{1}{1-\sigma}} \tag{A.21}$$

$$\hat{\lambda}_{ij}^{k}=\big(\frac{\hat{\tau_{ij}^{k}}\hat{c}_{i}^{k}}{\hat{P}_{j}^{k}}\big)^{1-\sigma} \tag{A.22}$$

$$Y_{i}^{k\prime}=\sum_{l}\eta_{i}^{kl}\sum_{j}\lambda_{ji}^{l}{}'Y_{j}^{l\prime}+\mu_{i}^{k}I_{i}' \tag{A.23}$$

$$I'=(w_{i}L_{i})\hat{w}_{i}+D_{i} \tag{A.24}$$

$$D_{i}=\sum_{k}\sum_{j}\lambda_{ij}^{k}{}'Y_{i}^{k\prime}-\sum_{k}\sum_{j}\lambda_{ji}^{k}{}'Y_{j}^{k\prime} \tag{A.25}$$

Lastly, the equilibrium change in welfare for each country is represented by the relative change in the real wage, $ln(\frac{\hat{w}_i}{\hat{P}_i})$, where $\hat{P}_i$ is the change in the aggregate price level. Recall that μ_i^k is the consumption share.

$$\hat{P}_i = \prod_k \hat{P_i^k}^{\mu_i^k} \tag{A.26}$$

Trade cost is calibrated as follows:

$$\tau_{ij} = exp\left(\frac{\alpha_1 * log(Dist_{ij}) + \alpha_2^k * log(Elev_{ij})}{1-\sigma^k}\right) \tag{A.27}$$

where α_1 is the coefficient on the log of route distance in the baseline regression, and α_2^k are the industry-heterogeneous coefficients on the log of bilateral elevation estimated in section 1.7.2.

$$\hat{\tau}_{ij} = \frac{\tau_{ij}^{'}}{\tau_{ij}} \tag{A.28}$$

A.2 More Extensions and Robustness Checks

A.2.1 Island Countries

As an additional robustness check, this section analyzes the validity of the bilateral elevation measure when island countries are included in the sample. Island countries are excluded from the baseline regression as they primarily engage in maritime trade, which is not the primary focus of this paper.

In this section, I illustrate that the existing measures of bilateral elevation effectively accommodate maritime trade by assuming a zero change in elevation over the ocean. Essentially, maritime trade is a way to circumvent elevation changes. Consequently, island countries exhibit minimal average bilateral elevation measures to the rest of the world.

Table A.1 presents the results from the regression which incorporates islands into the sample. The coefficients on bilateral elevations in columns (2) and (3) are observed to be larger than the baseline counterparts while remaining statistically significant.

VARIABLES	(1) $\log(X_{ijt}^k)$	(2) X_{ijt}^k	(3) $\log(X_{ijt}^k)$	(4) $\log(X_{ijt}^k)$	(5) X_{ijt}^k	(6) $\log(X_{ijt}^k)$
log(Route Distance)	-0.969***	-0.598***	-0.966***			
	(0.023)	(0.029)	(0.023)			
log(Bilateral Elevation)	-0.087***	-0.070***	-0.093***	-0.117***	-0.087***	-0.122***
	(0.007)	(0.016)	(0.008)	(0.007)	(0.016)	(0.008)
log(Straight Distance)				-0.985***	-0.586***	-0.984***
				(0.021)	(0.028)	(0.021)
Model	OLS	PPML	IV	OLS	PPML	IV
Kleibergen-Paap F-Statistic			70,508		72,285	

Standard errors in parentheses
**** p<0.01, ** p<0.05, * p<0.1*

Table A.1: Baseline Regression Including Island Countries

Note: This table shows the regression results with a larger sample with 84 countries in Europe and Asia, including island countries. Newly included island countries are: Japan(JPN), Philippines(PHL), Brunei(BRN), Sri Lanka(LKA), Indonesia(IDN), Cyprus(CYP), Ireland(IRL), Iceland(ISL) and Malta(MLT). Note that UK(GBR) and Singapore(SGP) are island countries but were included in the baseline sample because they are connected to the continent by bridges and tunnels. The number of observations is 1,099,062. Other aspects of the regressions are identical to the baseline regressions.

A.2.2 Bilateral Elevations Using Smaller Interval

This section serves as an additional robustness check, examining the impacts of using smaller intervals between sample points in the data-generating process of bilateral elevations. Specifically, I reduce the interval between sample points from 20 miles to 10 miles. This adjustment nearly doubles the number of sampled points along routes.

Table A.2 presents the impact of EBEs with smaller intervals, excluding island countries. First-stage regression results for IV can be found in Table A.11. Summary statistics for different versions of EBE measures can be found in Table A.12. In summary, the coefficients and their significance in Table A.2 are in line with the results presented in the main sections. Reducing the interval from 20 to 10 miles does not alter the benchmark findings. Since this paper's primary objective is to capture elevation changes along trade routes, the 20-mile interval proves sufficient for this purpose.

However, smaller intervals yield more detailed measures, albeit at the cost of longer processing times. Employing smaller intervals may be necessary for future research that focuses on analyzing

VARIABLES	(1) $\log(X^k_{ijt})$	(2) X^k_{ijt}	(3) $\log(X^k_{ijt})$	(4) $\log(X^k_{ijt})$	(5) X^k_{ijt}	(6) $\log(X^k_{ijt})$
log(Route Distance)	-0.987***	-0.596***	-0.984***			
	(0.027)	(0.030)	(0.027)			
log(Bilateral Elevation)	-0.044***	-0.042*	-0.056***	-0.078***	-0.058**	-0.090***
	(0.010)	(0.023)	(0.011)	(0.010)	(0.023)	(0.011)
log(Straight Distance)				-1.002***	-0.587***	-1.002***
				(0.024)	(0.029)	(0.024)
Model	OLS	PPML	IV	OLS	PPML	IV
Kleibergen-Paap F-Statistic			48,697		49,003	

Standard errors in parentheses
**** p<0.01, ** p<0.05, * p<0.1*

Table A.2: Effective Bilateral Elevation With Smaller Intervals

Note: The effective bilateral elevations used in these regressions are calculated with 10-mile intervals rather than 20-mile intervals. Other aspects of the regressions are identical to the baseline regressions.

specific infrastructure segments (e.g., tunnels) with lengths shorter than 20 miles. Smaller intervals may also be crucial if precise measurements of elevation changes along different routes are required. It's worth noting that updating the elevation data to finer levels becomes necessary when further reducing the interval. The elevation data used in this paper are at the 15-arc-second level.

A.2.3 Bilateral Elevation Based On Straight Lines

In this section, as an additional extension, I ask the following question: Does a bilateral elevation measure based on straight lines capture enough information on the actual changes in elevation traversed by vehicles? To answer this question, first, I generate straight lines between the capitals of the origin and destination. Second, I take many sampled points 20 miles apart, along straight lines, just like the process described in the main sections. Then, I hold other aspects of the process constant and calculate PBEs and EBEs based on straight lines. Lastly, I calculate the difference, Δ, between the EBE based on straight lines and based on actual routes.

$$\Delta = \frac{Elev_{ij}^{straight} - Elev_{ij}}{Elev_{ij}} * 100 \tag{A.29}$$

where $Elev_{ij}^{straight}$ is the EBE calculated based on straight lines between capitals, and $Elev_{ij}$ is the standard EBE based on routes.

Table A.3 summarizes the comparison result. The minimum in Table A.3 suggests that the EBE, $Elev_{ij}^{straight}$, that is based on straight lines, can be 93 percent lower than the corresponding EBE based on routes, $Elev_{ij}$. The maximum shows that the straight $Elev_{ij}^{straight}$ can be 39,104 percent higher than the corresponding route $Elev_{ij}$. On average, $Elev_{ij}^{straight}$ tends to overstate the actual $Elev_{ij}$ by 196.08 percent. The standard deviation, 1077, suggests that the variation of mis-measurement is substantial. I then calculated the percentage of observations such that $Elev_{ij}^{straight}$ is no more than 10% away from $Elev_{ij}$. Only 9.3 percent of the observations satisfy this criterion.

Variable	mean	sd	min	max
Δ	196.08	1077.10	-93.36	39104.32

Table A.3: Difference Between EBE Along Straight Lines and EBE Along Routes

Why is $Elev_{ij}^{straight}$ such a bad proxy for $Elev_{ij}$? There are at least three reasons: (1) $Elev_{ij}^{straight}$ may include too many mountains along the straight lines, which, in reality, are avoided by going around them. This is the primary reason why $Elev_{ij}^{straight}$ overstates. (2) Straight lines ignore many elevation changes within rugged areas, as actual routes in such terrain tend to zigzag and are longer than straight lines. Consequently, $Elev_{ij}^{straight}$ may underestimate elevation changes within mountainous regions. (3) $Elev_{ij}^{straight}$ may include excessive water bodies that actual roads typically avoid. This over-representation of water in straight lines can lead to an underestimation of elevation changes.

A.2.4 Bilateral Elevation Based on A Different Speed

In this section, as an additional robustness check, I test the validity of EBE if trucks' fuel consumption is calculated at a different speed. Recall equation (3) borrowed from MOPU (1990),

which calculates truck fuel consumption.

For uphill and flat roads($p \geq 0$):

$$c = 388.18 - 7.32 * Vcp + 0.0700 * Vcp^2 + 101.28 * p + 0.019 * Vcp * p + 7.85 * 10^{-3} * Vcp^2 * p$$

For downhill roads($p < 0$):

$$c = 213.31 - 6.15 * Vcp + 0.0742 * Vcp^2 + 6.08 * p + 0.0382 * Vcp * p + 7.27 * 10^{-4} * Vcp^2 * p$$

where p is the slopes of roads in percentage; c, in cubic centimeters(milliliters), is the fuel consumption per kilometer, and Vcp is the speed in kilometers per hour.

	(1)	**(2)**	**(3)**	**(4)**
VARIABLES	X_{ijt}^k	$\mathbf{log}(X_{ijt}^k)$	X_{ijt}^k	$\mathbf{log}(X_{ijt}^k)$
log(Route Distance)	-0.594***	-0.984***		
	(0.030)	(0.027)		
log(Bilateral Elevation)	-0.048*	-0.059***	-0.067***	-0.093***
	(0.025)	(0.011)	(0.025)	(0.011)
log(Straight Distance)			-0.586***	-1.001***
			(0.029)	(0.024)
Model	PPML	IV	PPML	IV
Kleibergen-Paap F-Statistic		49,372		49,760

Standard errors in parentheses

**** p<0.01, ** p<0.05, * p<0.1*

Table A.4: Bilateral Elevation Based on A Different Speed

Note: The table shows the results of PPML and IV regressions in which the effective bilateral elevation is calculated assuming the speed is 90km/h. This is different from the 50km/h speed in the main sections. Other aspects of the regressions are identical to the baseline counterpart.

In the main section of this paper, the speed has been assumed to be constant at 50km/h. In this section, I assume the speed to be 90 km/h and regenerate EBE using the benchmark 20-mile interval, holding other parts of the procedure constant. Then, I examine the impact of the updated EBE using the baseline PPML and IV regressions. Other aspects of the regressions (sample, controls, clustered standard errors, fixed effects, etc) are identical to their baseline counterpart. The results are shown in Table A.4. Table A.4 indicates that the choice of speed does not significantly alter the baseline results. The speed only affects the fuel-consumption ratio, w_{grade}, by a little bit. A comparison between fuel-consumption ratios for different versions of EBE can be found in Table A.13. First-stage regression results for IV can be found in Table A.11. Summary statistics for different versions of EBE measures can be found in Table A.12.

A.2.5 Bilateral Elevation Based On Other Transportation Literature

In this section, as an additional robustness check, I test the validity of effective bilateral elevation (EBE) if trucks' fuel consumption is calculated based on formulas in more recent transportation literature. The baseline fuel consumption in Section 1.2 follows MOPU (1990) because, to my knowledge, it is the only paper that calculates trucks' fuel consumption on both uphill and downhill roads. But, one may question whether the formulas from 1990 have been obsolete.

A more recent paper, Posada-Henao et al. (2022), conducts experiments with carefully chosen representative trucks in Colombia and evaluates trucks' fuel consumption only on uphill roads and overlooking downhill roads. The trucks used in Posada-Henao et al. (2022) are rigid-type trucks with three axles and articulated trucks with six axles (C3 and C3S3 as the official classification in Colombia, respectively), with engine powers of 350 HP (10,800 cc) and 400 HP (15,000 cc). Another recent transportation paper, Faria et al. (2019), attempts to measure fuel consumption for a sample of passenger cars in Portugal on both uphill and downhill roads.

I devise two alternative measures for EBE based on findings from recent literature. The first alternative integrates elements from Posada-Henao et al. (2022) and MOPU (1990). It combines the uphill fuel consumption formula for C3 type trucks from Posada-Henao et al. (2022) with the

downhill formula provided in MOPU (1990). EBE is recalculated with an assumed speed of 50 km/h.

The second alternative utilizes the fuel-consumption ratios for passenger cars as outlined in Faria et al. (2019). According to the findings in this paper, while the level of fuel consumption varies with speed, the fuel-consumption ratio remains relatively stable for non-aggressive drivers within the speed range of 50 km/h to 90 km/h. Consequently, I employ the stable fuel-consumption ratio applicable to speeds between 50 km/h and 90 km/h for non-aggressive drivers from Faria et al. (2019).

	(1)	**(2)**	**(3)**	**(4)**	**(5)**	**(6)**	**(7)**	**(8)**
VARIABLES	X_{ijt}^k	$\mathbf{log}(X_{ijt}^k)$	X_{ijt}^k	$\mathbf{log}(X_{ijt}^k)$	X_{ijt}^k	$\mathbf{log}(X_{ijt}^k)$	X_{ijt}^k	$\mathbf{log}(X_{ijt}^k)$
log(Route Distance)	-0.594***	-0.982***			-0.596***	-0.985***		
	(0.030)	(0.027)			(0.030)	(0.027)		
log(Bilateral Elevation)	-0.045*	-0.056***	-0.062**	-0.089***	-0.049*	-0.062***	-0.068**	-0.099***
	(0.024)	(0.011)	(0.024)	(0.010)	(0.027)	(0.012)	(0.027)	(0.012)
log(Straight Distance)			-0.585***	-0.998***			-0.589***	-1.003***
			(0.029)	(0.024)			(0.029)	(0.024)
Model	PPML	IV	PPML	IV	PPML	IV	PPML	IV
Kleibergen-Paap F-Statistic		43,666		44,020		54,645		54,871

Standard errors in parentheses

**** p<0.01, ** p<0.05, * p<0.1*

Table A.5: Bilateral Elevations Based On Different Transportation Literature

Note: This table shows the regression results for the alternative EBE measures based on fuel consumption results in Posada-Henao et al. (2022) and Faria et al. (2019). The bilateral elevation measure in columns (1)-(4) is a hybrid between Posada-Henao et al. (2022) and MOPU (1990). The uphill fuel consumption formula for C3 type trucks in Posada-Henao et al. (2022) is combined with the downhill formula in MOPU (1990). The bilateral elevation measure in columns (5)-(8) uses the fuel-consumption ratios for passenger cars in Faria et al. (2019). Other aspects (sample, controls, clustered standard errors, and fixed effects) of the regressions are identical to the baseline regressions.

I conduct the baseline PPML and IV regression using the two alternative measures. The regression outcomes are detailed in Table A.5. Columns (1)-(4) display the results of the first alternative EBE, while columns (5)-(8) exhibit the second. A comparison of fuel-consumption ratios is presented in Table A.13. It demonstrates that the fuel-consumption ratios derived from MOPU (1990) and Posada-Henao et al. (2022) exhibit striking similarity. Conversely, ratios derived from Faria et al. (2019) for passenger cars are considerably smaller compared to those for trucks. Despite the variance in fuel-consumption ratios, the alternative EBE measures effectively capture bilateral elevation, as evidenced by the coefficients in Table A.5, which align with those obtained in the baseline regressions.

A.3 Supplementary Tables and Figures

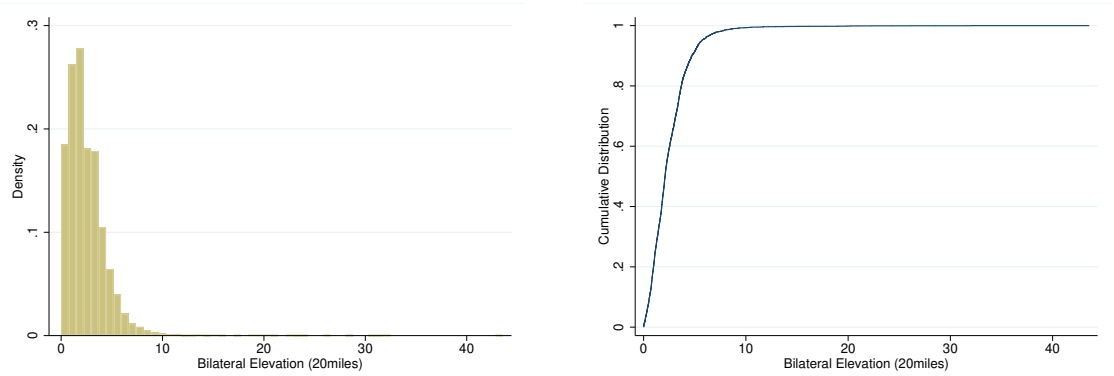

(a) Density (b) Cumulative Distribution

Figure A.1: Distribution of EBE

Notes: Panel (a) shows the density of baseline EBE measure. Panel (b) shows its cumulative distribution.

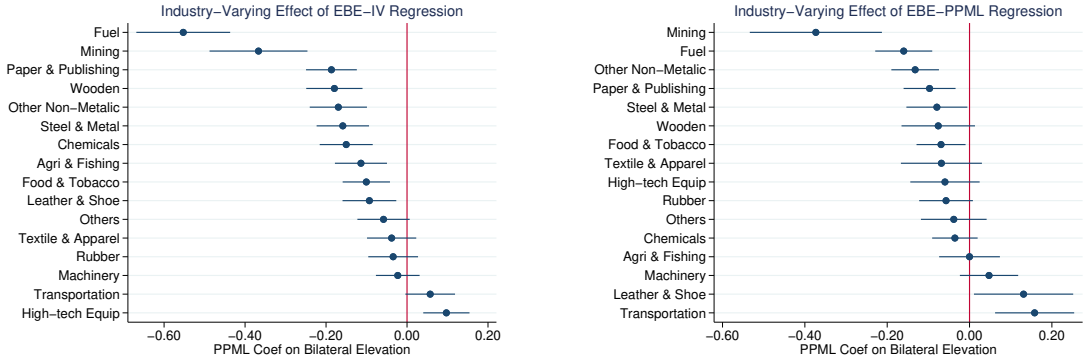

(a) IV (b) PPML

Figure A.2: Industry-Varying Effect of EBE

Note: These figures show the industry-varying effect of EBE, controlling for the great-circle distance. Panel (a) uses IV. Panel (b) uses PPML. The coefficients shown in these figures can be found in Table A.6 in the Appendix.

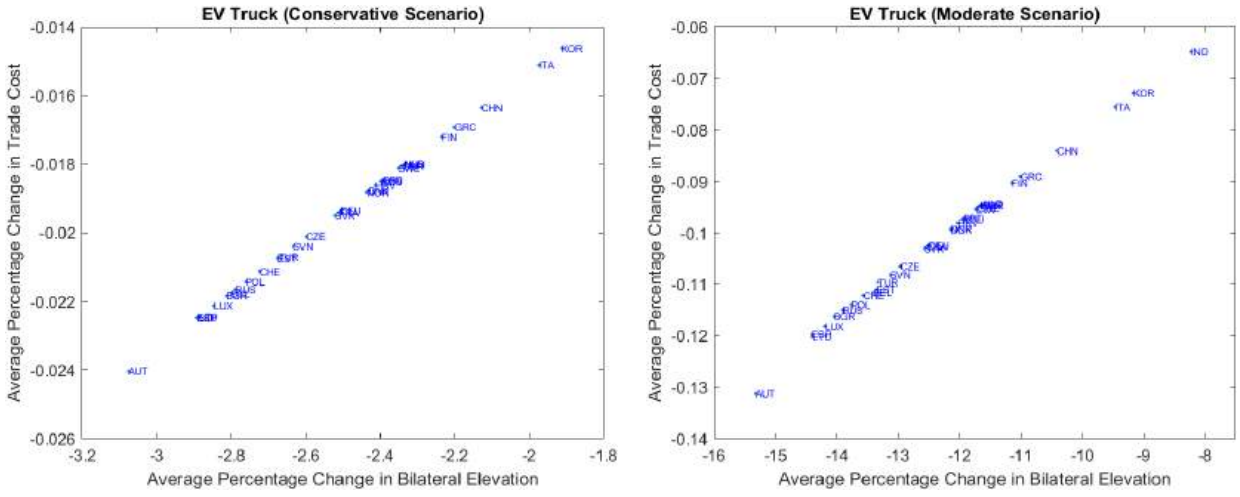

(a) (b)

Figure A.3: EBE, Trades Costs and EV Trucks

Note: Panels (a) and (b) show how reductions in EBE translate to reductions in trade costs with the prevalence of EV trucks. Panel (a) shows the conservative scenario. Panel (b) shows the moderate scenario.

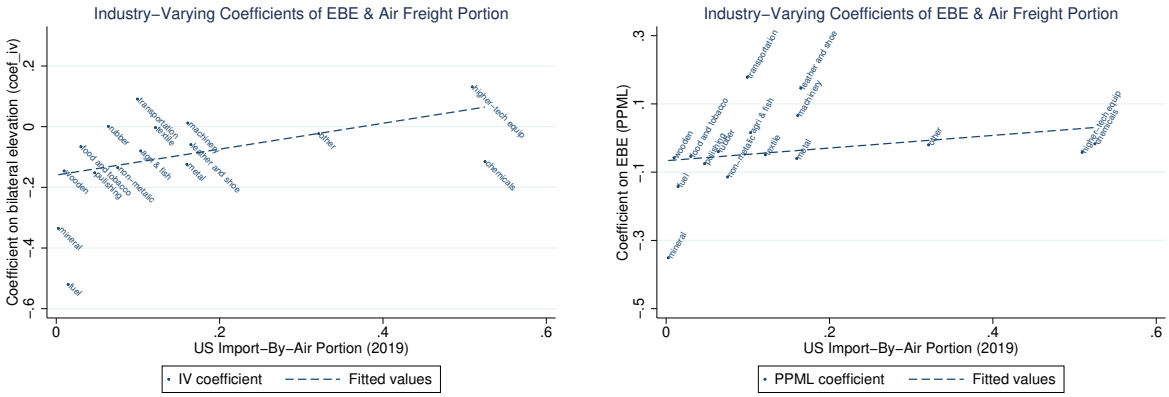

(a) IV

(b) PPML

Figure A.4: Industry-varying Coefficients on EBE and US Import-by-air Portion

Note: The figures presented depict the US import-by-air portion plotted against the coefficients on bilateral elevation for various grouped industries. Positive correlations in both panels imply that industries with less frequent use of air freight tend to exhibit more negative coefficients on Effective Bilateral Elevation (EBE). These correlations are relatively weak, suggesting that the US import-by-air portion for each industry may not be the most accurate proxy for assessing air transportation patterns in Eurasian countries. This limitation is attributed to the scarcity of data on international air freight between Eurasian countries.

		(1)	(2)	(3)	(4)	(5)	(6)
ISIC Rev.3.1 Grouped Industry	**VARIABLES**	**log(X^k_{ijt})**	**X^k_{ijt}**	**log(X^k_{ijt})**	**log(X^k_{ijt})**	**X^k_{ijt}**	**log(X^k_{ijt})**
	log(Dist)	-0.985***	-0.618***	-1.099***	-0.998***	-0.609***	-1.088***
		(0.027)	(0.029)	(0.022)	(0.024)	(0.029)	(0.020)
Agriculture, Fishing	Industry*log($Elev_{ij}$)	-0.036	0.016	-0.080**	-0.071**	-0.000	-0.114***
		(0.031)	(0.038)	(0.033)	(0.031)	(0.038)	(0.033)
Mining, Quarrying, Oil	Industry*log($Elev_{ij}$)	-0.298***	-0.351***	-0.335***	-0.333***	-0.373***	-0.367***
		(0.058)	(0.081)	(0.062)	(0.058)	(0.082)	(0.062)
Food, Tobacco	Industry*log($Elev_{ij}$)	-0.043	-0.054*	-0.066**	-0.079***	-0.069**	-0.101***
		(0.029)	(0.031)	(0.031)	(0.028)	(0.030)	(0.030)
Textile, Apparel	Industry*log($Elev_{ij}$)	0.017	-0.049	-0.003	-0.019	-0.068	-0.038
		(0.031)	(0.051)	(0.031)	(0.030)	(0.050)	(0.031)
Leather, Shoe	Industry*log($Elev_{ij}$)	-0.014	0.146**	-0.059*	-0.050	0.131**	-0.093***
		(0.033)	(0.061)	(0.034)	(0.033)	(0.062)	(0.034)
Wooden Products	Industry*log($Elev_{ij}$)	-0.115***	-0.058	-0.146***	-0.150***	-0.076*	-0.179***
		(0.035)	(0.046)	(0.036)	(0.035)	(0.046)	(0.035)
Paper, Publishing	Industry*log($Elev_{ij}$)	-0.127***	-0.075**	-0.152***	-0.162***	-0.097***	-0.187***
		(0.030)	(0.032)	(0.033)	(0.030)	(0.032)	(0.032)
Fuel	Industry*log($Elev_{ij}$)	-0.479***	-0.142***	-0.520***	-0.514***	-0.160***	-0.553***
		(0.053)	(0.036)	(0.060)	(0.053)	(0.035)	(0.059)
Chemicals	Industry*log($Elev_{ij}$)	-0.093***	-0.017	-0.115***	-0.129***	-0.036	-0.150***
		(0.032)	(0.028)	(0.034)	(0.031)	(0.028)	(0.033)
Rubber	Industry*log($Elev_{ij}$)	0.004	-0.040	0.001	-0.032	-0.057*	-0.034
		(0.030)	(0.033)	(0.032)	(0.030)	(0.033)	(0.031)
Other Non-Metallic Mineral	Industry*log($Elev_{ij}$)	-0.122***	-0.114***	-0.135***	-0.158***	-0.132***	-0.170***
		(0.034)	(0.030)	(0.037)	(0.034)	(0.029)	(0.036)
Basic Metal, Steel	Industry*log($Elev_{ij}$)	-0.126***	-0.060	-0.124***	-0.161***	-0.079**	-0.159***
		(0.032)	(0.038)	(0.034)	(0.032)	(0.038)	(0.033)
Machinery	Industry*log($Elev_{ij}$)	0.040	0.066*	0.012	0.004	0.047	-0.023
		(0.027)	(0.036)	(0.028)	(0.027)	(0.036)	(0.028)
Higher-Tech Machinery	Industry*log($Elev_{ij}$)	0.152***	-0.042	0.131***	0.117***	-0.060	0.097***
		(0.029)	(0.043)	(0.030)	(0.028)	(0.043)	(0.029)
Transportation	Industry*log($Elev_{ij}$)	0.101***	0.178***	0.091***	0.066**	0.158***	0.057*
		(0.030)	(0.049)	(0.032)	(0.030)	(0.049)	(0.031)
Others	Industry*log($Elev_{ij}$)	0.012	-0.020	-0.023	-0.024	-0.038	-0.058*
		(0.032)	(0.041)	(0.033)	(0.031)	(0.041)	(0.033)
Model		OLS	PPML	IV	OLS	PPML	IV
Kleibergen-Paap F-Statistic				2545			2503

Standard errors in parentheses

**** p<0.01, ** p<0.05, * p<0.1*

Table A.6: Industry-Varying Effects of EBE

Note: This table provides a list of 16 grouped sectors in the empirical analysis and summarizes the regression coefficients to show the heterogeneous impacts of EBE on different industry groups. It supplements the regressions in Section 1.7.2. Columns (1)-(3) use the shortest route distance from ArcGIS path-finding process as the distance variable. Columns (3)-(6) use the great-circle distance as the distance variable. The IV regressions in columns (3) and (6) are conducted by instrumenting $Industry * log(Elev_{ij})$ with $Industry * log(IV)$, where $Elev_{ij}$ is the EBE. Trade values are aggregated to two-digit ISIC industry levels and further grouped into 16 groups similar to that in the World-Input-Output Table. Standard errors are clustered at the country-pair-industry level. Destination-industry-year and origin-industry-year fixed effects are included. The sample includes 75 countries on the Eurasian landmass. The sample covers a period of time from 2014 to 2019. The number of observations is 869,709.

		(1)	(2)
ISIC Rev.3.1 Grouped Industry	**VARIABLES**	**log(X_{ijt}^k)**	**log(X_{ijt}^k)**
Agriculture, Fishing	Industry*log($Elev_{ij}$)	-0.013	-0.047
		(0.039)	(0.038)
Mining, Quarrying, Oil	Industry*log($Elev_{ij}$)	-0.315***	-0.356***
		(0.071)	(0.069)
Food, Tobacco	Industry*log($Elev_{ij}$)	0.017	-0.013
		(0.036)	(0.035)
Textile, Apparel	Industry*log($Elev_{ij}$)	-0.095***	-0.120***
		(0.033)	(0.033)
Leather, Shoe	Industry*log($Elev_{ij}$)	-0.117***	-0.146***
		(0.037)	(0.037)
Wooden Products	Industry*log($Elev_{ij}$)	-0.108**	-0.149***
		(0.042)	(0.041)
Paper, Publishing	Industry*log($Elev_{ij}$)	0.002	-0.039
		(0.039)	(0.037)
Fuel	Industry*log($Elev_{ij}$)	-0.266***	-0.326***
		(0.069)	(0.066)
Chemicals	Industry*log($Elev_{ij}$)	-0.109***	-0.145***
		(0.038)	(0.037)
Rubber	Industry*log($Elev_{ij}$)	0.034	-0.002
		(0.037)	(0.035)
Other Non-Metallic Mineral	Industry*log($Elev_{ij}$)	-0.084**	-0.122***
		(0.042)	(0.041)
Basic Metal, Steel	Industry*log($Elev_{ij}$)	-0.084**	-0.123***
		(0.039)	(0.037)
Machinery	Industry*log($Elev_{ij}$)	-0.062**	-0.093***
		(0.030)	(0.030)
Higher-Tech Machinery	Industry*log($Elev_{ij}$)	0.032	0.006
		(0.032)	(0.031)
Transportation	Industry*log($Elev_{ij}$)	0.055	0.027
		(0.034)	(0.033)
Others	Industry*log($Elev_{ij}$)	-0.038	-0.071**
		(0.037)	(0.036)
Model		Full-Gravity IV	Full-Gravity IV
Kleibergen-Paap F-Statistic		214.9	216.6

Standard errors in parentheses

**** p<0.01, ** p<0.05, * p<0.1*

Table A.7: Industry-Varying Effect of EBE: Full-Gravity IV

Note: This table provides the coefficients of the full-gravity IV regressions. $Industry * log(Elev_{ij})$ is instrumented by $Industry * log(IV)$, where $Elev_{ij}$ is the EBE. In addition, all variables in the regression (including the controls) are interacted with the industry dummies. It supplements the regressions in Section 1.7.2. Column (1) uses route distance as the distance variable, and column (2) uses straight distance. Trade values are aggregated to two-digit ISIC industry levels and further grouped into 16 groups similar to that in the World-Input-Output Table. Standard errors are clustered at the country-pair-industry level. Destination-industry-year and origin-industry-year fixed effects are included. The sample includes 75 countries on the Eurasian landmass. The sample covers a period from 2014 to 2019. The number of observations is 869,709.

Country	Country	Country	Country
Afghanistan(AFG)	Albania(ALB)	Andorra(AND)	United Arab Emirates(ARE)
Armenia(ARM)	Austria(AUT)	Azerbaijan(AZE)	Belgium(BEL)
Bangladesh(BGD)	Bulgaria(BGR)	Bahrain(BHR)	Bosnia and Herzegovina(BIH)
Belarus(BLR)	Bhutan(BTN)	Switzerland(CHE)	China(CHN)
Czech Republic(CZE)	Germany(DEU)	Denmark(DNK)	Spain(ESP)
Estonia(EST)	Finland(FIN)	France(FRA)	Great Britain(GBR)
Georgia(GEO)	Greece(GRC)	Croatia(HRV)	Hungary(HUN)
India(IND)	Iran(IRN)	Iraq(IRQ)	Israel(ISR)
Italy(ITA)	Jordan(JOR)	Kazakhstan(KAZ)	Kyrgyzstan(KGZ)
Cambodia(KHM)	South Korea(KOR)	Kuwait(KWT)	Laos(LAO)
Lebanon(LBN)	Lithuania(LTU)	Luxembourg(LUX)	Latvia(LVA)
Moldova(MDA)	North Macedonia(MKD)	Myanmar(MMR)	Mongolia(MNG)
Malaysia(MYS)	Netherland(NLD)	Norway(NOR)	Nepal(NPL)
Oman(OMN)	Pakistan(PAK)	Poland(POL)	Portugal(PRT)
Qatar(QAT)	Romania(ROU)	Russia(RUS)	Saudi Arabia(SAU)
Serbia(SER or SRB)	Singapore(SGP)	San Marino(SMR)	Slovakia(SVK)
Slovenia(SVN)	Sweden(SWE)	Syria(SYR)	Thailand(THA)
Tajikistan(TJK)	Turkmenistan(TKM)	Turkey(TUR)	Ukraine(UKR)
Uzbekistan(UZB)	Vietnam(VNM)	Yemen(YEM)	

Table A.8: List of 75 Countries in the Empirical Analysis

Note: Each country's ISO 3166-1 alpha-3 code is provided in the parenthesis. All countries are on Eurasian landmass except Singapore and Great Britain which are connected to the Eurasian continents via bridges and tunnels.

Left Column				Right Column			
Number	**Sector**	α_2^k	θ^k	**Number**	**Sector**	α_2^k	θ^k
1	Agriculture	-0.114	9.11	25	Water Transport	NA	10.4
2	Mining	-0.314	13.53	26	Air Transport	NA	10.4
3	Food Products	-0.056	2.62	27	Warehousing	NA	10.4
4	Textiles	-0.013	9.10	28	Postal	NA	10.4
5	Wooden Products	-0.130	11.50	29	Accommodation and Food Service	NA	10.4
6	Paper	-0.125	16.52	30	Publishing	NA	10.4
7	Refined Petroleum	-0.822	64.85	31	Video, Television Products	NA	10.4
8	Chemicals	-0.190	3.13	32	Telecommunication	NA	10.4
9	Rubber, Plastic	-0.039	1.67	33	Computer Programming	NA	10.4
10	Non-Metallic	-0.168	2.41	34	Financial Service	NA	10.4
11	Basic Metals	-0.122	3.28	35	Insurance	NA	10.4
12	Metals	-0.017	6.99	36	Financial	NA	10.4
13	Electronics	-0.046	12.95	37	Real Estate	NA	10.4
14	Electrical	-0.046	12.91	38	Legal and Accounting Service	NA	10.4
15	Machinery	-0.062	1.45	39	Architectural, Engineering	NA	10.4
16	Motor Vehicles	-0.046	1.84	40	Research	NA	10.4
17	Furniture	-0.038	3.98	41	Advertising	NA	10.4
18	Service on Machinery	NA	10.4	42	Other Professional	NA	10.4
19	Electricity, Gas	NA	10.4	43	Administrative	NA	10.4
20	Construction	NA	10.4	44	Public Defence	NA	10.4
21	Motor and Service	NA	10.4	45	Education	NA	10.4
22	Wholesale Trade	NA	10.4	46	Human Health	NA	10.4
23	Retail Trade	NA	10.4	47	Other Services	NA	10.4
24	Transport on Land	NA	10.4				

Table A.9: List of 47 Sectors and Coefficients in the Counterfactual Analysis

Note: Grouped Manufacturing sectors are number 1-17. Similar to Section 1.7.2, the coefficient on EBE is estimated by including interaction terms between EBE and the industry dummies in an IV regression that uses data from the 2014 World Input-Output Table. If a coefficient is positive for a sector, it is replaced with the corresponding coefficient from the full-gravity IV regression. If it is still positive, it's replaced with the coefficient in the baseline model, -0.046. Service sectors are number 18-47, and they do not have coefficients because they are assumed to be unaffected by changes in bilateral elevation. The θ^k is the trade elasticity taken from the 99% sample in Table 1 of Caliendo and Parro (2015). θ_k is used to calibrate σ^k in the model, where $\sigma^k = \theta^k + 1$. The trade elasticity for the service sectors is 10.4, the average between those of the manufacturing sectors.

Country	Country	Country	Country
Austria(AUT)	Belgium(BEL)	Bulgaria(BGR)	Switzerland(CHE)
China(CHN)	Czech Republic(CZE)	Germany(DEU)	Denmark(DNK)
Spain(ESP)	Estonia(EST)	Finland(FIN)	France(FRA)
Great Britain (GBR)	Greece(GRC)	Croatia(HRV)	Hungary(HUN)
India(IND)	Italy(ITA)	South Korea(KOR)	Lithuania(LTU)
Luxembourg(LUX)	Latvia(LVA)	Netherland(NLD)	Norway(NOR)
Poland(POL)	Portugal(PRT)	Romania(ROU)	Russia(RUS)
Slovakia(SVK)	Slovenia(SVN)	Sweden(SWE)	Turkey(TUR)

Table A.10: List of 32 Countries in the Counterfactual Analysis

Note: Each country's ISO 3166-1 alpha-3 code is provided in the parenthesis. Due to data limitations, the counterfactual analysis utilizes fewer countries than in the empirical analysis.

	(1)	(2)	(3)	(4)	(5)
VARIABLES	**log**($Elev_{ij}$)	**log**($Elev_{ij}$)	**log**($Elev_{ij}$)	**log**($Elev_{ij}$)	**log**($Elev_{ij}$)
log(IV)	0.914***	0.925***	0.936***	0.838***	0.890***
	(0.004)	(0.004)	(0.004)	(0.004)	(0.004)
Model	First Stage	First Stage	First Stage	First Stage	First Stage

Standard errors in parentheses

**** p<0.01, ** p<0.05, * p<0.1*

Table A.11: First-Stage Regressions Results

Note: The independent variable is the log of IV for EBE specified in section 1.3.2. All columns show strong correlations between the effective bilateral elevation (EBE) and the instrumental variable. The dependent variable in column (1) is the EBE based on the trucks' fuel consumption formula in MOPU (1990). In column (2), it is the EBE with smaller (10 miles) intervals. In column (3), it is the EBE in which the trucks' fuel consumption ratios for uphill roads are calculated using formulas in Posada-Henao et al. (2022). In column (4), the dependent variable is the EBE in which the fuel consumption ratios are taken from Faria et al. (2019) for passenger cars. In column (5), it is the EBE based on MOPU (1990) in which speed is changed to 90km/h from 50km/h. The regressions here use the same sample, controls, and fixed effects as in the baseline regression. Standard errors are clustered at the country-pair-industry level, as in the baseline regressions. The number of observations is 869,709. The period of study spans from 2014-2019.

VARIABLES	mean	sd	min	max
EBE (Baseline)	2.51	2.07	0.01	43.58
EBE (Speed 90)	2.91	2.28	0.01	44.26
EBE (10-Mile Interval)	4.23	3.82	0.01	83.91
EBE (Straight Lines)	4.75	3.84	0.01	55.01
EBE (Faria et al. 2019)	2.45	1.70	0.01	27.54
EBE (Posada-Henao et al. 2022)	2.77	2.40	0.01	52.42

Table A.12: Summary Statistics of EBE Measures

Note: EBE (Baseline) uses fuel-consumption formulas in MOPU (1990) for trucks, takes points along routes, and uses the 20-mile interval between sampled points, assuming speed is 50 km/h. EBE (Speed 90) changes the speed to 90 km/h. EBE (10-Mile Interval) changes the interval to 10 miles between sampled points. EBE (Straight Lines) take sampled points along straight lines between capitals rather than along the routes. EBE (Faria et al. 2019) uses the fuel-consumption data for passenger cars from Faria et al. (2019). EBE (Posada-Henao et al. 2022) combines the trucks' uphill fuel-consumption formula from Posada-Henao et al. (2022) with the downhill fuel-consumption formula in MOPU (1990).

	(1)	(2)	(3)	(4)	(5)	(6)
Grade(%) (Slope)	MOPU (1990)	MOPU (1990)	Posada-Henao et al.(2022)	Faria et al. (2019)	EV Truck (Conservative Scenario)	EV Truck (Moderate Scenario)
7	5.33	4.92	4.65	3	5.33	5.33
6	4.71	4.37	4.64	3	4.71	4.71
5	4.09	3.82	4.34	3	4.09	4.09
4	3.47	3.25	3.74	1.85	3.47	3.47
3	2.85	2.69	2.84	1.85	2.85	2.85
2	2.23	2.13	2.14	1.35	2.23	2.23
1	1.62	1.56	1.82	1.35	1.62	1.62
0	1	1	1	1	1	1
-1	0.41	0.83	NA	0.7	0.37	0.21
-2	0.36	0.78	NA	0.7	0.32	0.18
-3	0.31	0.72	NA	0.4	0.28	0.16
-4	0.26	0.67	NA	0.4	0.23	0.13
-5	0.21	0.62	NA	0.2	0	0
-6	0.16	0.57	NA	0.2	-0.1	-0.2
-7	0.11	0.52	NA	0.2	-0.2	-0.4

Table A.13: Comparison of Fuel-Consumption Ratios

Note: This table provides examples of fuel-consumption ratios at various road slopes and compares them from different literature. Column (1) displays the fuel-consumption ratio, $\frac{c_{\text{grade}}}{c_{\text{grade}=0}}$, based on formulas in MOPU (1990) assuming a speed of 50 km/h, where $grade$ is the technical term for road slope. Column (2) is derived from MOPU (1990) assuming a speed of 90 km/h. Column (3) utilizes the formulas for C3 trucks outlined in Posada-Henao et al. (2022) assuming a speed of 50 km/h. Note that Posada-Henao et al. (2022) overlooks downhill roads (with negative slopes). Column (4) employs the data from Faria et al. (2019), which examines the fuel-consumption ratios for sampled passenger cars. Columns (5) and (6) present conservative and moderate scenarios on EV trucks' fuel-consumption ratios. In columns (5) and (6), the numbers for positive slopes are identical to those in column (1). In column (5), for slopes between -5 and 0, the ratios in column (1) are multiplied by 0.9. In column (6), for slopes between -5 and 0, the ratios in column (1) are multiplied by 0.5. A value of 0 denotes no additional electricity consumption. Negative numbers indicate electricity recharge. For example, -0.1 suggests that an EV truck can regenerate 10 percent of the electricity consumed when driving on flat roads. Note that MOPU (1990) and Posada-Henao et al. (2022) provide continuous functions in their studies, which are utilized in this paper. The step functions depicted in columns (1)-(3) and (5)-(6) are solely for illustrative purposes. Since Faria et al. (2019) does not provide continuous functions in their study, the step function in column (4) is used in this paper.

Appendix B

Appendix for Chapter Two

B.1 Theory

B.1.1 FOC and Marginal Utility for Planner's Problems

The national government's problem is as follows:

$$\underset{(\phi^r_{upper,n},\phi^t_{upper,n})}{Max} \bar{U} = \Gamma(\frac{\epsilon-1}{\epsilon})\Bigg[\sum_{n\in N}(v_n/P_n^{\alpha}r_n^{1-\alpha})^{\epsilon}\Bigg]^{\frac{1}{\epsilon}}$$

subject to (a) budget constraint

$$Z \geq \sum_{n\in N} w_n L_n^{infra}$$

(b) construction worker supply constraint

$$\frac{\sum_{n\in N} L_n^{infra}}{\sum_{n\in N} L_n} \leq 1$$

(c) goods market clears:

$$w_n L_n = \sum_{n\in N} \pi_{in} w_n L_n = \sum_{n\in N} \frac{(1-\lambda)L_i}{\sigma F}(\frac{\sigma}{\sigma-1}\frac{w_i}{A_i}T_{in})^{1-\sigma} P_n^{\sigma-1}\, w_n L_n$$

(d) trade cost along the least-cost paths:

$$\text{argmin} T_{kl} = \prod_{in\in\mathcal{L}} (t_{in}|\mathcal{I}^{in}_{kl}=1) \quad \forall k,l \in N$$

(e)labor market clears:

$$L_n = \pi_n(\omega) * L = \frac{(v_n/P_n^{\alpha}r_n^{1-\alpha})^{\epsilon}}{\sum_{k\in N}(v_k/P_k^{\alpha}r_k^{1-\alpha})^{\epsilon}} L \tag{B.1}$$

where the price index is given by:

$$P_n^{1-\sigma} = \sum_k \frac{(1-\lambda)L_k}{\sigma F}(\frac{\sigma}{\sigma-1}\frac{w_k}{A_k}T_{kn})^{1-\sigma}$$

the rent is given by:

$$r_n = \frac{1-\alpha}{\alpha}\frac{w_n L_n}{H_n}$$

and $\sum_i L_i = L$

The Lagrangian of the national government's problem is as follows:

$$\begin{aligned}\mathcal{L} =&\Gamma(\frac{\epsilon-1}{\epsilon})\Bigg[\sum_{n\in N}(v_n/P_n^{\alpha}r_n^{1-\alpha})^{\epsilon}\Bigg]^{\frac{1}{\epsilon}}\\ &-\sum_n^N \mu_{n,1}\Bigg[w_n L_n - \sum_{i\in N}\frac{(1-\lambda)L_i}{\sigma F}(\frac{\sigma}{\sigma-1}\frac{w_i}{A_i}T_{in})^{1-\sigma}P_n^{\sigma-1}w_n L_n\Bigg]\\ &-\sum_n^N \mu_{n,2}\Bigg[\frac{(v_n/P_n^{\alpha}r_n^{1-\alpha})^{\epsilon}}{\sum_{k\in N}(v_k/P_k^{\alpha}r_k^{1-\alpha})^{\epsilon}} - \frac{L_n}{L}\Bigg]\\ &-\sum_{kl\in\mathcal{L}}\mu_{kl,3}\Bigg[\prod_{in\in\mathcal{L}}(t_{in}|\mathcal{I}_{kl}^{in}=1) - T_{kl}\Bigg]\\ &-\mu_4(\sum_{n\in N} w_n(c_n^r\phi_{upper,n}^r + c_n^t\phi_{upper,n}^t) - Z)\\ &-\mu_5(\frac{\sum_{n\in N}L_n^{infra}}{\sum_{n\in N}L_n} - 1)\end{aligned} \tag{B.2}$$

where $\mu_{n,1}$, $\mu_{n,2}$, $\mu_{kl,3}$, μ_4 and μ_5 are the Lagrangian multipliers. In practice, the construction worker supply constraint is not binding, so that $\mu_5 = 0$. The first-order condition with respect to $\phi_{upper,n}^r$ implies:

$$\begin{aligned}&\frac{\partial\mathcal{L}}{\partial\phi_{upper,m}^r} = 0:\\ &\underbrace{\frac{\partial\bar{U}}{\partial\phi_{upper,m}^r}}_{\text{Direct Effect}} + \underbrace{\sum_n\sum_i \mu_{n,1}\frac{\partial x_{in}}{\partial\phi_{upper,m}^r}}_{\text{Wage Effect}} + \underbrace{\sum_n\sum_i \mu_{n,2}\frac{\partial\frac{L_n}{L}}{\partial\phi_{upper,m}^r}}_{\text{Labor Effect}} + \underbrace{\mu_3\frac{\partial T_{kl}}{\partial\phi_{upper,m}^r}}_{\text{Path Effect}} = \underbrace{\mu_4 w_m c_m^r}_{MC}\end{aligned} \tag{B.3}$$

where $x_{in} = M_i p_{in}^{1-\sigma} = \frac{(1-\lambda)L_n}{\sigma F}(\frac{\sigma}{\sigma-1}\frac{w_i}{A_i}T_{in})^{1-\sigma}$ is the expenditure on goods produced in i and consumed in n.

For simpler intuitions, let's focus on the direct effect in Equation (2.36). Let $U_n = v_n/P_n^{\alpha} r_n^{1-\alpha}$. The marginal utility from investment on highways is:

$$\begin{aligned}
\frac{\partial \bar{U}}{\partial \phi^r_{upper,m}} &= \frac{1}{\epsilon}(\bar{U})^{-1}\frac{\partial \sum_n^N U_n^{\epsilon}}{\partial \phi^r_{upper,m}} \\
&= \frac{1}{\epsilon}(\bar{U})^{-1}\epsilon\sum_n^N U_n^{\epsilon-1}\frac{\partial U_n}{\partial \phi^r_{upper,m}} \\
&= (\bar{U})^{-1}\sum_n^N U_n^{\epsilon-1}\frac{v_n}{r_n^{1-\alpha}}\frac{\partial P_n^{-\alpha}}{\partial \phi^r_{upper,m}} \\
&= -\alpha(\bar{U})^{-1}\sum_n^N U_n^{\epsilon}\frac{1}{P_n}\frac{\partial P_n}{\partial \phi^r_{upper,m}} \\
&= \underbrace{-\alpha(\bar{U})^{-1}\sum_n^N U_n^{\epsilon}P_n^{\sigma-1}}_{\equiv C_1}\sum_i^N M_n p_{in}^{(1-\sigma)}T_{in}^{-1}\frac{\partial T_{in}}{\partial \phi^r_{upper,m}} \\
&= C_1 * \sum_i^N x_{in}T_{in}^{-1}T_{in}\Big[\sum_x^V \mathcal{I}_{in}^{xm,mx}\cdot\frac{1}{t_{xm,mx}}\cdot\frac{\partial t_{xm,mx}}{\partial \phi^r_{upper,m}}\Big] \\
&= \frac{1}{2}C_1 * \sum_i^N x_{in} * \Big[\sum_x^V \mathcal{I}_{kl}^{xm}\underbrace{\frac{1}{1-\sigma}}_{C_2}\big[\frac{\beta^r_{dist}log(dist)_{xm}}{area_m}\big] + \sum_x^V \mathcal{I}_{kl}^{mx}\underbrace{\frac{1}{1-\sigma}}_{C_2}\big[\frac{\beta^r_{dist}log(dist)_{mx}}{area_m}\big]\Big] \\
&= \frac{1}{2}C_1C_2 * \sum_i^N x_{in} * \Big[\sum_x^V \mathcal{I}_{kl}^{xm}\frac{\beta^r_{dist}log(dist)_{xm}}{area_m} + \sum_x^V \mathcal{I}_{kl}^{mx}\frac{\beta^r_{dist}log(dist)_{mx}}{area_m}\Big] \qquad \text{(B.4)}
\end{aligned}$$

where $x_{in} = M_n p_{in}^{(1-\sigma)} = \frac{(1-\lambda)L_n}{\sigma F} * (\frac{\sigma}{\sigma-1}\frac{w_i}{A_i}T_{in})^{(1-\sigma)}$. $\mathcal{I}_{in}^{xm,mx} = 1$ if edge xm or mx is on the least cost-path from k to l. V is the set of all locations near m. Similarly, one can derive the marginal utility with respect to investment in tunnels, where, generally speaking, $elev_{xm} \neq elev_{mx}$.

$$\frac{\partial \bar{U}}{\partial \phi^r_{upper,m}} = \frac{1}{2}C_1C_2 * \sum_i^N x_{in} * \Big[\sum_x^V \mathcal{I}_{in}^{xm}\frac{\beta^t_{elev}log(elev_{xm})}{area_m} + \sum_x^V \mathcal{I}_{in}^{mx}\frac{\beta^t_{elev}log(elev_{mx})}{area_m}\Big] \qquad \text{(B.5)}$$

Let's consider the relative marginal utility per dollar between highways and tunnels in region m.

$$\begin{aligned}
&\frac{MU^r_{upper,m}/MC^r_m}{MU^t_{upper,m}/MC^t_m} \\
&= \frac{\frac{1}{2}C_1C_2 * \sum_n x_{in} * \Big[\sum_x^V \mathcal{I}_{in}^{xm}\frac{\beta^r_{dist}log(dist)_{xm}}{area_m} + \sum_x^V \mathcal{I}_{in}^{mx}\frac{\beta^r_{dist}log(dist)_{mx}}{area_m}\Big]}{\frac{1}{2}C_1C_2 * \sum_n x_{in} * \Big[\sum_x^V \mathcal{I}_{in}^{xm}\frac{\beta^t_{elev}log(elev_{xm})}{area_m} + \sum_x^V \mathcal{I}_{in}^{mx}\frac{\beta^t_{elev}log(elev_{mx})}{area_m}\Big]} * \frac{w_m c^t_m}{w_m c^r_m} \\
&= \frac{\sum_x^V \mathcal{I}_{in}^{xm}\beta^r_{dist}log(dist_{xm}) + \sum_x^V \mathcal{I}_{in}^{mx}\beta^r_{dist}log(dist)_{mx}}{\sum_x^V \mathcal{I}_{in}^{xm}\beta^t_{elev}log(elev_{xm}) + \sum_x^V \mathcal{I}_{in}^{mx}\beta^t_{elev}log(elev_{mx})} * \frac{c^t_m}{c^r_m} \qquad \text{(B.6)}
\end{aligned}$$

Similarly, one can solve the marginal utility of highways and tunnels for provincial governments' problems. The difference is that provincial governors only consider the welfare of residents within their governed province p. Let $C_1^{'} = -\alpha(\bar{U}_p)^{-1}\sum_{n\in p} U_n^{\epsilon} P_n^{\sigma-1}$, where $\bar{U}_p$ is the expected utility within province p, $\bar{U}_p = \Gamma(\frac{\epsilon-1}{\epsilon})\left[\sum_{n\in p}(v_n/P_n^{\alpha} r_n^{1-\alpha})^{\epsilon}\right]^{\frac{1}{\epsilon}}$.

$$\frac{\partial \bar{U}_p}{\partial \phi^r_{lower,m}} = \frac{1}{2} C_1 C_2 * \sum_i^p x_{in} * \left[\sum_x^{V'\in p} \mathcal{I}_{in}^{xm} \frac{\beta^r_{dist} log(dist)_{xm}}{area_m} + \sum_x^{V'\in p} \mathcal{I}_{in}^{mx} \frac{\beta^r_{dist} log(dist)_{mx}}{area_m}\right] \tag{B.7}$$

$$\frac{\partial \bar{U}_p}{\partial \phi^t_{lower,m}} = \frac{1}{2} C_1^{'} C_2 * \sum_i^p x_{in} * \left[\sum_x^{V'\in p} \mathcal{I}_{in}^{xm} \frac{\beta^t_{elev} log(elev_{xm})}{area_m} + \sum_x^{V'\in p} \mathcal{I}_{in}^{mx} \frac{\beta^t_{elev} log(elev_{mx})}{area_m}\right] \tag{B.8}$$

where V' is the set of all locations adjacent to x and within province p.

The relative marginal utility per dollar between provincial and national highways is as follows:

$$\frac{MU^r_{lower,m}/MC^r_n}{MU^r_{upper,m}/MC^r_n} = \frac{C_1^{'} * \sum_i^p x_{in} * \sum_x^{V'\in p} \mathcal{I}_{in}^{xm}\left[\frac{\beta^r_{dist} log(dist_{xm})}{area_m}\right]}{C_1 * \sum_i^N x_{in} * \sum_x^V \mathcal{I}_{in}^{xm}\left[\frac{\beta^r_{dist} log(dist_{xm})}{area_m}\right]} \tag{B.9}$$

where the marginal costs cancel out because the construction cost is the same for both tiers of government.

B.1.2 Equivalence Variation

This paper defines equivalence variation (EV) as the change in real wages in the baseline setting that would achieve the same utility level after a counterfactual change in infrastructure investments.

Consider two equilibrium infrastructure investment outcomes: the baseline outcome $\phi_n = \phi_{upper,n} + \phi_{lower,n}$ and the counterfactual outcome $\phi_n^{'} = \phi_{upper,n}^{'} + \phi_{lower,n}^{'}$. They lead to two different levels of expected utility for the country, $\bar{U}$ and $\bar{U}^{'}$. Define $\frac{\bar{U}}{\bar{U}'} \equiv b$. Using the expected utility in equation (2.14), one can calculate the wage $\mathfrak{w}_n$ that achieves the counterfactual expected

utility under the baseline equilibrium.

$$\begin{aligned}\bar{U}' = \frac{\bar{U}}{b} &= \Gamma(\frac{\epsilon-1}{\epsilon})\Big[\sum_{n\in N}(v_n/P_n^{\alpha}r_n^{1-\alpha})^{\epsilon}\Big]^{\frac{1}{\epsilon}} * b^{-1} \\ &= \Gamma(\frac{\epsilon-1}{\epsilon})\Big[\sum_{n\in N}(w_n\alpha^{-1}b^{-1})/P_n^{\alpha}r_n^{1-\alpha})^{\epsilon}\Big]^{\frac{1}{\epsilon}} \end{aligned} \tag{B.10}$$

where $v_n = \frac{w_n}{\alpha}$ is the total landlord income, including labor and rent income. w_n is the nominal wage. Equation (B.11) shows that the wage that achieves the counterfactual expected utility under the baseline equilibrium is $\mathfrak{w}_n = \frac{w_n}{b}$. In other words, by plugging $\mathfrak{w}_n = \frac{w_n}{b}$ into the expected utility with baseline variable values, one will get $\bar{U}'$. The EV is the difference between the two real wages:

$$EV_n = \frac{\mathfrak{w}_n}{P_n} - \frac{w_n}{P_n} = \frac{w_n}{P_n}(\frac{1-b}{b}) \tag{B.11}$$

EV_n is a constant markup over the baseline real wage, which does not depend on location n. For convenience, define the EV margin as $(\frac{1-b}{b}) * 100$. The EV margin tells the percentage of real wage that each consumer must be compensated (if the margin is positive) or charged (if the margin is negative) so that they are indifferent between the baseline and the counterfactual scenarios. On the other hand, EV_n tells the amount.

In addition, note that if one plugs in the value of b, where $b = \frac{\bar{U}}{\bar{U}'}$, into the formula of EV margin, one will conclude that EV margin, $(\frac{1-b}{b}) * 100$, is the same as the percentage change in the expected utility, $\frac{\bar{U}'-\bar{U}}{\bar{U}} * 100$.

B.2 Tables and Figures

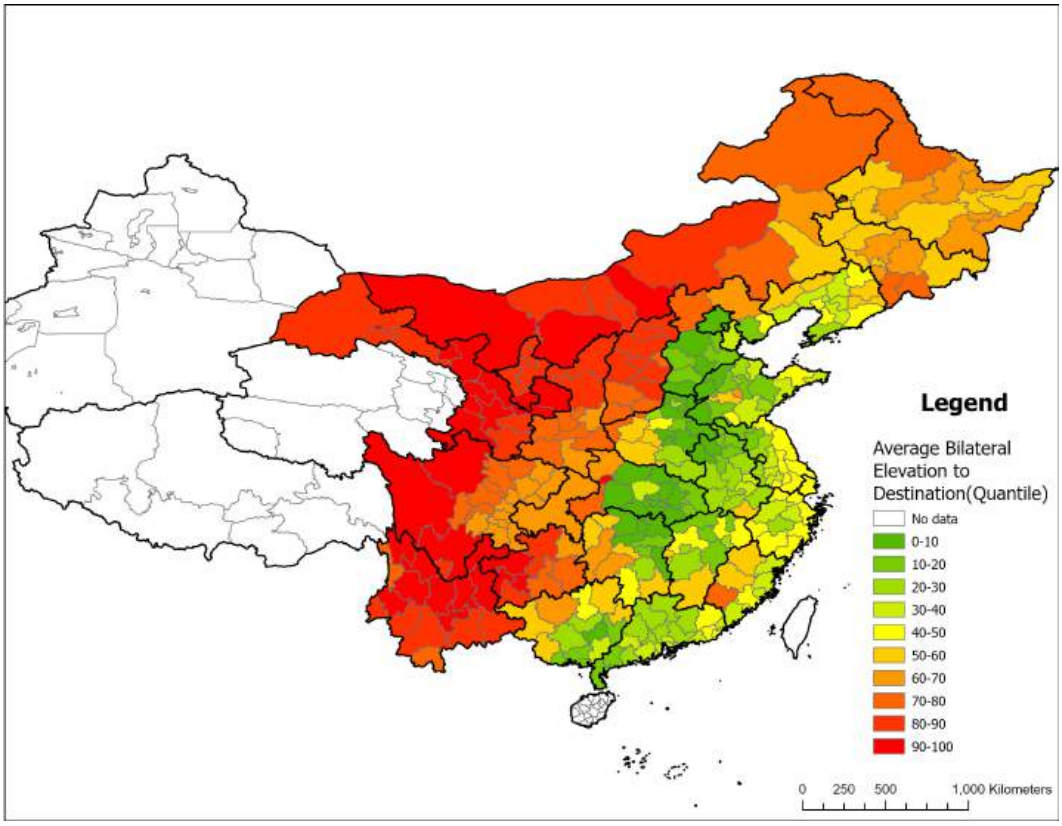

Figure B.1: Average Bilateral Elevation

Note: This figure shows each prefecture's average effective bilateral elevation to the rest of the prefectures in the sample. The regions in lower percentiles have relatively flatter routes than the rest of the country. Note that the bilateral elevation in this paper is simplified from Sun (2023).

No.	Port Name	Value(10,000 TEU)
1	Shanghai	4330
2	Ningbo	2753
3	Shenzhen	2577
4	Guangzhou	2283
5	Qingdao	2101
6	Tianjin	1730
7	Xiamen	1112
8	Dalian	876
9	Yingkou	548
10	Lianyungang	478
11	Rizhao	450
12	Beibu Gulf(including Qinzhou, Fangchenggang, Beihai)	382
13	Dongguan	368
14	Fuzhou	354
15	Yantai	310
16	Tangshan	294
17	Quanzhou	258
18	Zhuhai	256
19	Haikou	197
20	Jinzhou	188
21	Jiaxing	187
22	Zhongshan	141
23	Shantou	135
24	Zhanjiang	112
25	Weihai	103

Table B.1: Container Throughput of Top 25 Coastal Ports in China, 2019

Note: This table provides the 2019 container throughput (measured in 10,000 TEU, Twenty-foot Equivalent Units) for the top 25 coastal ports in China. Beibu Gulf, represent combined figures for multiple ports (Qinzhou, Fangchenggang, Beihai). Data comes from Ministry of Transport of China.

Province	**Share of Total Budget (%)**
Hebei	7.17
Shanxi	10.58
Inner Mongolia	2.05
Liaoning	1.91
Jilin	1.29
Heilongjiang	1.70
Jiangsu	4.51
Zhejiang	7.15
Anhui	3.59
Fujian	7.66
Jiangxi	5.96
Shandong	3.81
Henan	6.60
Hubei	4.55
Hunan	6.27
Guangdong	8.34
Guangxi	3.54
Sichuan	8.82
Guizhou	2.21
Yunnan	0.57
Shaanxi	0.77
Gansu	0.17
Ningxia	0.78

Table B.2: Share of Total Budget Allocation by Province

Note: This table shows the percentage of the total budget allocated to each province in the sample, proportional to the share of provincial highways in each province in 2019. Although the total budget allocated to all provincial governments differs in the baseline and the counterfactual analysis, the share to each province is the same.

Variables	Moment	Baseline	Counterfactual 1	Counterfactual 2
Hwy Length	Mean	358.11	263.79	198.69
	SD	349.99	317.74	188.28
Ntnl Hwy Length	Mean	267.53	263.79	0.00
	SD	325.50	317.74	0.00
Prvn Hwy Length	Mean	90.58	0.00	198.69
	SD	183.94	0.00	188.28
Tnnl Length	Mean	9.43	7.25	5.01
	SD	11.43	10.66	6.61
Ntnl Tnnl Length	Mean	6.67	7.25	0.00
	SD	10.75	10.66	0.00
Prvn Tnnl Length	Mean	2.75	0.00	5.01
	SD	5.74	0.00	6.61

Table B.3: Counterfactual Result Summary

Note: This table summarizes the baseline and counterfactual infrastructure length values. The unit for length is 1 kilometer. The variables from top to bottom are highway length, national highway length, provincial highway length, tunnel length, national tunnel length, and provincial tunnel length.

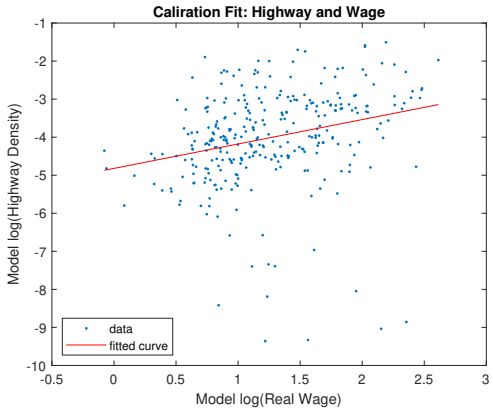

(a) Highway and Income

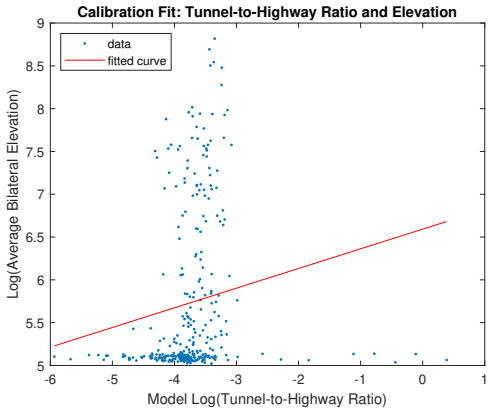

(b) Tunnel Highway and Elevation

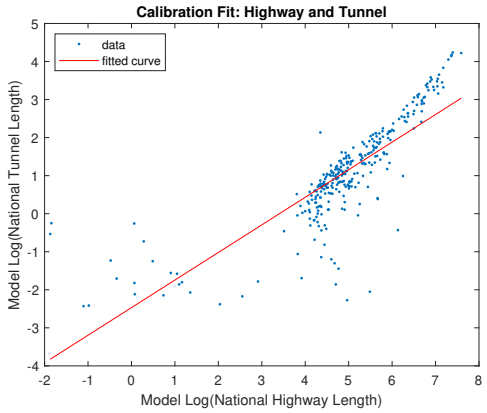

(c) National Highway and Tunnels

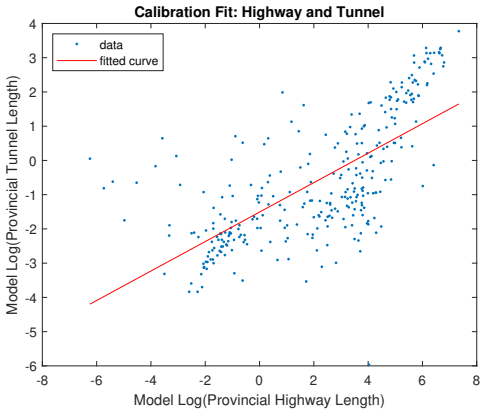

(d) Provincial Highway and Tunnels

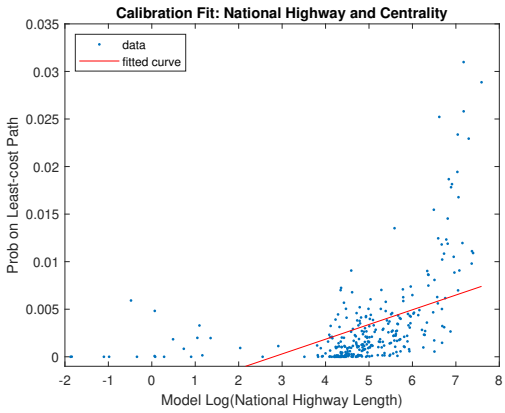

(e) National Highway and Centrality

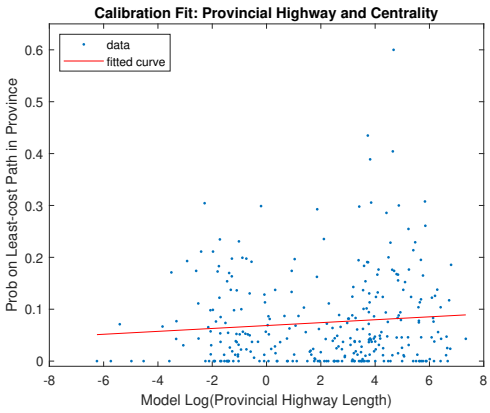

(f) Provincial Highway and Centrality

Figure B.2: Model Replication of Stylized Facts

Note: This figure presents six panels illustrating how the baseline model replicates stylized facts in Section (2.3). Aligned with the data, the model predicts that (a) highways are positively correlated with income, (b) tunnel-to-highway ratio is positively correlated with average bilateral elevation to the rest of the regions, highways are positively correlated with tunnels from (c) national planning and (d) provincial planning, and highways are positively correlated with centrality within the jurisdiction at the (e) national level and (f) provincial level.

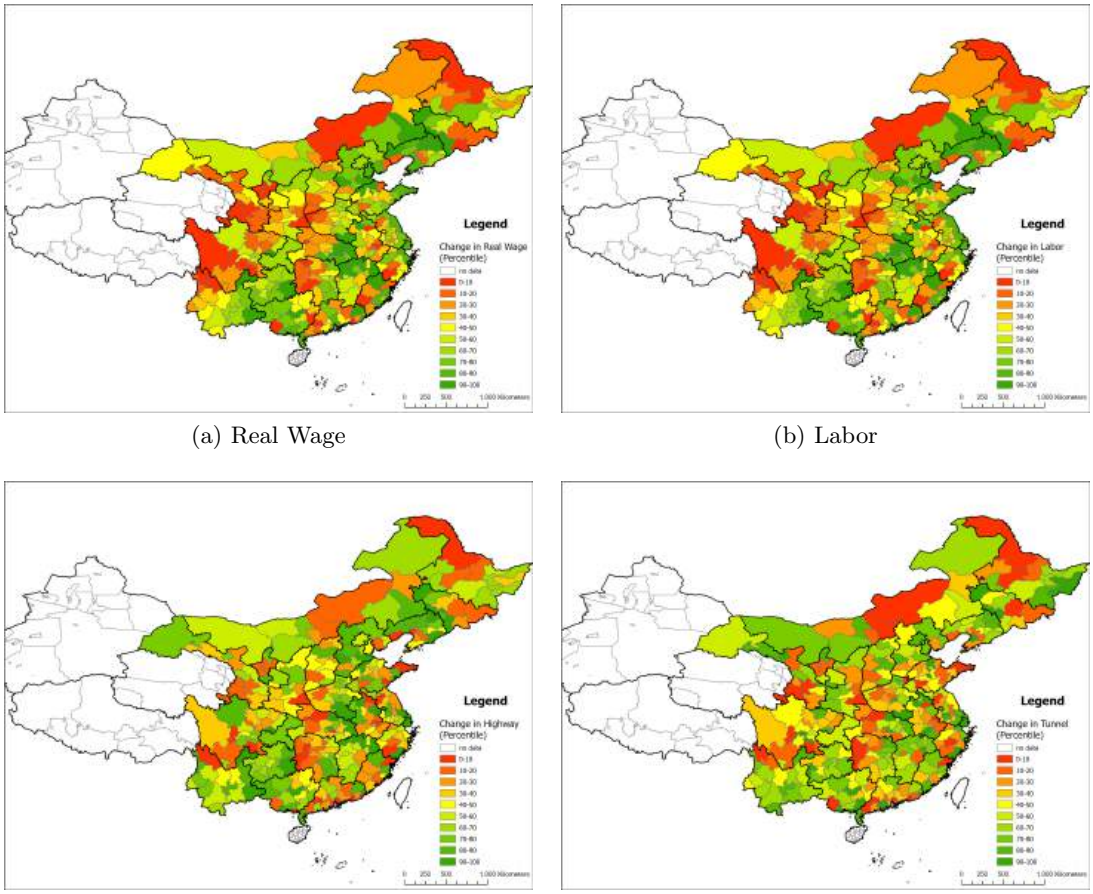

(a) Real Wage (b) Labor

(c) Highway (d) Tunnel

Figure B.3: Counterfactual Result: Distribution of Changes Under Complete Centralization

Note: This figure illustrates the distributional impacts of complete centralization in infrastructure planning across four key variables: (a) real wage, (b) labor, (c) highway, and (d) tunnel.

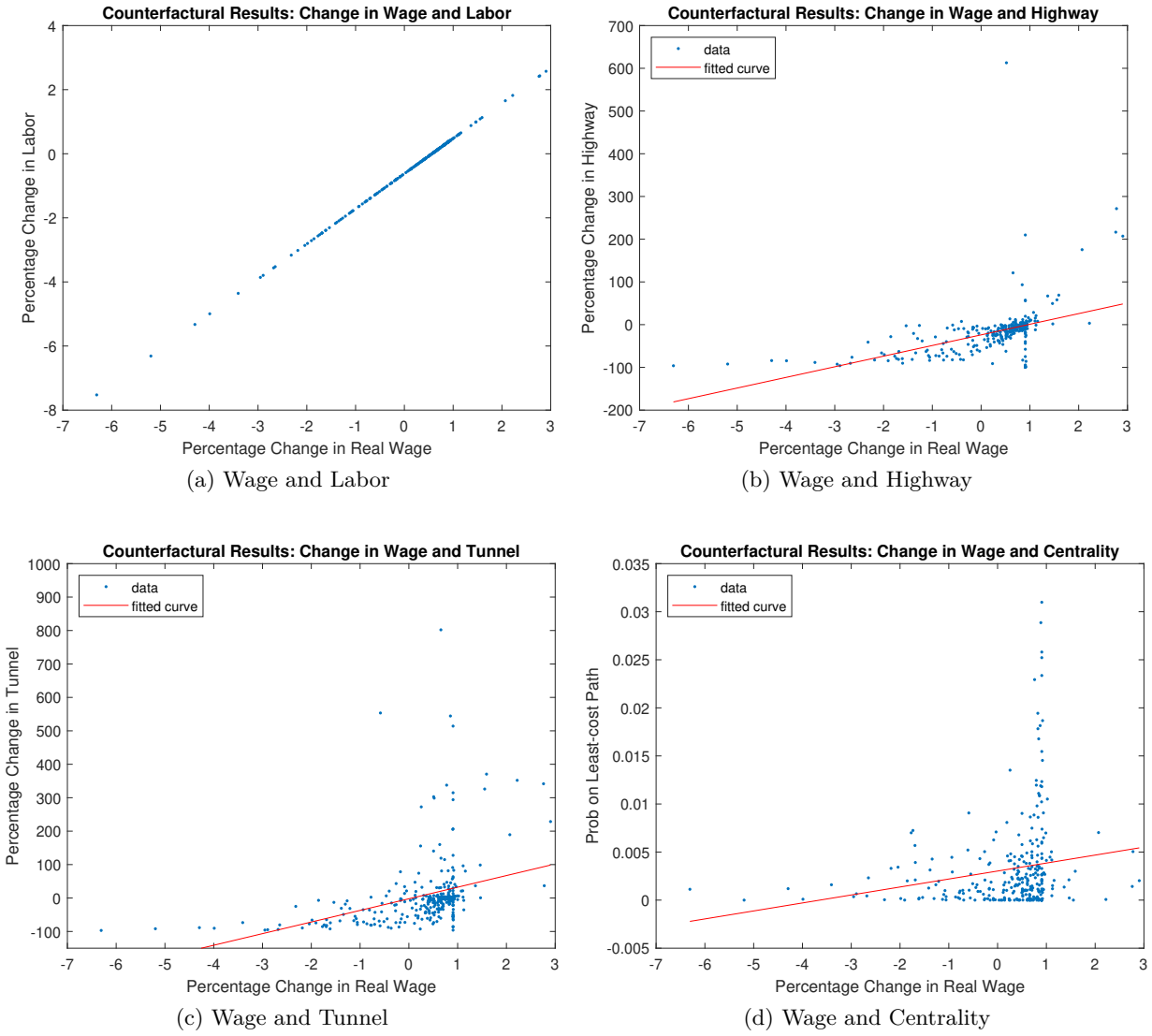

(a) Wage and Labor

(b) Wage and Highway

(c) Wage and Tunnel

(d) Wage and Centrality

Figure B.4: Counterfactual Result: Relationship of Changes Under Complete Centralization

This figure presents the relationship between real wage changes and various key variables (labor, highway, tunnel, and centrality) under the complete centralization scenario. Panel (a) shows that, after the counterfactual change, labor is migrated to the regions with higher changes in real wages. Panel (b) and (c) explain the mechanism of change in real wage: Regions that experienced a greater increase in infrastructure investment see greater rises in real wage. Panel (d) further explains the distributional pattern of the changes: Regions with a greater probability of being on the least path experience the most substantial changes in the real wage.

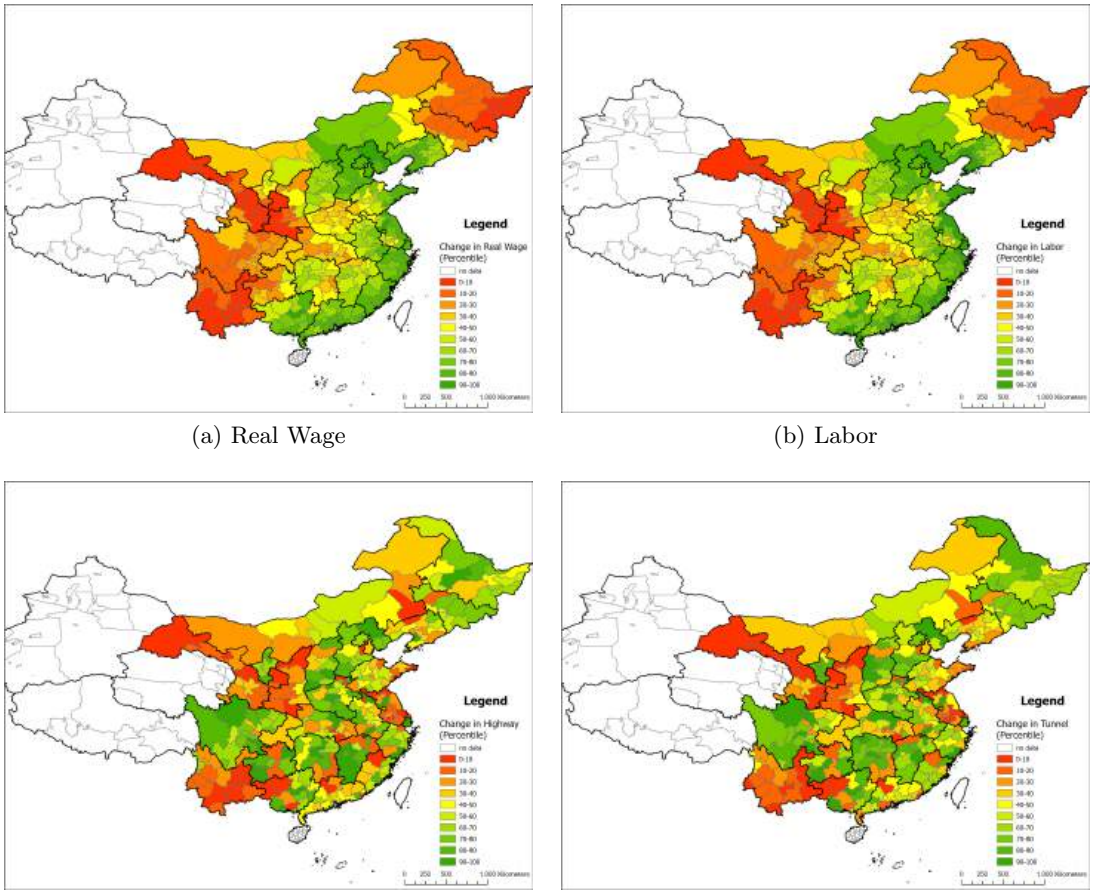

(a) Real Wage (b) Labor

(c) Highway (d) Tunnel

Figure B.5: Counterfactual Result: Distribution of Changes Under Complete Decentralization

Note: This figure illustrates the distributional impacts of complete decentralization in infrastructure planning across four key variables: (a) real wage, (b) labor, (c) highway, and (d) tunnel.

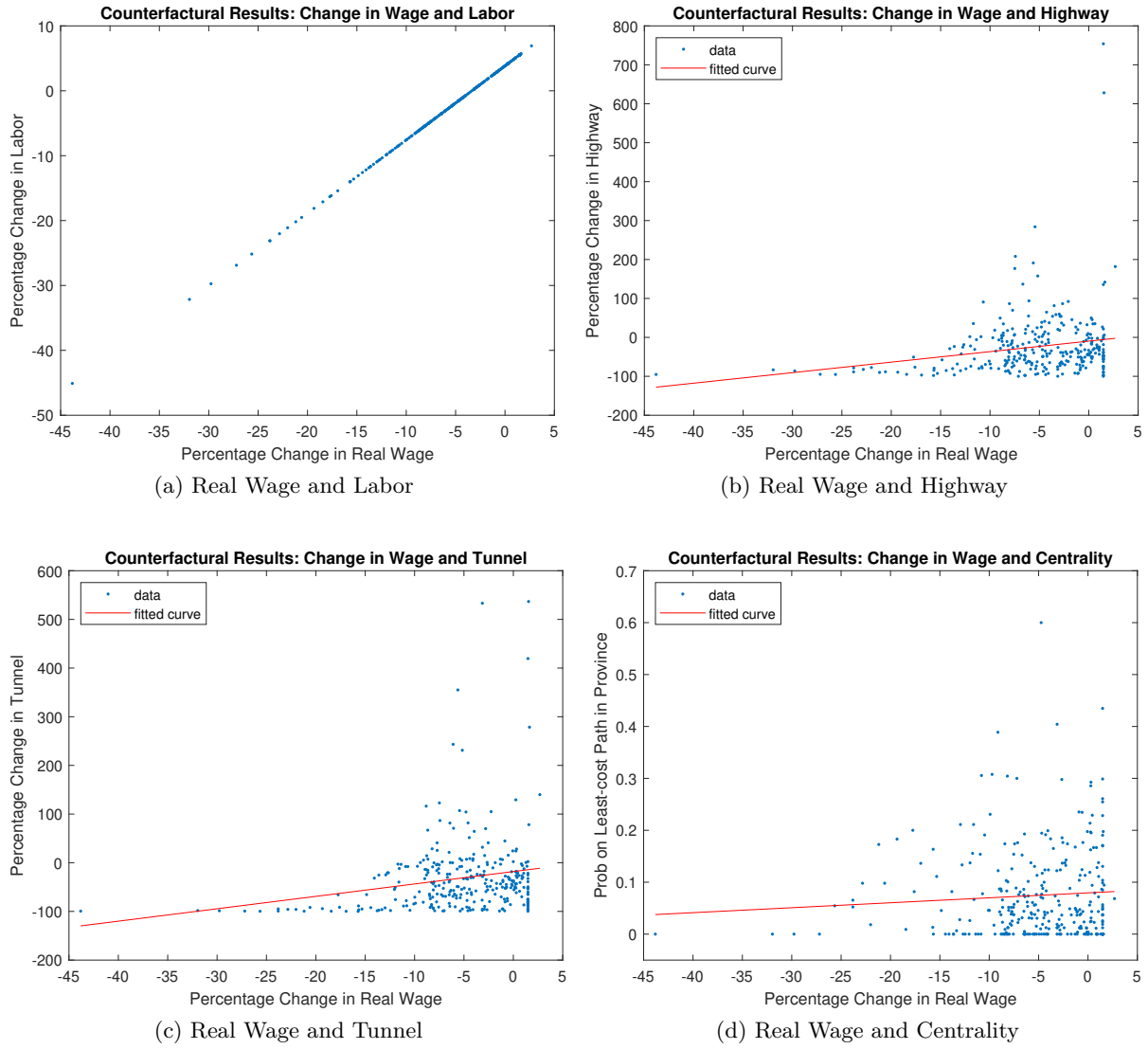

(a) Real Wage and Labor

(b) Real Wage and Highway

(c) Real Wage and Tunnel

(d) Real Wage and Centrality

Figure B.6: Counterfactual Result: Relationship of Changes Under Complete Decentralization

Note: This figure presents the relationship between real wage changes and various key variables (labor, highway, tunnel, and centrality) under the complete decentralization scenario. Panel (a) shows that, after the counterfactual change, labor is migrated to the regions with higher changes in real wages. Panel (b) and (c) explain the mechanism of change in real wage: Regions that experienced a greater increase in infrastructure investment see greater rises in real wage. Panel (d) further explains the distributional pattern of the changes: Regions with a greater probability of being on the least path in the province experience the most substantial changes in the real wage.

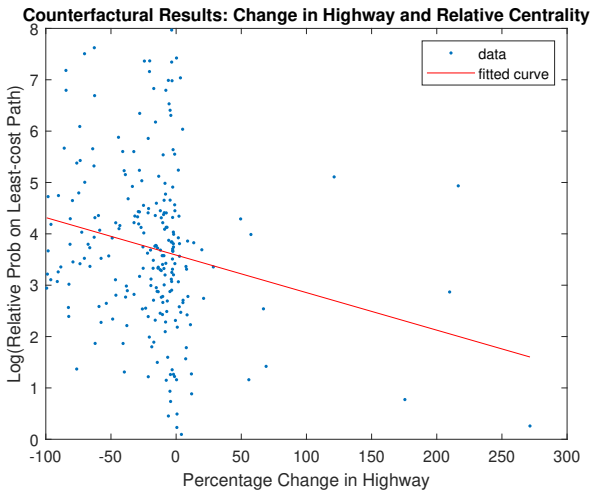

(a) Highway

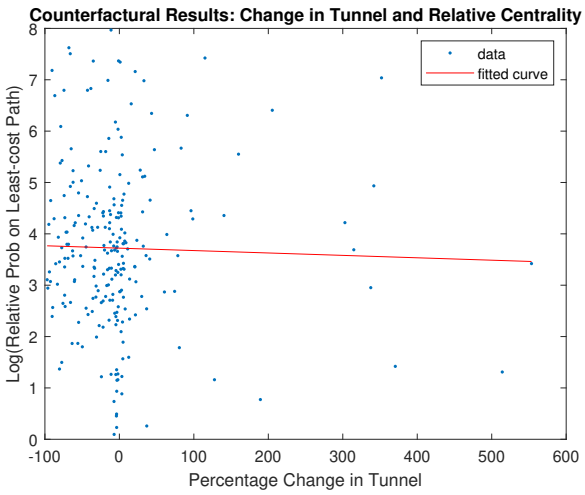

(b) Tunnel

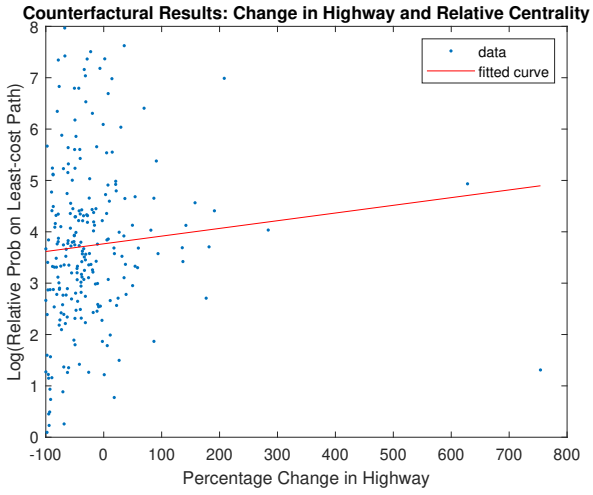

(c) Highway

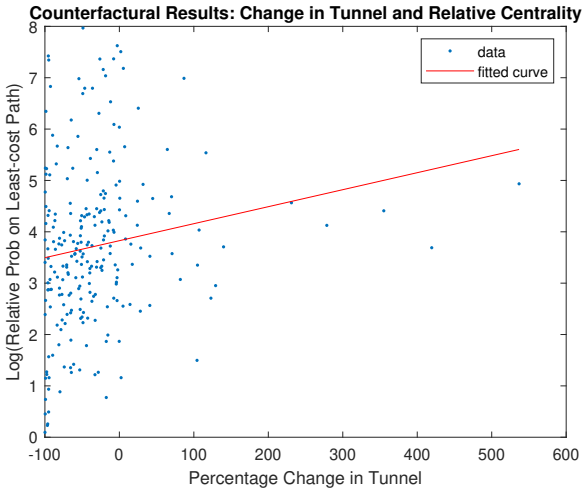

(d) Tunnel

Table B.4: Counterfactual Result: Change in Wage and Relative Centrality

Note: In the tables, the variable on the x-axis is the percentage change in infrastructure in counterfactual 1 (Panels (a) and (b)) and in counterfactual 2(Panels (c) and (d)). The variable on the y-axis is the log of relative probability on the least-cost path (the probability of being on the least-cost path within a province divided by the probability of being on the least-cost path within the whole country).

Province	Data Hwy	Baseline Hwy	Data Tnnl	Baseline Tnnl
Hebei	8267.29	6202.63	1116.69	145.44
Shanxi	4040.14	3236.02	1929.72	101.58
Inner Mongolia	5897.23	4118.59	335.27	115.04
Liaoning	3683.21	3870.97	489.56	98.33
Jilin	2913.39	2498.48	174.23	58.01
Heilongjiang	4520.96	3375.11	87.58	88.87
Jiangsu	5786.74	8305.14	133.81	145.28
Zhejiang	2591.06	4441.09	1664.34	93.42
Anhui	4743.06	4619.54	410.70	90.36
Fujian	2172.65	4033.64	2467.07	103.66
Jiangxi	5815.31	3728.85	473.70	97.85
Shandong	6092.25	6187.10	126.47	152.35
Henan	7212.01	6120.22	252.10	163.28
Hubei	6477.43	5771.93	1210.98	143.05
Hunan	6359.01	5066.10	611.99	125.54
Guangdong	7337.19	7116.51	1169.30	149.83
Guangxi	5136.53	7180.51	430.06	245.64
Sichuan	8254.74	9328.63	3620.87	311.23
Guizhou	3662.50	4407.69	877.20	167.92
Yunnan	5302.60	4644.63	1232.28	137.73
Shaanxi	3676.85	3606.02	2512.54	103.78
Gansu	3590.03	2194.73	1169.54	60.08
Ningxia	1558.98	602.34	69.72	14.97

Table B.5: Calibration fit: infrastructure lengths by province

Note: This table provides a detailed overview of the lengths of highways and tunnels across various provinces in China, comparing actual data (Data Hwy and Data Tnnl) with baseline model predictions (Baseline Hwy and Baseline Tnnl). The unit is in kilometers.

Province	Data NTL Hwy	Baseline NTL Hwy	Data NTL Tnnl	Baseline NTL Tnnl
Hebei	6866.22	5880.61	770.10	131.55
Shanxi	3573.85	2738.00	985.80	80.15
Inner Mongolia	3886.37	3494.52	116.18	91.86
Liaoning	3501.73	2985.45	397.65	78.53
Jilin	2115.29	1806.12	63.82	41.03
Heilongjiang	3321.06	1907.07	14.55	40.10
Jiangsu	3813.13	6191.39	85.76	108.29
Zhejiang	2898.61	2767.55	941.55	45.25
Anhui	3578.97	3045.25	340.16	44.97
Fujian	3266.66	2946.78	1665.21	85.25
Jiangxi	4010.67	3501.51	245.03	89.60
Shandong	4393.43	4146.51	100.89	98.18
Henan	3963.66	4342.59	101.52	87.56
Hubei	4033.83	4056.18	576.84	81.69
Hunan	4089.22	3127.89	313.53	74.89
Guangdong	5623.73	3675.68	750.24	72.27
Guangxi	4045.46	6822.33	349.04	236.90
Sichuan	7632.02	5980.67	2916.63	182.14
Guizhou	1707.62	4392.35	357.11	163.47
Yunnan	2405.06	3900.66	534.27	106.35
Shaanxi	4892.26	2869.08	2500.26	73.46
Gansu	3348.98	1726.11	1017.38	40.83
Ningxia	1348.68	362.12	34.03	8.13

Table B.6: Calibration fit: national infrastructure lengths by province

Note: This table provides a detailed overview of the lengths of highways and tunnels in the National Expressway network across various provinces in China, comparing actual data with baseline model predictions. The unit is in kilometers.

Province	Data Prvn Hwy	Baseline Prvn Hwy	Data Prvn Tnnl	Baseline Prvn Tnnl
Hebei	2517.76	322.01	346.59	13.89
Shanxi	2396.01	498.02	943.92	21.43
Inner Mongolia	1023.35	624.07	0.00	23.18
Liaoning	671.04	885.52	91.91	19.80
Jilin	531.40	692.35	37.38	16.98
Heilongjiang	846.55	1468.05	0.00	48.76
Jiangsu	2107.43	2113.75	48.06	36.98
Zhejiang	1356.80	1673.54	722.79	48.17
Anhui	1574.79	1574.30	70.55	45.39
Fujian	1373.06	1086.87	801.86	18.41
Jiangxi	2278.33	227.34	228.66	8.25
Shandong	1825.30	2040.58	25.58	54.16
Henan	3059.53	1777.64	77.55	75.72
Hubei	1449.95	1715.74	269.00	61.37
Hunan	2440.85	1938.21	225.43	50.64
Guangdong	2882.76	3440.84	419.06	77.57
Guangxi	1521.12	358.18	81.02	8.74
Sichuan	2920.81	3347.97	485.15	129.09
Guizhou	627.45	15.34	154.95	4.45
Yunnan	161.49	743.97	40.75	31.38
Shaanxi	347.57	736.95	12.29	30.32
Gansu	67.46	468.62	6.10	19.25
Ningxia	280.02	240.23	35.69	6.84

Table B.7: Calibration fit: provincial infrastructure length by province

Note: This table provides a detailed overview of the lengths of highways and tunnels in the Provincial Expressway network across various provinces in China, comparing actual data with baseline model predictions. The unit is in kilometers.

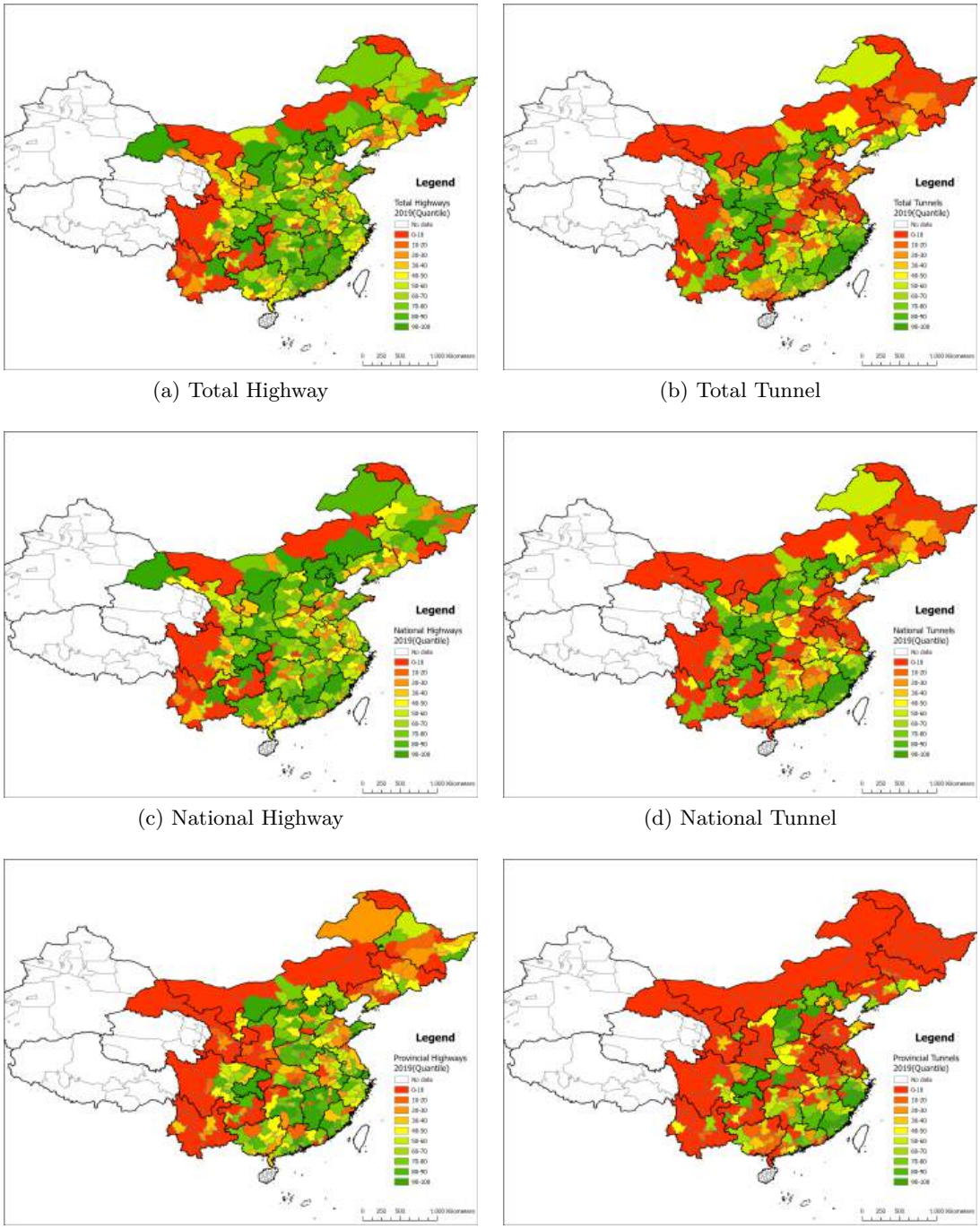

(a) Total Highway (b) Total Tunnel

(c) National Highway (d) National Tunnel

(e) Provincial Highway (f) Provincial Tunnel

Figure B.7: China's Highway and Tunnel Distribution 2019

Note: This table provides the distribution of highways and tunnels in the National and Provincial Expressway network in 2019.